HYDROGEOLOGICAL AND HYDROCHEMICAL INVESTIGATION OF THE DURBAN METROPOLITAN DISTRICT, EASTERN SOUTH AFRICA

by

MINENHLE SIPHESIHLE NDLOVU

Submitted in fulfilment of the academic requirements of Master of Science

In hydrogeology

Discipline of Geological Sciences,

School of Agricultural, Earth and Environmental Sciences,

University of KwaZulu-Natal,

Durban

South Africa

December 2018

ABSTRACT

Population and economic growth within the Durban Metropolitan region in eastern South Africa has increased the demand for water supply. This ever-increasing demand means that all available water supply sources including groundwater will be looked at, particularly in urban and peri-urban areas. However, the state of the groundwater resource in the region is poorly understood. This study aims to contribute towards improved understanding of the state of groundwater resources in the Metropolitan District through an integrated hydrogeological, hydrochemical and environmental isotope investigations. Results of hydrogeological and hydrogeochemical characterization identified at least five hydrostratigraphic units of varying hydraulic and hydrochemical characteristics. 1) The weathered and fractured Granitic basement aquifers of the Mapumulo Group and Oribi Gorge Suite characterized by average borehole yield and transmissivity (T) of 1.2 l/s and 3.9 m^2/day, respectively, with hydrochemical facies of Ca-Mg-HCO_3. 2) The fractured Natal Group sandstone, characterized by average borehole yield and hydraulic conductivity (K) of 5.6 l/s and 2.8 m/day, respectively with Na-Mg-HCO_3-Cl as dominant water type; 3) The fractured aquifers of the Dwyka Group diamictite and tillite are characterized by average borehole yield of 0.4 l/s and T of 1.3 m^2/day and Na-Cl-HCO_3 as the dominant water type; 4) The Vryheid Formation, which is part of the Ecca Group, is characterized by a mean borehole yield of 2.5 l/s, T of 4.9 m^2/day, K of 0.17 m/day and Na-Cl-HCO_3 water type; 5) The intergranular primary aquifers of the Maputaland Group which consists the Bluff, Berea Formations and recent alluvium and estuarine deposits (locally called harbour beds Formation) have average borehole yield of 14.8 l/s and transmissivity of up to 406 m^2/day with a mainly Na-Cl-HCO_3 hydrochemical signature. The region receives mean annual precipitation (MAP) of 935 mm/yr of which 9.2% infiltrates to recharge the various aquifers. Environmental isotope information (^2H, ^{18}O and ^3H) indicated that groundwater recharge is of modern precipitation. Groundwater tritium values of 37.4 and 92 TU are measured around the Bul Bul Drive and Bisasar Road Landfill sites, respectively, indicating groundwater contamination from landfill leachate leakage. Based on the main hydrogeological, hydrogeochemical and environmental isotope findings, a regional hydrogeological conceptual model is developed that characterizes the hydrogeological and hydrochemical conditions of the Durban Metropolitan region.

Keyword/Phrases: Environmental isotopes; hydrogeochemistry; Hydrostratigraphic units; weathered and fractured aquifers; Urban and peri-urban groundwater, South Africa

PREFACE

The research contained in this dissertation was completed by the candidate while based in the Discipline of Geological Sciences, School of Agricultural, Earth and Environmental Sciences of the College of Agriculture, Engineering and Science, University of KwaZulu-Natal, Westville Campus, South Africa. The research was financially supported by the school through Dr Molla Demlie.

The contents of this work have not been submitted in any form to another university and, except where the work of others is acknowledged in the text, the results reported are due to investigations by the candidate.

_____ _____**03/12/2018**_____

Signed (Supervisor) Date

Declaration 1 -Plagiarism

I, Minenhle Siphesihle Ndlovu declare that:

I. The research reported in this dissertation, except where otherwise indicated, is my original research.

II. This dissertation has not been submitted for any degree or examination at any other university.

III. This dissertation does not contain other persons' data, pictures, graphs or other information, unless specifically acknowledged as being sourced from other persons.

IV. This dissertation does not contain other persons' writing, unless specifically acknowledged as being sourced from other researchers. Where other written sources have been quoted, then:

   a. Their words have been re-written, but the general information attributed to them has been referenced

   b. Where their exact words have been used, then their writing has been placed in italics and inside quotation marks and referenced.

V. This dissertation does not contain text, graphics or tables copied and pasted from the internet, unless specifically acknowledged, and the source being detailed in the thesis and in the References section.

…….....

Signed: Minenhle Siphesihle Ndlovu

03 December 2018

DECLARATION 2 –PUBLICATIONS

Publication 1 (Chapter 6 and 7): Submitted to the South African Journal of Geology

Ndlovu, M.S and Demlie, M. (2018). Hydrogeological setting and hydrogeochemical characteristics of the Durban Metropolitan District, Eastern South Africa.

Contribution: As first author on the paper, I was responsible for sample collection (with the aid of my supervisor), undertaking of hydrogeological and hydrochemical analyses, collection and interpretation of all data, writing, editing and preparation of the manuscript, figures, Table and the development of the conceptual model. The second author is my supervisor, who provided guidance throughout the project as well as editing the manuscript.

…….....**.....**

Signed: Minenhle Siphesihle Ndlovu

03 December 2018

Table of Contents

List of Figures

List of Tables

List of Acronyms

amsl	Above mean sea level
bmsl	Below mean sea level
C	Runoff coefficient
Cl_p	Chloride concentration in precipitation (mg/l)
Cl_{sw}	Chloride concentration in soil water (mg/l)
CMB	Chloride Mass Balance
DEM	Digital Elevation Model
DO	Dissolved Oxygen (ppm)
DWA	Department of Water Affairs
DWS	Department of Water and Sanitation
EC	Electrical conductivity (µS/m)
Eh	Reduction potential (mV)
ETo	Reference crop evapotranspiration
ETc	Crop evapotranspiration under standard conditions (mm day-1)
FAO	Food and Agriculture Organisation
G	Soil heat flux (MJ m-2 day-1)
GMWL	Global Meteoric Water Line
GRIP	Groundwater Resource Information Project
IAEA	International Atomic Energy Agency
I	Thermal index
IC	Ion-Chromatograph
ICP-MS	Inductively Coupled Plasma Mass Spectrometry
LMWL	Local Meteoric Water Line
Nm	Latitude correction factor
n	Actual duration of sunshine in a day (hour)

ORP	Oxygen Reduction Potential (mV)
P	Precipitation (mm/month)
Q	Peak runoff rate (m3/s)
Q	Yield (usually in l/s or m3/d)
q	Monthly runoff (mm)
S	Storativity or specific yield
SAWS	South African Weather Services
SRTM	Shuttle Radar Topography Mission
T	Transmissivity (m2/d)
T	Air temperature (°C)
TDS	Total dissolved solids (mg/l)
V-SMOW	Vienna Standard Mean Ocean Water

Acknowledgements

I would like to thank Dr. Molla B. Demlie, my supervisor, for his guidance and support throughout the study. Thank you for keeping me on track and for providing assistance whenever it was needed and for encouragingly supporting my academic development. Your guidance was invaluable and thank you for financial assistance throughout the course of this research.

I would like to thank Michael Maluleke from the Department of Water and Sanitation for providing all the groundwater related data and for the consultations, without you the research would have not been a success.

The South African Weather Services (SAWS) is acknowledged for providing the necessary climatic data for the research.

To the Durban Solid Waste Unit engineers as well as onsite personnel at the various landfills at the eThekwini Municipality, thank you for assisting and allowing for data collection necessary for this research.

I would like to thank my fellow office mates, Hlumela Mduduma, Nkule Dladla, Tammy Wanda, Xolani and Kgaugelo for being the best office mates and for providing a break from reality when much needed.

To Felicia Dimba, Thanks for the support, for always cheering me up and keeping me on my toes words cannot express how grateful I am.

To my family, thank you for supporting and encouraging me throughout the course of this research, may God bless you all.

Finally, I thank my God, my good Father, for letting me through all the difficulties. I have experienced your guidance day by day. You are the one who let me finish my degree. I will keep on trusting You for my future. Thank you, Lord.

CHAPTER 1

INTRODUCTION

1.1. Background and Rationale

Population in urbanized areas grows exceptionally rapidly forcing cities to expand beyond their current borders resulting in an increased demand for basic infrastructure and services including water supply and sanitation, waste disposal among others (Howard, 2002). Daily activities in urban areas affect groundwater conditions both directly and indirectly and are often lastly considered (Rogers, 1994; Strohschon *et al*., 2013). The rapid growth of urban areas has two basic effects on groundwater resources including effects on natural recharge of aquifers due to sealing of the ground surface with concrete and pollution of groundwater due to leakage from drains, sewers, industrial waste including effluents (Foster, 1990; Lerner, 2002; Baier *et al*., 2014). This gives rise to great implications for management policies, particularly in rapid growing cities. According to Department of Water Affairs (DWA, 2010), South Africa's main water supply schemes are dependent on surface water sources. As these surface water sources are gradually fully exploited, groundwater resources are becoming increasingly important to supplement the water supply shortfall.

From a resource perspective, groundwater represents the largest and most important source of potable water (Foster, 1990). Problems begin when groundwater's utility becomes compromised by urban growth, intensifying demand and degradation of water quality through the release and spread of contaminants (Shahin, 1990). According to Changnon (1976); Bornstein and Lin (2000), urban development alters all aspects of the water cycle: the climate; quantity and quality of surface water and groundwater regimes. It affects local climate by altering surface temperatures, albedo, evaporation, transpiration, precipitation rates and the energy balance in the atmosphere.

The impervious land surface cover in urban areas enhances runoff and limits infiltration resulting into reduced natural groundwater recharge (Leopold, 1968). However, new sources of recharge in the form of leakage from water and wastewater collection and distribution systems, leaks from storm sewers and irrigation return flow from lawns, parks, and golf courses occur (Lerner, 1986). Thus, quantifying groundwater recharge in urban areas becomes a challenge due to the complexity

of its environment, not only due to the heterogeneity of shallow aquifers underneath, but due the variety of overlapping and coexisting land uses.

In the past, groundwater in KwaZulu-Natal has been exploited to a very limited extent compared to other drier parts of South Africa as surface water was readily available to satisfy the various demands. However, the impact of the prolonged drought in surface water resources in recent years has resulted into an increase in exploitation of the groundwater resource (DWA, 2010). The Durban Metropolitan District relies highly on good quality and quantity of fresh water from catchment areas outside of its boundaries (i.e. Ugu, uMgungundlovu & iLembe Districts) and this requires the improvement of relationships with neighboring District municipalities (IPD, 2017). Growth in population within the Durban Metropolitan will impose an increased demand on surface water supply, which will then require an additional source of water supply. According to IDP (2017), in 2001 the population of the Durban Metropolitan was 3.09 million and has grown at an average rate of 1.13% per annum to reach 3.44 million in 2011 and 3.72 million in 2016. Statistics South Africa (2011) projected that the population will grow up to 3.85 million by 2020. IDP (2017) reported that climate change also results into a decrease in water availability due to changes in rainfall patterns and increased evaporation within the District Municipality. An increase in frequency and intensity of drought severity has been observed over the past 48 years in KwaZulu-Natal province in general and within the Durban region in particular (Ndlovu and Demlie, 2018a). A decline in groundwater level in the Durban area at a rate of 0.05 m/year over the past 14 years has been observed (Ndlovu and Demlie, 2018b).

The increase in demand for water supply in eThekwini District Municipality requires that groundwater resources be developed and protected in line with the South African National Water Act (Act No.36 of 1998). This act legislates the way in which all South Africa's surface and groundwater resources are protected, used, developed, conserved, managed and controlled. The objective of which is to ensure that there is enough water of good quality available for distribution to municipalities, water boards, water use associations and other water service institution for current and future generations. The water act also stipulates provisions for monitoring, recording, assessing and disseminating information on water resources. This includes an establishment of local monitoring systems on water resources for collecting appropriate data to assess the quality and quantity, and the rehabilitation of water resources.

Thus, population and economic growth within the Durban Metropolitan region in eastern South Africa have increased the demand for water supply. Though the region's water supply comes mainly from surface water resources, the ever-increasing demand means that all available water supply sources including groundwater will be looked at, particularly in the peri-urban areas. However, the state of the groundwater resource including detailed aquifer characteristics, recharge conditions, their hydrochemical composition and extent is poorly understood. Thus, this M.Sc. research envisages to contribute towards improved understanding of the state of groundwater resources by characterizing the hydrogeological setting and hydrochemical characteristics across the Durban Metropolitan District.

1.2. Research Aims and Objectives

The overall aim of this study is to contribute towards an improved understanding of the complex hydrogeological setting of the Durban Metropolitan District by collecting, integrating and analyzing hydrogeological and hydrochemical data.

The specific objectives are:

- To characterize the aquifers including their extent, hydraulic parameters and rates of recharge
- To understand surface water – groundwater interconnection
- To understand the hydrochemistry of the area
- To assess the impact of various land use activities on the water resources quality in the area, mainly around landfill sites
- To develop a regional conceptual hydrogeological model for improved understanding of hydrogeological and hydrochemical characteristics.

1. 3. Dissertation Structure

This dissertation is divided into seven chapters and comprises the following;

Chapter 1 is the introductory chapter outlining the background, rationale, aims and objective of the research.

Chapter 2 provides an overview of the study area in terms of location, demography, physiography, and drainage; hydrogeological and hydro-meteorological aspects and geological setting of

the study area. The geological characteristics are described through lithology, stratigraphy and structure.

Chapter 3 reviews literature related to previous work on the study area and worldwide scientific methods applied in analyzing geological, hydrogeological, hydrochemical, and environmental isotope data. This chapter also reviews methodologies related to the determination of water balance components such as groundwater recharge, surface runoff and evapotranspiration. Background information on developing a conceptual hydrogeological model is reviewed as well.

Chapter 4 outlines the research approaches and methodology applied during the collection, analyses and presentation of different hydrogeological, hydrochemical, and environmental isotope data.

Chapter 5 presents the main results and discussions which include both primary and secondary data interpretations. This chapter discusses all the components used in developing a hydrogeological conceptual model for the study area. This includes, water balance components of the study area, groundwater level and depth to groundwater contour maps, hydrochemistry, geological cross sections and hydrostratigraphy,

Chapter 6 provides the pollution aspect of the study area which includes landfills. The hydrochemistry and environmental isotope results for water resources around landfill sites are presented and discussed in this chapter.

Chapter 7 presents the main conclusions and recommendations emanating from the research. Summary of the main results of the hydrogeological conceptual model of the study area is provided in this chapter. And optimized groundwater monitoring network within the municipality using hydrogeological, water quality, and environmental isotope data has been recommended.

All scientific papers, books, reports and memoirs referred and cited during this study are listed as references. The appendix sections provide tables of results for water budget components, maps, geological logs and original hydrochemical, water quality, and environmental isotopic data used during the course of the study.

CHAPTER 2

DESCRIPTION OF THE STUDY AREA

2.1. Location of the study area

The Durban Metropolitan District Municipality is located in the southeastern coastal area of KwaZulu-Natal Province, South Africa (Figure 2.1). The Metropolitan District covers an area of approximately 2500 square kilometers (IDP, 2017). The boundary extends northwards towards the suburb of Tongaat while the southern boundary limits extends to south of Umkomaas. The Durban Metropolitan District is home to 3.56 million people which is 7.3% of total population in South Africa (IDP, 2017). The settlement characteristics of the Metropolitan District comprises of 45% rural, 30% peri-urban and 25% urban areas.

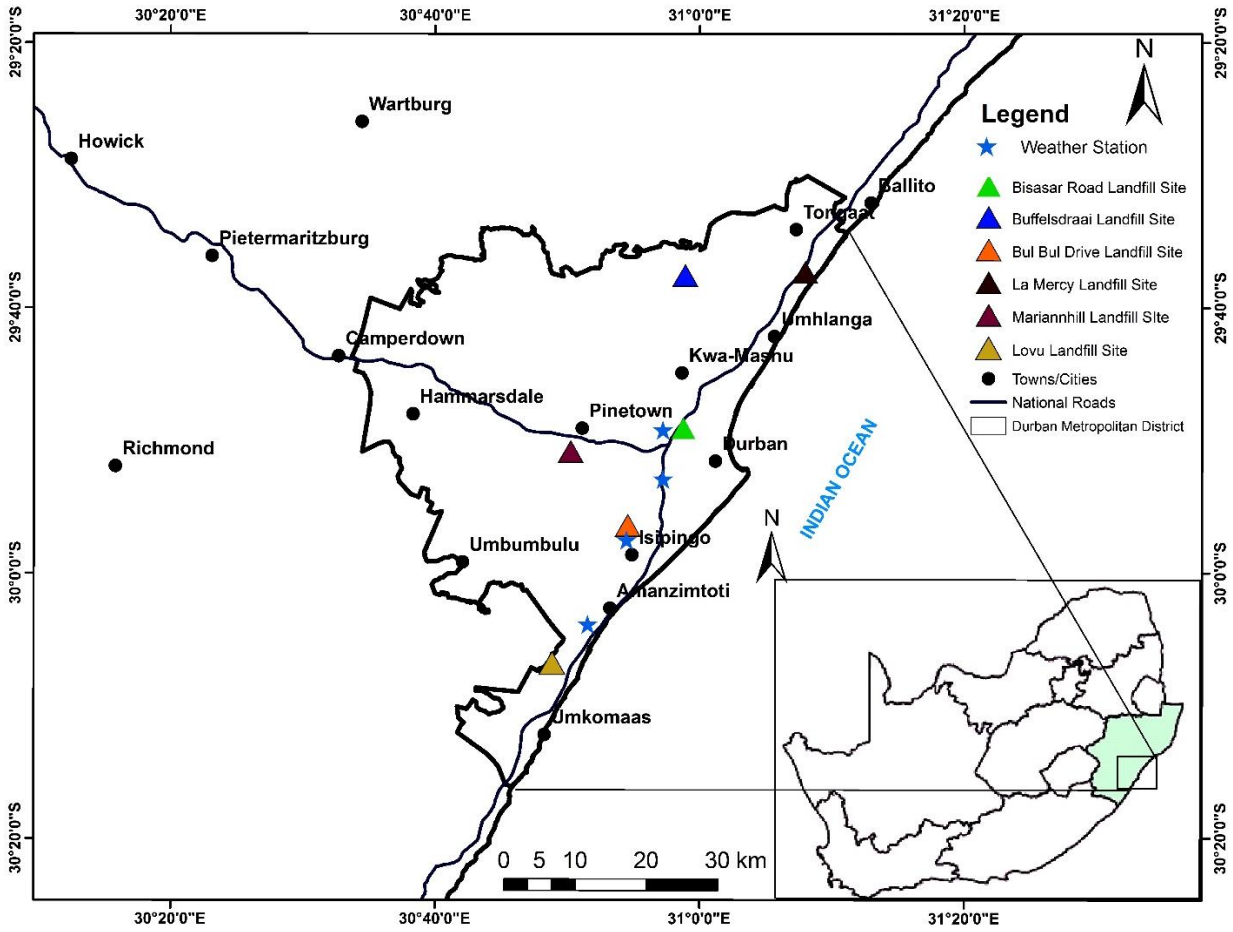

Figure 2.1: Location map of the study area along with Landfill sites.

2.2. Climate, Topography and Drainage

The Durban Metropolitan Region has a subtropical climate, where winters are dry and cold, while summers are hot, humid and wet. The average summer and winter temperatures are 26 °C and 17 °C, respectively (Figure 2.2). The main rainy season is from September to March (summer months). The average annual rainfall is just over 1000 mm/yr with highest and lowest rainfall of 125 and 23 mm recorded in January and June, respectively (SAWS, 2017). The main rivers that drain the study area from south to north are; uMkomazi, uBivana, uMlazi, uMbilo, uMngeni, uMdloti and uTongati, all of which are perennial (Figure 2.3).

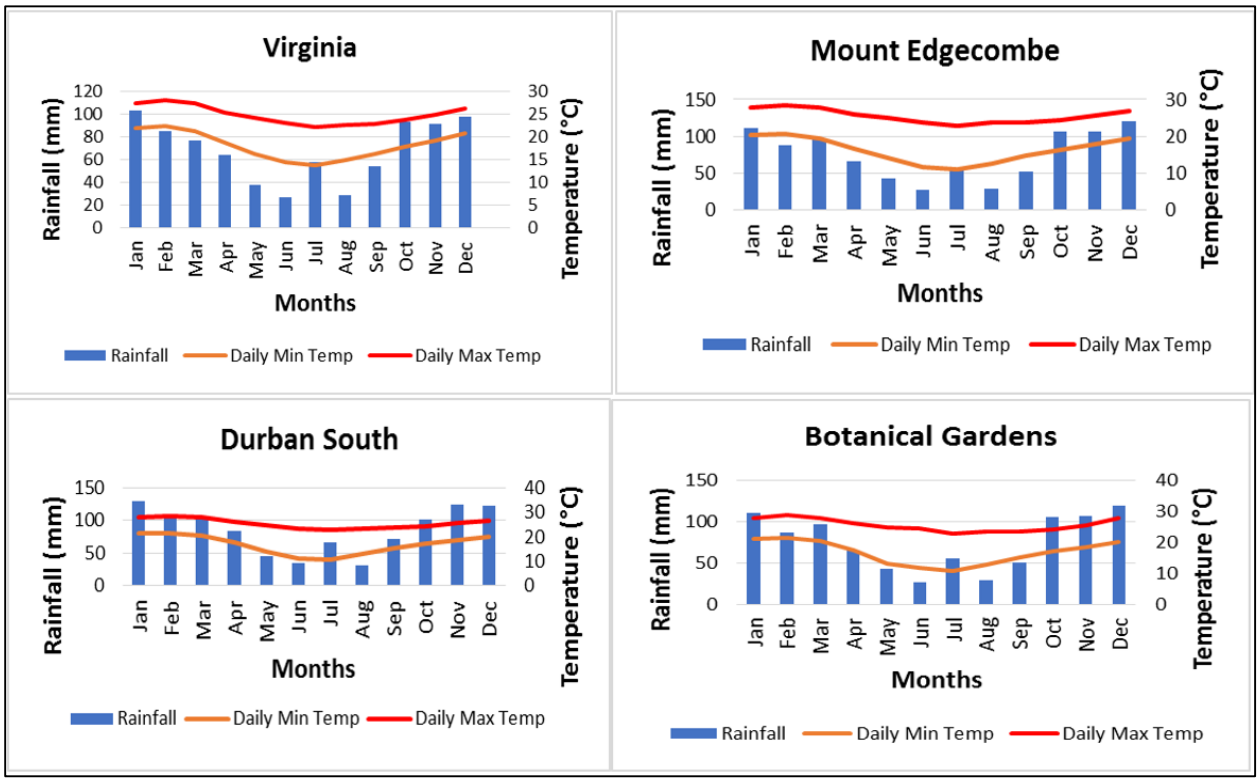

Figure 2.2: Mean monthly rainfall and temperature from 1995-2016 from weather stations located across the study area (data sourced from SAWS, 2017).

2.3. Land use and Land cover

About 68% of the District Municipal area is considered rural, with pockets of dense settlements where 10% of the rural areas comprise commercial farms. 90% of the rural area is defined by geospatial features, such rugged, hilly terrain, and dispersed settlement patterns in traditional dwellings. This presents a number of challenges to the municipality particularly with respect to

land, planning and urban management. The remainder of the municipal area, approximately 32%, is urban area dominated by residential, commercial and industrial land uses (IDP, 2017). Industrial/Commercial activities are mainly concentrated in Pinetown, Isipingo and Mobeni.

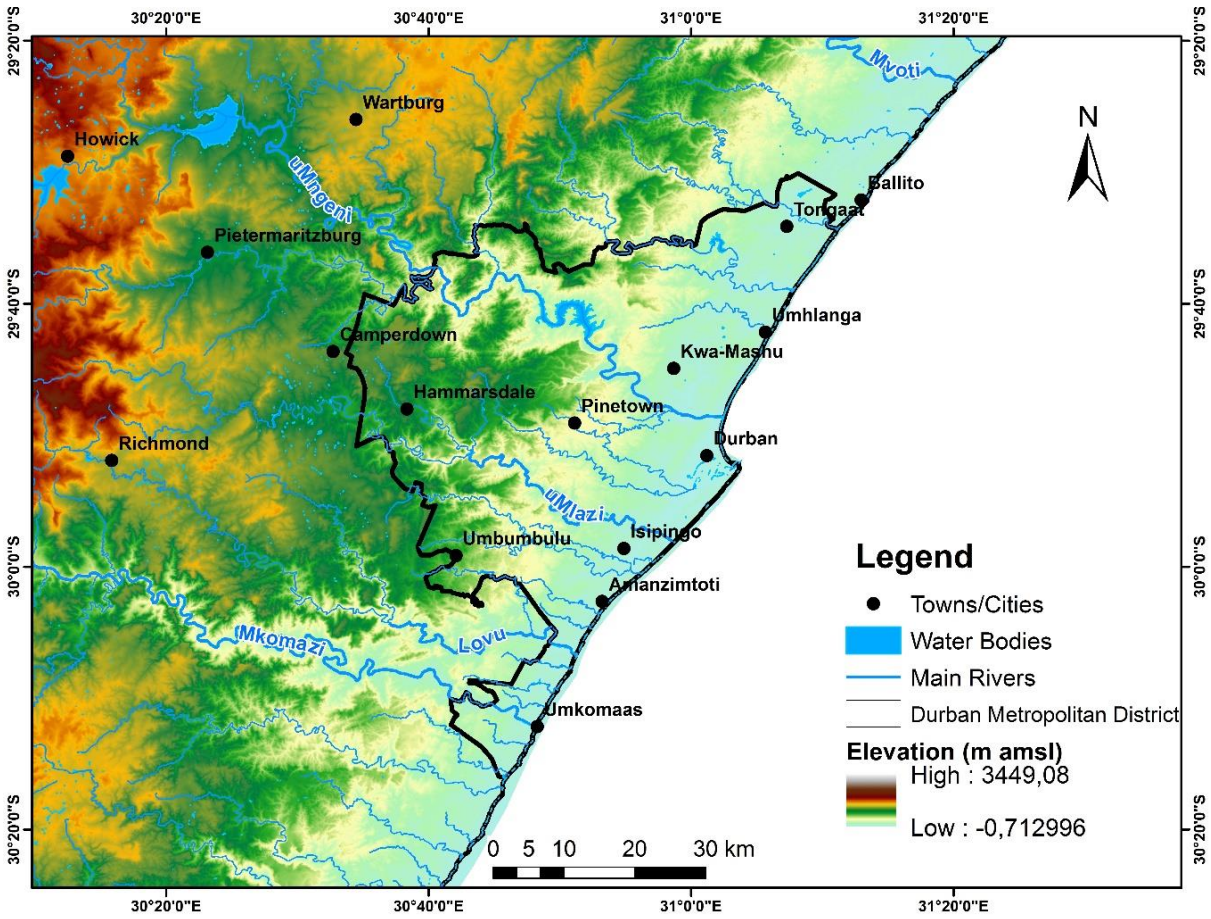

Figure 2.3: Topographical and Drainage Map of eThekwini Municipality, South Africa (data sourced from DWS, 2017).

Agricultural land use is primarily of sugar cane farming (Figure 2.4). These land use activities control the amount of water that infiltrates the ground to recharge groundwater. The species rich natural vegetation consists of grasslands, savannas, forests thickets and wetlands (Figure 2.4). The land use activities are incorporated into the water budget studies, as they have the ability to alter the water budget, soil properties, surface and groundwater chemistry of the area.

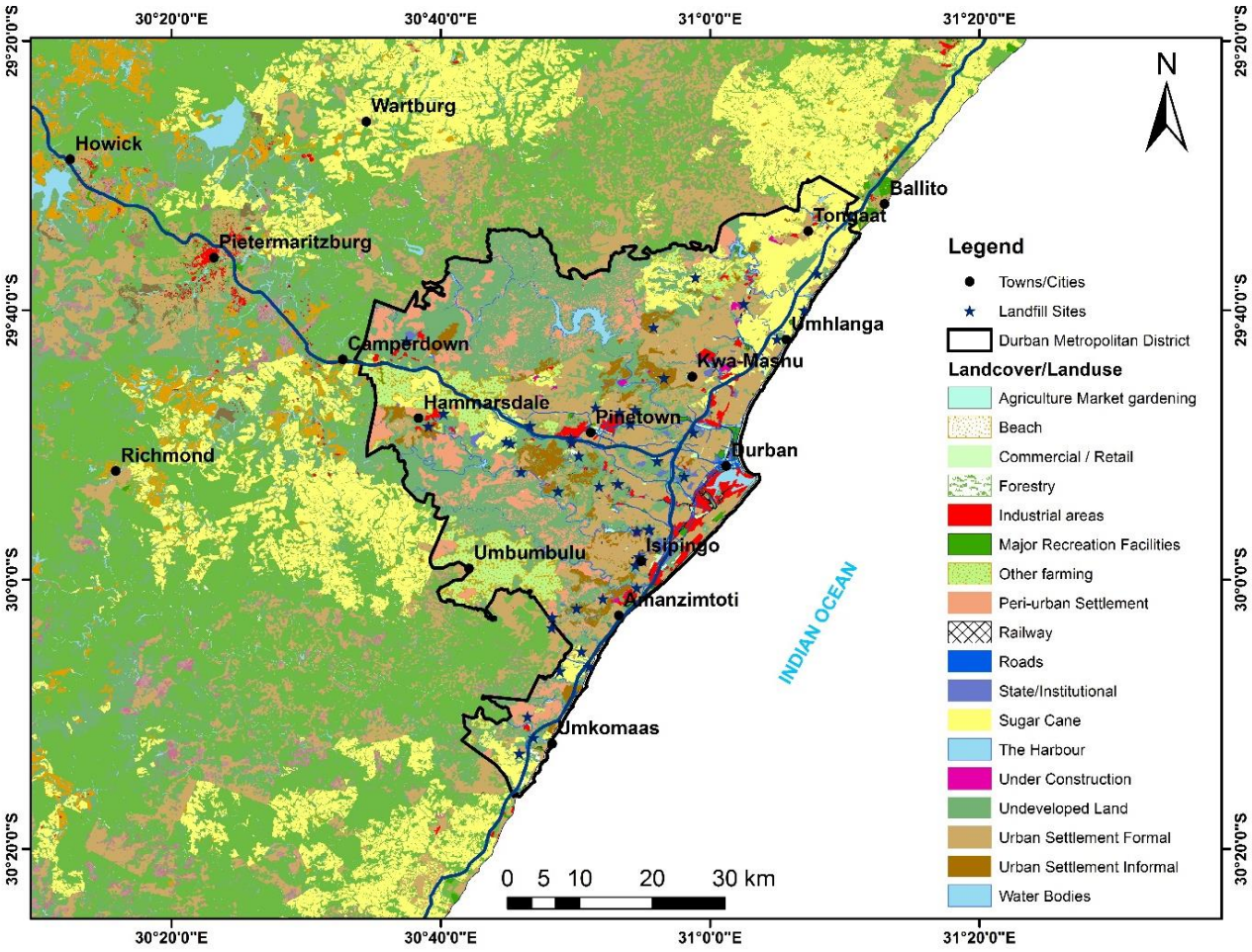

Figure 2.4: Land use and land cover map of the study area (KZN-PPC, 2016).

2.4. Geological Setting.

2.4.1 Regional Geology

The geological history of the Durban Metropolitan region extends back to approximately 1200 million years. The basement Natal Metamorphic Province (NMP) comprising of granite-gneisses uncorfomarbly overlain by the Ordovician-Silurian Natal Group which is made up of sandstones, siltstones and subordinate conglomerates. This is in turn overlain uncorfomably by the Lower Karoo sequence mainly the Dwyka and Ecca Groups. The Dwyka Group consist of diamictite and tillite, whereas the Ecca Group consist of shale, siltstone and sandstones. All these rocks are intruded by Jurassic Dolerite dykes and sills. The recent Tertiary-Quaternary aeolian beach deposits of the Maputaland Group forms the youngest rocks units completing the geological sequence of the Durban region (Figure 2.5).

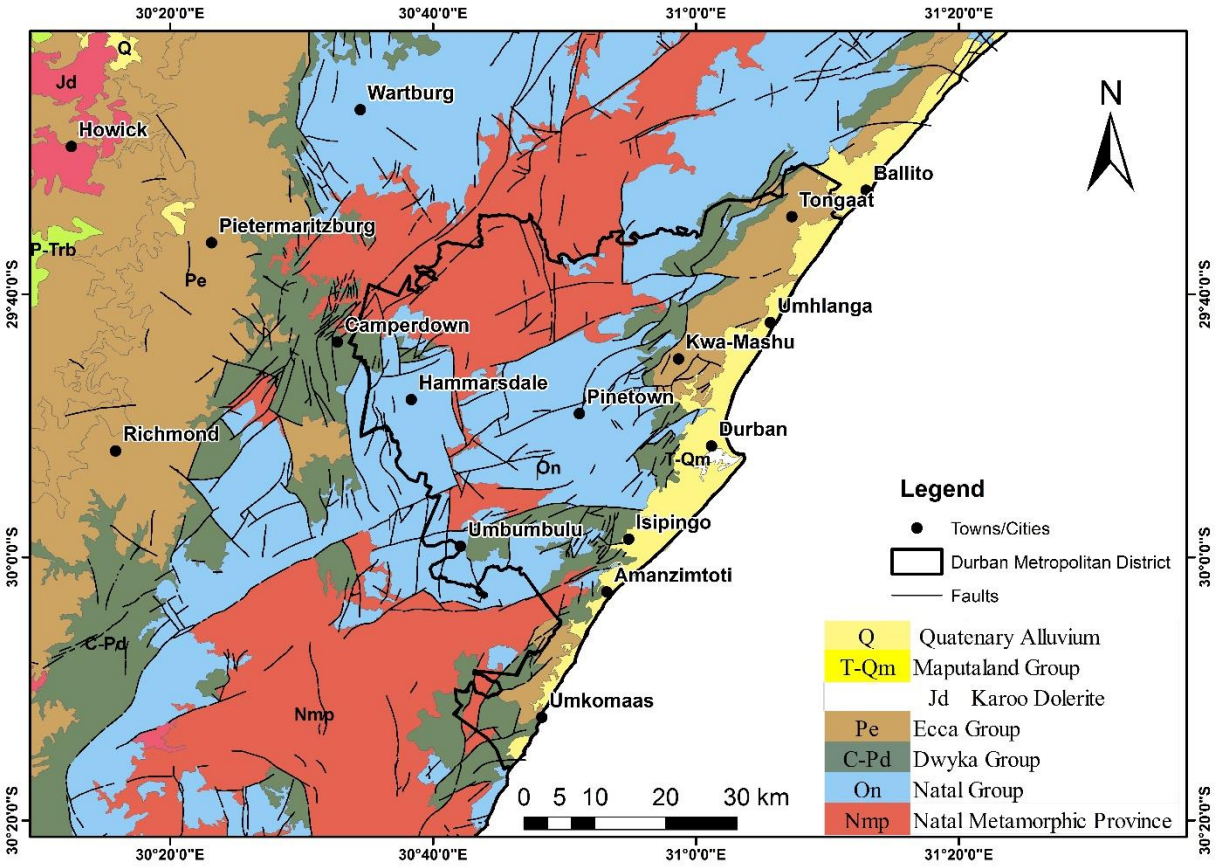

Figure 2.5: Geological map of Durban Metropolitan District (Source: Council for Geosciences, 1988a).

2.4.2. Detailed local geology of the Durban Metropolitan District and Surrounding areas.

Granitic Basement rocks of Natal Metamorphic Province

The Precambrian Natal sector of the Namaqua-Natal Province that forms the basement unit of study area is the Mzumbe Terrane comprising upper amphibolite facies of the Oribi Gorge Granitoid Suite. The Mzumbe Terrane is bounded in the north by the Lilani-Matigulu Shear Zone and in the south by the Mellville Thrust (Thomas, 1988). This terrane is made up of amphibolite grade supra crustal gneisses intruded by pre-, syn- and late tectonic granite suites. The older gniesses of the Mzumbe terrane collectively known as Mapumulo Group is subdivided into the Quha and Ndonyane Formation, with the former comprising grey biotite-hornblende-quartz gneiss and migmatite. The Ndonyane Formation is characterized by leucocratic gneisses with quartz-microcline assemblages (Cornell *et al*., 1996). The Mzumbe Terrane is also characterized in the

south by several suites of sheet-like, gneissic granites and granitoids (Thomas, 1988). These include Mkomazi, Mzimlilo and Mahlongwa Suites comprising coarse grained, megacrystic, garnet biotite orthogneisses, leocogranitic rocks (Evans *et al*., 1987; Thomas; 1990; Thomas, 1991; Clarke, 2008).

Natal Group

The Ordovician-Silurian Natal Group (Figure 2.6) unconformably overlying the granitoid rocks of the Natal Metamorphic Province comprises conglomerates, sandstones, siltstones and mudrocks which are divided into Marianhill and Durban Formations attaining a total thickness of approximately 200 m. The araneceous rocks are predominantly coarse to very coarse grained and comprise mainly subarkose and subordinate quartz arenite, with minor arkose and litharenite (Marshall, 2006).

Durban Formation

The Durban Formation is further subdivided into the Ulundi, Eshowe, Kranskloof, Situndu, Dassenhoek and Melmoth Members. The Ulundi Member predominantly comprises monomict boulder to pebble conglomerate with subordinate interbedded sandstone and mudrock. Overlying this unit is the Eshowe Member which is present throughout the basin comprising interbedded beds of mudrock and siltstone. The Kranskloof Member consists mainly of silicified quartz arenite and subarkose with subordinate interbedded mudrocks. The Situndu Member overlies the Kranskloof Member and consists of coarse arkosic pebbly sandstone with mudrock interbeds attaining a total thickness of about 84 m. The Dassenhoek Member forms the youngest unit of the Durban Formation and rests conformably on the Situndu Member occurring from just north of Verulam and Wartburg comprising silicified quartz arenite attaining a thickness of 42 m (Marshall, 2006)

Marianhill Formation

The Marianhill Formation is subdivided into Tulini, Newspaper and Westville Members. Tulini Member consists of matrix and clast supported conglomerate with interbedded coarse grained to very-coarse grained, subarkosic to arkosic sandstone and granite clast supported conglomerates with minor micaceous shale. The Tulini Member is conformably overlain by the Newspaper Member comprising feldspathic sandstone and subordinate granite clast conglomerate, siltstone and mudrock. The Westville Member forms the youngest unit of the Marianhill Formation resting

conformably on the Newspaper Member and is overlain by the Dwyka Group. This Member comprises of matrix-supported polymict conglomerate with clasts of quartz, chert and quartzite (Marshall, 2006).

Karoo Supergroup

The late Carboniferous to middle Jurassic Karoo Supergroup is subdivided into the Dwyka and Ecca Group rocks within the study area. The Dwyka Group (Figure 2.6) lies unconformably on the Natal Group and is predominantly composed of massive dark bluish grey tillite with abundant inclusion of older rock deposited during the permo-carboniferious glaciation (Johnson et al., 2006). The Elandsvei Formation of the Dwyka Group within the Durban Metropolitan region consists of diamictite with poorly to well defined bedding planes with alteration of diamictite, mudrock, sandstone and conglomerate beds in which Diamictite is the predominant constituent (Bell and Maud, 2000).

The Permain Ecca Group comprises the Pietermaritzburg and Vryheid Formations within the study area (Figure 2.6). The Pietermaritzburg Formation is the lower most unit of the Ecca Group and generally overlies the Dwyka Group with a sharp contact. It comprises dark silty mudrock, which coarsen upward with bioturbated deformed sandy and silty beds towards the top (Johnson et al., 2006). The Vryheid Formation is represented by alteration of bioturbated immature sand, dark siltstone and mudstone deposited in anoxic water of moderate depth. The coal seams that are hosted in this Formation originate as peat swamps developed on broad abandoned alluvial plains and less commonly in interfluves (Van Vuuren, 1981).

Maputaland Group

The Quaternary coastal deposits are the youngest within geological units in the study area. They are characterized by the Umkwelane, Kosi Bay, Isipingo, Sibayi and Berea Formations (Botha *et al*., 2003). The Pleistocene Berea Formation, the weathered product of the Bluff Formation, forms part of the coastal dune deposited unconformably on the Ecca Group to a considerable distance inland and is a result of marine transgression. The Berea Formation occupies the upper inner part of the Durban Bluff, as well as the Berea Ridge which runs parallel to the coast immediately to the west of the central city and harbor area (Bell and Maud, 2000). The Isipingo Formation is the rocky shoreline along the Bluff in Durban. This late middle Pleistocene to Holocene Formation

incorporates basal aeolianites truncated locally by the late interglacial age calcified beach and dune deposits at 4-5 m above mean sea level (Ramsay and Cooper, 2002). The Isipingo Formation replaces the poorly constrained Bluff Formation and can be subdivided into genetically significant shallow marine, beach and various dune lithological units recording sea level changes. These cemented deposits are readily distinguished from the non-calcareous Kosi Bay Formation sands in areas where they occur in close proximity (Maud, 1986). The Isipingo Formation extends to a depth of about 100m below present sea level at the northern end of the Durban Bluff, while towards its southern end at Umlazi Canal outfall occur within aeolianite succession at a depth of 37 m below sea level (Ramsay *et al*., 1993).

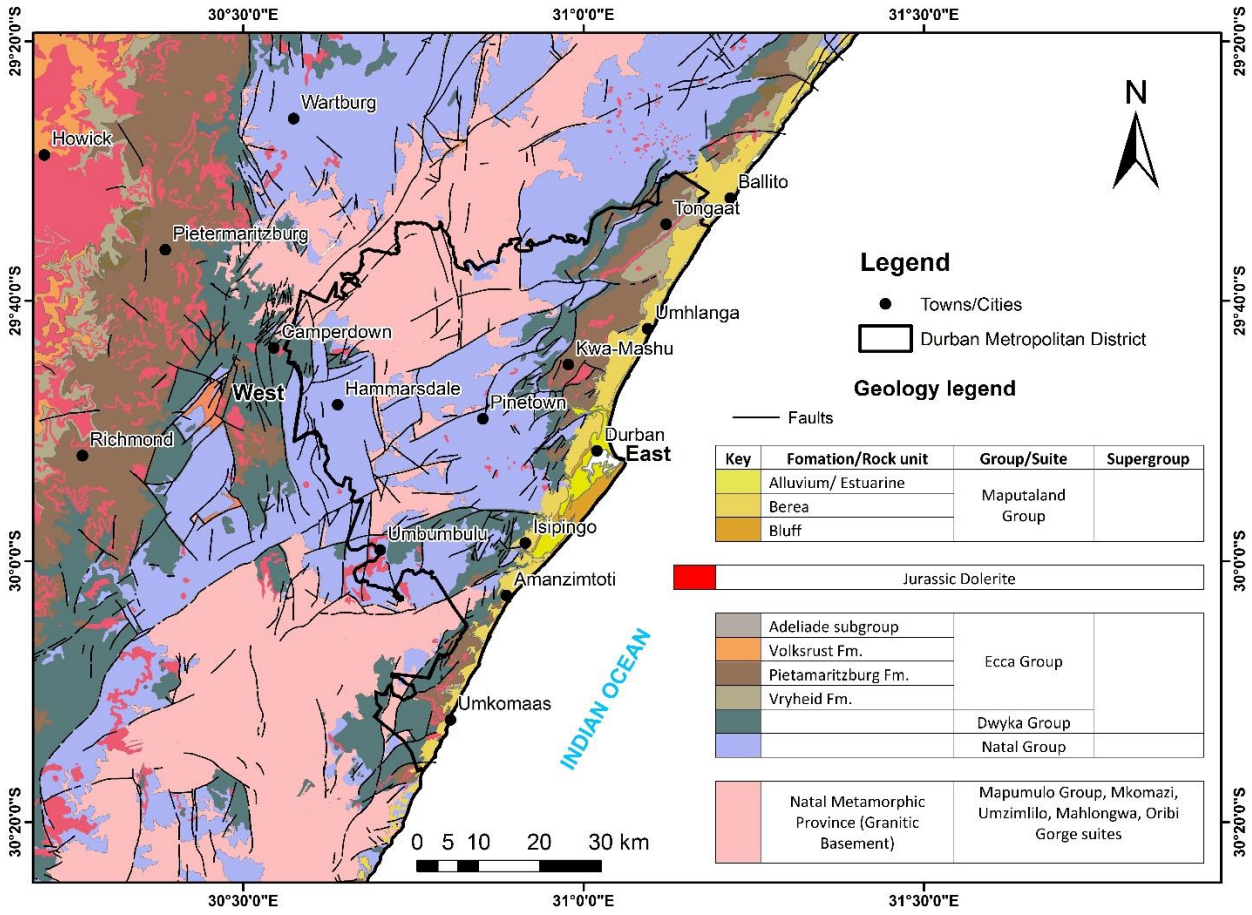

Figure. 2.6: Detailed geology map of the Dubarn District Municipality and surrounding areas (Source: Council for geoscience, 1988a,b and 2015)

2.5. Hydrogeological Setting

The hydrogeological setting of the Durban Metropolitan region comprises three modes of groundwater occurrence (Figure 2.7). These are (King, 2002):

- Intergranular aquifers of the Maputaland Group coastal deposits.
- Fractured aquifers of the Natal Group and Dwyka Group
- Weathered and fractured aquifers represented by the basement crystalline rocks of the Natal Metamorphic Province, lower Karoo Supergroup sedimentary rocks, and the Karoo dolerite intrusions.

2.5.1. Intergranular Aquifers

Intergranular aquifers occur in the unconsolidated coastal deposits of the Maputaland Group (Figure 2.7). This sedimentary sequence, formed during the marine regressions and transgression, which created unconsolidated formations. The Maputaland Group contains quaternary sediments which form primary aquifers in KwaZulu-Natal Province (Kelbe *et al*., 2013). The Berea Formation, often found on dune ridges, is the weathered components of dune sands which contains fine grained material. The groundwater potential in these sands is low due to the elevated positions they are found in, but in places where the dune overlies the bedrock at shallow depths, groundwater can be encountered at the contact. Average hydraulic conductivities of 5 m/day, specific yield values of approximately 0.18 and borehole yields in excess of 50 l/s have been reported (King, 2002). Groundwater levels are generally shallow, usually between 2 and 7 m below ground level. The quality of groundwater in this aquifer is influenced by the sedimentary depositional environment, proximity to the coast and industrial activities. This has resulted into increase in the electrical conductivities that are higher than the surrounding aquifers averaging 1000 µS/cm.

2.5.2. Fractured Aquifers

The Natal Group sandstones and Msikaba Formation are one of the best hydrolithological prospects for groundwater in KwaZulu-Natal compared to other units (Demlie and Titus, 2015). The average porosity of the Natal Group sandstones ranges between 9.0 and 16.9% (Van Wyk, 1963). According to Demlie and Titus (2015), this may be attributed to the presence of extensive faulting and fracturing which provided favorable conditions for storage and movement of groundwater. The borehole yields of the Natal Group sandstones range from 0.2 to 2.0 L/s. High

yielding boreholes are associated with a network of intersecting fractures and faults. Bedding planes and joints contribute to the occurrence of groundwater in these Formations (Bell and Maud, 2000). The range of known hydraulic conductivities is from 0.4 - 7.7 m/day and an estimated storativity of 0.0005. The quality of groundwater is usually very good with less than 70 mS/m of electrical conductivity unless polluted (King, 2002).

The Dwyka Group diamictite and shale have very low hydraulic conductivities and virtually no primary voids. The Dwyka Group constitutes a very low-yielding fractured aquifer and water is confined within narrow discontinuities like jointing and fracturing. Therefore, the Dwyka Group tend to form aquitards rather than aquifers (Bell and Maud, 2000). The porosity of the Dwyka Group determined by Van Wyk (1963) ranges between 0.5– 13%, The Dwyka Group is characterized by borehole yields of between 0.2 – 0.25 L/s with the most favorable borehole yields found in the tillite at low-lying sites on faults and major joints. The contact between the Dwyka Group and the underlying Natal Group has been found to be a high yielding aquifer with a transmissivity of 30 m^2/day (King, 2002).

2.5.3. Weathered and Fractured aquifers.

The Basement granitic rocks of the Mapumulo Group, Oribi Gorge and Mkomazi Suites have groundwater stored in fractures and near surfaces in weathered zones. Weathering of these rocks results into a material with high porosity but low hydraulic conductivity due to clay content from feldspars (King, 1997). The borehole yields in the intergranular zone are between 0.1 and 0.5 L/s, whereas in the underlying factures have yields greater than 0.5 L/s. Rowsell and de Swardt (1976) reported that the permeabilities of Ecca Group sandstones are usually very low. The main reason is that the sandstones are usually poorly sorted, and that their primary porosities have been lowered considerably by diagenesis. However, the Vryheid Formation sandstones in KwaZulu-Natal appear to be more permeable, with an average borehole yield of 0.33 ℓ/s and with 62% boreholes yielding greater than 1 ℓ/s.

Karoo Dolerite dykes are vertical to sub-vertical discontinuities that, in general, represent thin, linear zones of relatively higher permeability which act as conduits for groundwater flow within the aquifer. They may also act as semi- to impermeable barriers to the movement of groundwater. Van Wyk (1963) reported that more than 80% of the successful boreholes (> 0.13 ℓ/s) drilled into Karoo sediments are directly or indirectly related to dolerite intrusions. High permeability of the

dyke contact zones is a result of shrinkage joints developed during cooling of the intrusion (Van Wyk, 1963). Groundwater in these units is contained in intergranular interstices in the saturated weathered zone as well as in joints and fractures. The borehole yields range from 0.5-2.0 ℓ/s, hydraulic conductivities range between 0.05 and 0.5 m/day and storativity vary between $1x10^{-4}$ and $1x10^{-3}$ (Van Wyk, 1963).

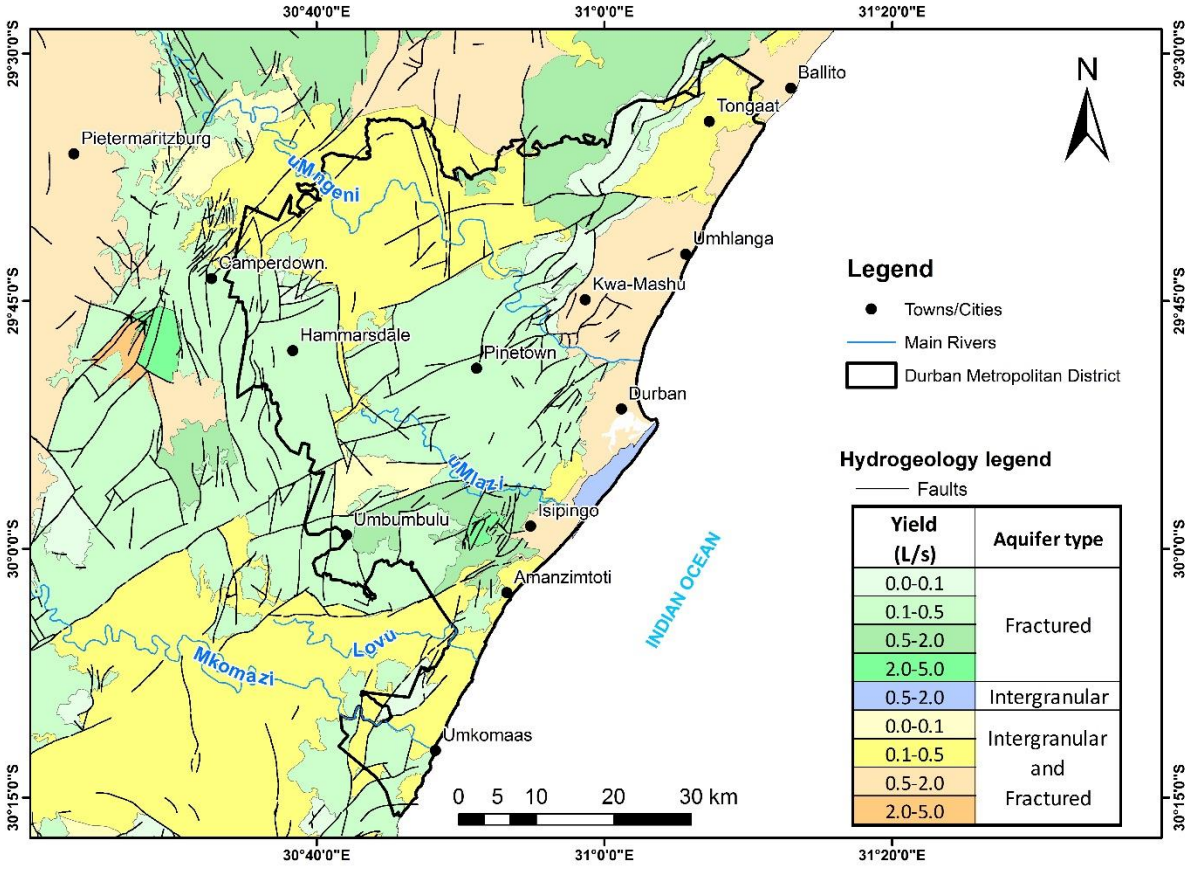

Figure 2.7: Hydrogeological map of Durban Metropolitan District showing borehole yields for different aquifer types (Source: DWAF, 1998).

CHAPTER 3

LITERATURE REVIEW

This research aims to contribute towards an improved understanding of the complex hydrogeology of the Durban Metropolitan Region through literature review, collection of existing data and by newly generated data. The collected data was collated and interpreted to characterize the aquifers in the region and to develop a conceptual hydrogeological model. A hydrogeological model is a simplified representation of the complex hydrogeological system by summarizing what is known about the hydrogeology in the form of written text, 2D and 3D graphs, cross-sections and tables (Wang and Anderson, 1982). The conceptual model expresses the past and current state of the system. The purpose of modelling is to understand the state of the hydrogeological system. Conceptual models provide a framework for designing numerical groundwater flow models that are capable of predicting the effect of some future actions or a change on the hydrological system (Anderson *et al*., 2015).

3.1. Hydrogeological conceptual modelling.

A conceptual model is a simplified method of representing how and why a hydrological system behaves in a particular manner and it is an effective way of representing the interaction between groundwater and surface water across landscapes. A conceptual model is usually built for a site-specific hydrogeological setting but can also be constructed using generic geological settings (Winter, 2001). The level of detail of a model is determined by the modelling purpose, the available field data and the practical limits. Defining the purpose of the model, which could include, amongst other, several purposes is the prediction of changes in groundwater flow direction due to abstraction, spread of contaminants from the source of pollution or changes in groundwater chemistry along flow paths. Defining the purpose of the model makes it possible to determine the governing equations (Anderson and Woessner, 1992). Anderson *et al*. (2015), defined a conceptual model to be a qualitative representation of a groundwater system that conforms to hydrogeological principles and is based on geological, geophysical, hydrological, hydro-geochemical and other Ancillary information. According to Kolm (1996), a conceptual model should consider nine aspects: geomorphology, geology, geophysics, climate, vegetation, soils, hydrology, hydrochemistry and anthropogenic aspects.

In developing a conceptual model, the modeler organizes, analyzes, and synthesizes relevant hydrogeological data often with a help of a database tool such as a Geographic Information System (GIS). Key components of a conceptual model include boundaries, hydrostratigraphy and estimates of hydrogeological parameters including water budget such as water sources (recharge rates), discharge rates (abstraction) and general groundwater flow directions (Anderson *et al*., 2015). These components of the conceptual model are discussed in the following sections.

3.1.1. Components of a conceptual model

Model Boundaries

Boundary conditions are key components of a mathematical model and strongly influence the flow directions calculated by a steady-state numerical model and most transient models. Boundaries include hydraulic features such as groundwater divides and physical features such as surface water bodies and relatively impermeably rocks (Anderson *et al*., 2015). Water table usually forms the upper boundary of a three-dimensional numerical model. Bottom and lateral boundaries should be aligned with physical or hydraulic features that are stable or do not change with changing hydrologic conditions. These include relatively stable groundwater divides; the ocean and stable saltwater-freshwater interface in a coastal aquifer; large lakes and rivers that are interconnected to groundwater system, relatively impermeable rocks and fault zones.

According to Winter *et al*. (2003), boundaries are classified from topographic, potentiometric and geologic maps of the region. There are three main types of boundaries, namely; Type 1 or Dirichlet boundary condition (constant heady boundary), type 2 or Neuman boundary condition (specified flux boundary) and Type 3 or Cauchy (specified head and gradient) boundary conditions (Barnett *et al*., 2012).

Hydrostratigraphy and hydrogeological properties

Traditionally, a groundwater system is characterized as an aquifer or sequence of aquifers and confining beds. According to Kresic and Mikszewski (2013), an aquifer is a "geological unit, or series of hydraulically connected geological units, that stores and transmits significant amounts of groundwater." Hydrostratigraphic units are defined based on the nature and connectivity of the openings in the rocks, which determines transmission and storage properties. Information on depositional setting, geologic history, and generalization about hydraulic properties of

hydrostratigraphic units should be included in a conceptual model. This will be useful in determining parameter values for the conceptual and numerical model. Thickness of hydrostratigraphic units can be determined from isopach maps or borehole logs (Lunt and Bridge, 2004). The hydraulic properties, including hydraulic conductivity, transmissivity and storativity of a hydrologic unit can be determined through the use of pumping tests data. Natural heterogeneous systems are generally represented by homogeneous models assuming isotropic conditions for hydrostratigraphic units, consequently producing less accurate results, are considered in modelling (Butler and Liu, 1991).

Groundwater sources and flow directions

According to Anderson et al. (2015), groundwater flow directions are determined from contour maps of the water table and the potentiometric surface, from areas of recharge to areas of discharge. The flow path direction is affected by anisotropy. Long-term monitored groundwater level data should be included in the development of a conceptual model, so as to identify whether a transient or steady state model is needed to address the modelling objective (Taylor and Alley, 2002). Groundwater sources should be identified and described using chemical constituents of groundwater, including environmental isotopes. The common source of groundwater is precipitation which infiltrates the land surface and becomes groundwater recharge. Other forms of recharge include, runoff from hill slopes and seepage of surface water. In urban areas, recharge can come from storm drainage and leakage of sewerage pipes.

Groundwater budget components.

Estimates of groundwater budget components should be part of every conceptual model to provide an initial understanding of model inflows and outflows. Groundwater budget is developed for the area represented by the conceptual model and for a specified period in order to help evaluate how all the components and processes of the groundwater system interact. Generally conceptual models often rely on reasonable estimates of water budget components. Hydrologic budget parameters include precipitation, evaporation, evapotranspiration, and surface water flows and groundwater inflows such as recharge from precipitation or other sources, seepage from surface water bodies, recharge from irrigation and from storm water in urban areas. Groundwater outflow includes groundwater discharge to surface water bodies, evapotranspiration, pumping, spring flows and discharge through seepage and groundwater abstraction (Alley *et al*., 1999).

3.2. Water Budget

Water budget forms the basis of investigating a hydrogeology system and is used to predict changes in a system. It is used to quantify the flow of water in and out of a system by using directly measured and estimated parameters, such as recharge, evaporation, evapotranspiration, precipitation, runoff, base flow, abstraction rate and the change in storage (Fetter, 2001; Betts, 2004). It is essential to consider the surface and subsurface hydrogeological boundaries in the evaluation of the water budget and ascertain an understanding of the relationships between various components of the environment, i.e. water and solid earth materials present (Fetter, 2001). According to Conrad *et al.* (2004), recharge quantification is a critical step in the development of a conceptual model and a requirement for the sustainable use and management of groundwater resources.

3.2.1 Groundwater recharge estimation

Groundwater recharge is defined as an addition of water to a groundwater reservoir and can be distinguished into four main domains, downward flow of water through the unsaturated zone reaching the water table, lateral and/or vertical inter-aquifer flow, induced recharge from nearby surface water bodies and, artificial recharge such as from borehole injection or man-made infiltration ponds (Xu and Beekman, 2003).

Direct recharge in urban areas takes place by percolation in unpaved areas, and to a lesser extent through paved surfaces which are not always fully impervious. Direct recharge can be estimated by assessing the amount of pervious cover in the city. Precipitation and potential evapotranspiration data are transformed into effective precipitation with a daily soil moisture balance (Lerner *et al.*, 1993). This method uses root constants and wilting points to account for different crops and soil types. According to Lerner (2002), a proportion of the impervious surface should be treated as permeable.

Indirect recharge is the sum of the recharge coming from seepage out of surface water bodies, leakage from water mains, wastewater, and storm sewers, and onsite sanitation systems. A simple way to assess the water available for recharge is to make a balance of water served versus the waste water treated. The most efficient cities report losses to leakage of 10%. In arid areas, the amount of water distributed in a city is often significantly greater than rainfall (Foster *et al.*, 1994). Thus,

the mains leakage is a considerable source of indirect groundwater recharge. Localized recharge takes place through faults and fractures and depends mainly on the geologic formation characteristics and structures, as well as soil types in each area.

In urban areas, natural groundwater recharge can be inhibited by impervious cover which enhances runoff and limits infiltration (Leopold, 1968; Coldwey and Meber, 1997). However, urban development introduces new sources of recharge; leakage from water and wastewater collection and distribution system, leaks from storm water sewers and return flow from irrigation of parks, and golf courses (Lerner, 1986). Thus, quantifying recharge in urban areas becomes challenging due to the complex urban environment as a result of the heterogeneity of shallow aquifers, and the variety of land-uses that coexist and overlap. The uncertainties in quantifying different sources of groundwater recharge and discharge makes it desirable to estimate water balances based on the amount of groundwater abstractions, imports, water use and wastewater outflows (Garcia-Fresca, 2004). Barrett et al. (1999) summarized sources and pathways of urban recharge (Figure 3.1)

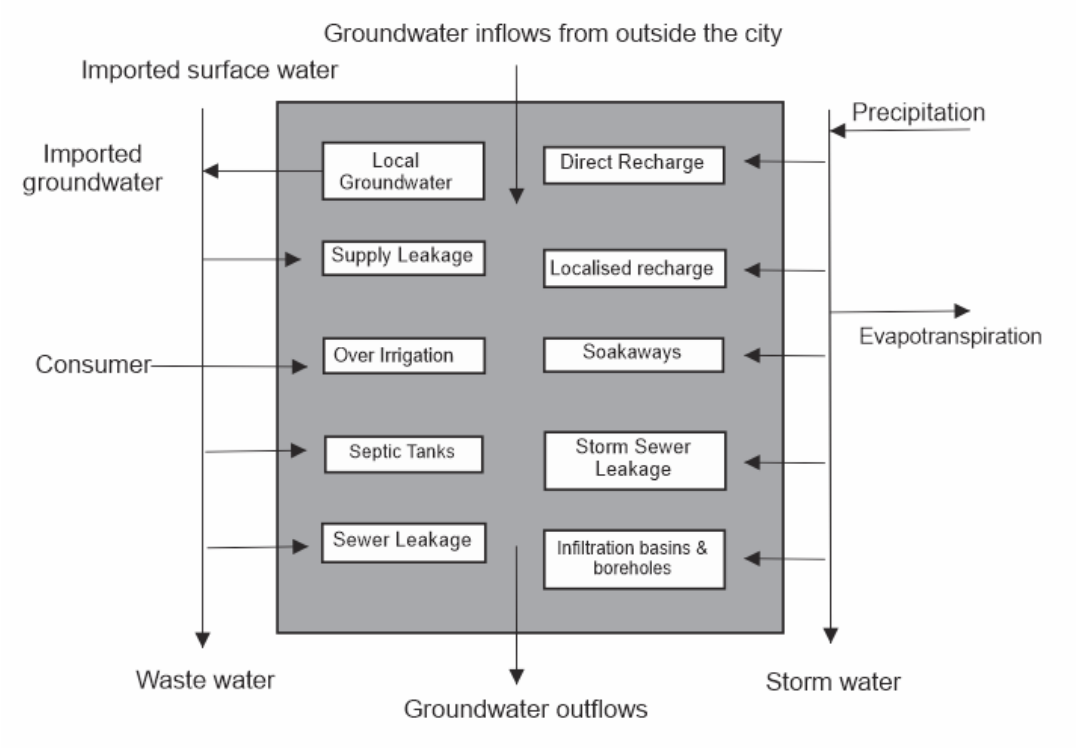

Figure 3.1: Urban recharge sources and pathways (Barrett et al., 1999).

Water directly applied to parks and lawns in excess of their plant requirement will percolate and recharge the groundwater, which is known as irrigation return flow. This source of recharge is significant in arid and semi-arid climates. Recharge from excess irrigation can be quantified following mass balancing approaches by considering water supply, water use, the physical properties of the soils, and evapotranspiration (Berg *et al*., 1996). Determination of groundwater recharge in arid and semi-arid areas is quite challenging as a consequence of the time variability of precipitation in arid and semi-arid climates, and spatial variability in soil characteristics, topography, vegetation and land uses (Lerner *et al.*, 1990). Furthermore, recharge results are normally small in comparison to the resolution of the estimation method. According to Scanlon *et al*. (2002), the objective of recharge study should be known prior to the selection of the appropriate method for quantifying groundwater recharge as it may dictate the required space and time scales of the recharge estimate.

Developing a recharge conceptual model should be preceded by selection of appropriate recharge estimation method in order to reduce the uncertainty of quantifying recharge. A recharge model needs to describe the location, timing, and probable mechanism of recharge and provide initial estimates based on climatic, topographic, land use and land cover, soil and vegetation types. Commonly used groundwater recharge estimation method in semi-arid Southern Africa include, but not limited to; Chloride Mass Balance (CMB), Water Table Fluctuation (WTF), Cumulative Rainfall departure (CRD) and Saturated Volume Fluctuation (SVF). Van Tonder and Xu (2000) developed an excel based spreadsheet recharge estimation model, while Beekman *et al*. (1999) developed combined chemical mass balance approach on moisture and groundwater using the CMB method and groundwater dating method using ^{14}C.

Chloride Mass Balance (CMB)

The environmental tracer chloride (Cl^-) has been extensively applied in estimation of groundwater recharge. The CMB method developed by Eriksson and Khunakasem (1969) is simple, inexpensive and the most universal method for recharge estimation in semi-arid regions. It is based on the assumption of conservation of mass between the input of the atmospheric chloride and the chloride flux in the subsurface. It is used for estimating moisture flux in the unsaturated zone by means of a profiling technique when diffuse flow is assumed. CMB based recharge mechanism can also be used in the assessment of vulnerability of groundwater resources to pollution. A site-

specific moisture flux can be calculated for the unsaturated zone based on a steady state chloride flux at the surface and the chloride flux beneath an upper zone where evapotranspiration and mixing of rainfall takes place using the relationship of equation 3.1(Eriksson and Khunakasem, 1969):

$$R_{sm}\frac{P*Cl_p}{Cl_{sm}} = \frac{TD}{Cl_{sm}} \qquad (3.1)$$

Where R_{sm} is the moisture flux (mm/yr), P is the mean annual rainfall (mm/yr), Cl_p and Cl_{sm} are chloride concentration in rainfall and soil moisture (mg/l), respectively and D is dry chloride deposition ($mgm^{-2}yr^{-1}$). Therefore, $P*Cl_p$ and D is referred to as "Total chloride atmospheric Deposition" (TD) originating from precipitation and dry fall out.

According to Allison *et al*. (1984), the chloride concentration increases relative to the amount of rainwater as a result of interception, soil evaporation and root water uptake by vegetation. Hence, vegetation cover is important in assessing the recharge potential at a site. When CMB method is applied, the following assumptions are made (Allison *et al*., 1984):

- The chloride ion behaves conservatively, i.e. it is not taken up by or leached from vegetation, aquifer formations and unsaturated zone sediments,
- Atmospheric input of chloride consisting wet and dry deposition is normally considered to be constant with time over longer periods,
- A piston flow regime is assumed but can be invalidated by complex transport of moisture vertically and horizontally and this may occur in unsaturated zones as a result of variability in rainfall and evapotranspiration or uneven topography.

Limitations arising with the application of chloride as a tracer in the unsaturated zone includes (Allison *et al*., 1984):

- When recharge rate is based on tracer estimates in the root zone, tracer techniques can over estimate recharge, unless the tracer has move below the root zone.
- Plant tissues contain a significant amount of chloride and upon decay may release it.
- Mineralogical composition of sediments can contribute chloride to the soil water or groundwater through dissolution and weathering of disruptive evaporite minerals

- Input from agricultural activities may contribute chloride and affect the mass-balance approach.

3.2.2. Evapotranspiration

Evapotranspiration (ET) refers to the loss of water to the atmosphere by the combined processes of evaporation from the soil surface and transpiration from plants (Zhang *et al*., 1999). Evapotranspiration is one of the major hydrological components during the water budget calculation and is indispensable for the calculation of a reliable recharge and evaporation losses when groundwater flow analysis is undertaken. Thus, reliable and consistent estimation of evapotranspiration is of great importance for the effective management of water resources. The quantification of referable reference evapotranspiration (ET_o) is necessary in the context of many issues, i.e. crop production, management of water resources, scheduling of irrigation, evaluation of the effects of changing land use on water yields and environmental assessment (Allen *et al*., 1998). Widely used evapotranspiration estimation methods include, but not limited to, Thornthwaite, Penman-Monteith, Hargreaves and Hamon methods.

3.2.2.1. Thornthwaite Method

The Thornthwaite method (Thornthwaite, 1948; Mather, 1978; 1979) is generally used in humid regions where air temperature is the only input data. The Thornthwaite monthly (ETo) is determined with the equation proposed by Thornthwaite (1948) for a standard month of 30 days and days with 12 hour photoperiod, by using the monthly mean temperature as follows:

$$ETm = 16Nm\,(10/I)^{a}, \quad 0℃ \le T \le 26℃ \tag{3.2}$$

$$I = \sum_{n=1}^{12}(0.2T)^{1.514}\ ,\ T > 0℃ \tag{3.3}$$

$$a = 6.75 \times 10^{-7}I^{3} - 7.71 \times 10^{-5}\,I^{2} + 1.7912 \times 10^{-2}I + 0.49239 \tag{3.4}$$

Where, ET_m is the monthly ETo in mm/month; Nm is the latitude correction factor; I is the thermal index; a is the exponent of Equation (3.2) and T is the monthly mean temperature in °C. This method underestimates monthly ETo under dry and arid climates because the equation does not consider the saturation vapor deficit of the air (Pelton *et al*., 1960; Pruitt, 1964; Doorenbos and Pruitt, 1977).

3.2.2.2. Penman-Monteith Method.

The Penman-Monteith Method requires a range of climatic data for an area and is recommended as the standard method for accurately estimating the reference evapotranspiration across a range of climatic conditions (Allen *et al*., 1998). This method is based on several inputs, including the average monthly precipitation, temperature, humidity, and wind speed. This method requires the quantification of various parameters and is given by (Allen et al., 1998):

$$ETo = \frac{0.408\Delta(R_n - G) + \gamma \frac{900}{T+273} u_2 (e_s - e_a)}{\Delta + \gamma\,(1 + 0.34U_2)} \quad (3.5)$$

Where, ETo is the reference evapotranspiration [mm day^{-1}], Rn the net radiation at the crop surface [MJ/m^2 day^{-1}], G the soil heat flux density [MJ m^{-2} day^{-1}], T represents the mean daily air temperature at 2 m height [°C], U_2 is the wind speed at 2 m height [m s^{-1}], e_s is the saturation vapour pressure [kPa], e_a is the actual vapour pressure [kPa], e_s-e_a is the saturation vapour pressure deficit [kPa], Δ is the slope of the vapour pressure curve [kPa °C-1] and γ is the psychometric constant [kPa°C^{-1}]. The reference crop evapotranspiration represents the evapotranspiration from a standardized vegetated surface.

3.2.3. Runoff

Runoff is an important component of water balance whereby excess precipitation flows on the surface along streams, and rivers. The magnitude of runoff varies on the basis of precipitation and land surface and is heavily influenced by vegetation, soil type and degree of disturbance, catchment slope and the number and nature of watercourses in the catchment. Tripathi and Singh (1998) conducted studies on small basins in India and developed the following relationship for the estimation of Peak discharge:

$$Q = 1/360\ CI_rA_{ha} \quad (3.6)$$

Where Q is the peak rate of runoff (m^3/s) for given rainfall frequency; C is the runoff coefficient; A_{ah} is the area of the basin [ha]; and I_r is the intensity of rainfall [mm/h] for the design frequency for duration equal to the time of concentration. Equation 3.6 was modified to take monthly precipitation into account, and to determine the monthly runoff rate. Thus providing:

$$q_{(t)} = 1/360\ CP_{(t)} \quad (3.7)$$

Where q is the runoff rate (mm), C is the runoff coefficient, and P is the precipitation (mm), for a given time (t).

In view of the numerous variables and uncertainties governing surface runoff estimation, conceptual models are useful approaches of analysis (Beven, 1983; McCuen, 2003). However, these models must be calibrated and verified using field measurements. Among the lumped parameter models used for predicting surface runoff in agricultural watersheds, the curve number (CN) method (USDA, 1986) is widely used method due to its simplicity and limited number of parameters required for runoff estimation (Bhuyan *et al*., 2003). The SCS Runoff Curve Number method is given by (SCS, 1986);

$$Q = \frac{(P - 0.1S)^2}{(P - 0.8S)} \quad (3.8)$$

Where; Q is the runoff (mm), P is the rainfall (mm), S is the potential maximum retention after runoff begin (mm) and I_a is the initial abstraction. Initial abstraction (I_a) is all losses before runoff begins, It includes water retained in surface depression, water intercepted by vegetation and infiltration where S is related to the soil and cover conditions of the water shed through CN. With CN ranging from 0 to 100 and is related to CN by:

$$S = \frac{25400}{CN} - 245 \quad (3.9)$$

The major factors considered in determining runoff curve numbers are the hydrologic soil group (HSG), type of land cover, hydrologic condition and antecedent moisture condition.

3.3. Ancillary Information for Conceptual model development

Ancillary information includes data such as water chemistry, geophysical data, soils and land uses, which are helpful in developing a conceptual model. Chemical analysis of water samples includes concentrations of major cations (Ca^{2+}, Mg^{2+}, Na^{+}, and K^{+}) and anions (SO_4^{-2}, HCO_3^{-}, Cl), specific electrical conductivity (EC), total dissolved solids, dissolved oxygen, temperature, and pH. Chemical analysis may also include trace metals, stable and radiogenic isotopes, and organic compounds. Water chemistry helps in identifying groundwater of similar geochemical composition, groundwater recharge sources and assist in the identification of groundwater flow directions. Environmental and artificial tracers are useful for identifying groundwater flow paths (Roy *et al*., 2014). Isotopic data gives insight on sources of recharge, age and direction of

groundwater flow and interaction with surface waters (Hunt *et al*., 2006). According to Hunt *et al*. (2005); Cook *et al*. (2006) environmental isotopic analysis including tritium, stable isotopes of oxygen, hydrogen and strontium which assist in identifying sources, amount of recharge and groundwater flow rates. The procedure and type of data needed to develop both hydrogeological conceptual and numerical groundwater flow model is summarized in Figure 3.2.

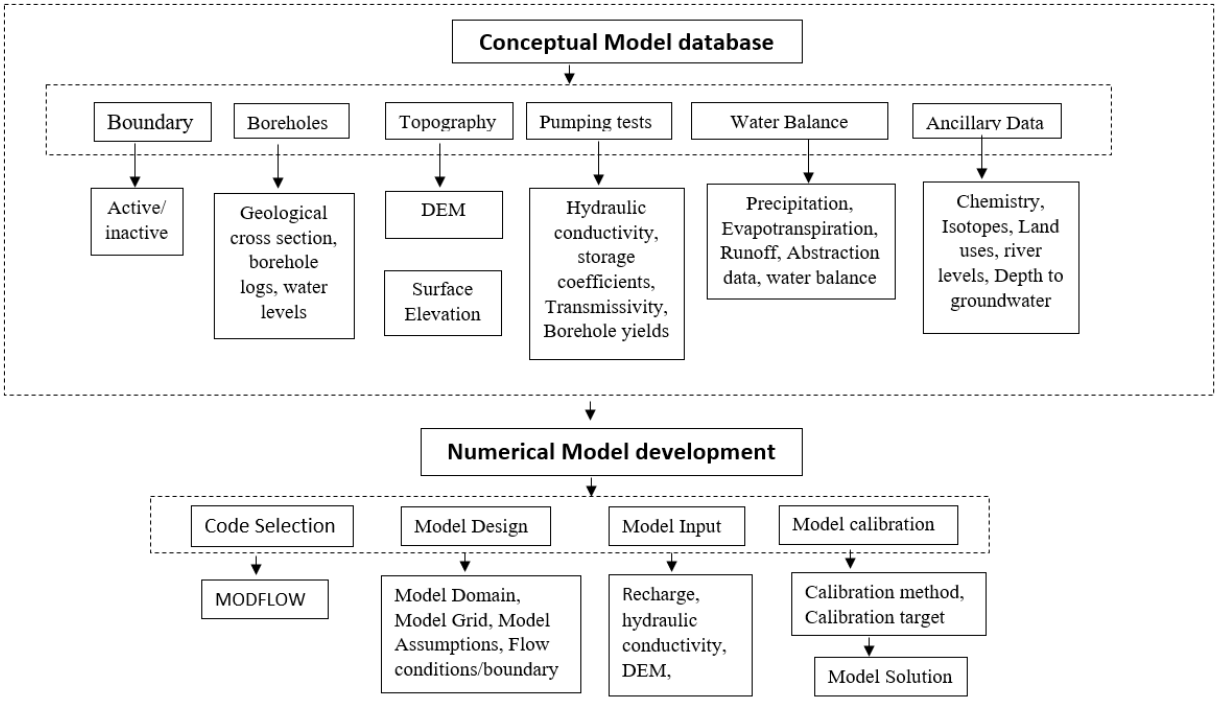

Figure 3.2: Procedure and data required in groundwater modelling (modified after Del Bon *et al*., 2015).

3.3.1 Hydrochemistry Chemical composition of natural waters

Hydrogeochemical processes and hydro-geochemistry of groundwater vary spatially and temporally, depending on the geology and chemical characteristics of the aquifer. Fresh groundwater flowing through different aquifers may be identified and differentiated by their characteristic salinity levels and ionic ratios (Rosenthal, 1987). A number of factors influences the chemical composition of groundwater. These include the mineralogy of the rock type forming catchments or aquifers, overlying land uses, proximity to the coast, recharge source, soil type, aquifer structure and the age of water itself.

Major changes in groundwater quality first occur in the soil or saturated zone above the water table and are driven by biochemical processes (Freeze and Cherry, 1979). The soil's influence is more apparent on groundwater recharged by vertically infiltrating rainwater. Its effect may be less important where river recharge is dominant, and the influence of the organic rich soil horizon is less. The soil zone represents a thin layer within the water cycle highly influencing the chemistry of the surrounding groundwater due its unique ability to generate carbonic acid (H_2CO_2) formed by the mixing of water and carbon dioxide (CO_2). According to Freeze and Cherry (1979), carbon dioxide is more abundant in the soil layer than anywhere else in the travel path of groundwater.

The chemical composition of groundwater evolves during regional flow due to hydrochemical reactions along flow paths. This evolution can be generalized by considering the water types that are typically found in different zones of groundwater flow systems. Weathering, ion exchange, salt dissolution, and saline water encroachment tend to cause water to evolve from a dilute calcium carbonate type in recharge areas toward a more concentrated sodium chloride or calcium chloride type (Ingebritsen *et al*., 2006). As flow through the system progresses, ion exchange between groundwater and clay minerals tends to play a more significant role in controlling the overall solute chemistry. The existence of soluble salt deposits within the regional aquifer system can have a profound effect on the groundwater chemistry. Gypsum or anhydride beds are the major sources of calcium and sulphate (Ingebritsen *et al*., 2006). Mixing of meteoric groundwater with sea water can also exert a controlling factor and due to greater density of sea water with respect to groundwater, sea water will exist as a coastal wedge beneath a lighter freshwater lens. Direct input of solute from hydrothermal sources can affect the regional groundwater chemistry (Plummer et al., 1979). Clays and clay rich geologic media can impede the movement of solutes relative to groundwater thus affecting the groundwater chemistry.

Under natural conditions, groundwater chemistry is determined by:

- The sum of soil-modified atmospheric input, water interaction taking place at the soil bedrock interface and from the long-term reactions taking place along flow paths in the saturated zone.
- The initial composition resembles the parent geology for some elements, thus providing a primary groundwater signature. The groundwater will then undergo geochemical reactions

(dissolution, precipitation, ion-exchange or redox reactions) as water moves down gradient.

- Other processes that affect groundwater chemistry are dry deposition, evapotranspiration, Selective uptake of ions by vegetation and mixing of different water chemistries.

3.3.2 Groundwater Contamination

Anthropogenic activities can thoroughly change the chemistry of groundwater. Groundwater contamination may be caused by the discharge of waste into streams which feed the groundwater, leaks from sewers, overflow or leakages from sewage tanks or structural failures, with a resulting massive, localized infiltration of waste water (Erikson, 1985). This is where compounds such as NO_3^-, NO_2^-, SO_4^{2-} and various cations make their appearance, including elements such as Cl^-. Leaching of waste from landfills also affects the groundwater chemistry as the leachate may contains compounds such as HCO_3 and CH_4. As the polluted groundwater moves down gradient, iron and other metals may precipitate. Mining waste and water pumped from mines are capable of polluting groundwater, particularly when they contain very soluble substances. This process if referred to acid mine drainage. The large amounts of NO_3^- and pesticides leaching from agricultural fields also have a huge influence on the groundwater chemistry (Erikson, 1985).

Groundwater pollution in urban areas

Urbanization does not only impact groundwater quantity through the modification of recharge pathways, but also impacts underlying groundwater quality. Changes in land-use such as industrial development, agricultural activities and wastewater generation may impact the underlying groundwater quality. Agricultural and industrial impacts are dependent upon the degree of development of the city. In urban areas, sewage contamination is the major issue. Depending upon whether waterborne sewerage or on-site sanitation is employed, the sources and pathways will differ. Whilst sewerage systems reduce the impacts on underlying groundwater, they do not eliminate them.

According to Forster *et al*. (1998) and Barret *et al*. (2000), sewage contamination of groundwater results not only from direct infiltration from onsite sanitation and leaking sewerage systems, but also surface runoff entering poorly designed or maintained springs and boreholes, i.e. through cracked concrete. The latter pathway is of most significance where sanitary coverage is poor, and

human waste are discarded on the land surface. Where urban sewage contains human waste as the dominant contaminant source such as in unsewered cities, faecal bacteria, viruses and nitrogen species are the main pollutants that may reach the underlying groundwater (Forster et al., 1998).

Industrial contamination of urban groundwater is controlled by a combination of the stage of industrial development of the overlying city, the type of industries present, and the underlying geology, particularly with regard to the natural attenuation capacity. Table 3.1 and Table 3.2 list potential contaminants that may be found in urban recharge along with the potential sources.

Table 3.1: Potential markers for urban recharge (Barrett et al., 1999).

Category	**Group**	**Species**
Inorganic		
	Major cation	Ca Mg K Na
	Major anion	HCO_3 SO_4 Cl
	Nitrogen Species	NO_3 NH_4 (plus organic nitrogen)
	Other minor Ions	B PO4 Sr F Br CN
	Metals	Fe PO_4 Mn Trace metals
Organic	Atmospheric	Chlorofluorocarbons (CFCs)
	Chlorination by products	Trihalomethanes (THMs)
	Faecal	Coprostanol, 1-aminopropanone
	Detergent related	Optical Brighteners, EDTA, limonene
	Industrial	Chlorinated solvents, hydrocarbons etc.
	Faecal microbiological	E. coli, Faecal streptococci, Organic, inorganic
Particulate	Colloidal	
Isotope	Stable Isotopes	^{2}H ^{15}N ^{18}O ^{35}S

Contaminants that may be present in urban groundwater include the following (USEPA, 1983):

- Inorganic contaminants, such as salts and metal ions, which may be present naturally in soil or rocks, or may enter the water as a result of urban storm water runoff, industrial or domestic wastewater discharges, landfill leakage, etc.
- Organic chemical contaminants, including synthetic and volatile organic chemicals, which are by-products of industrial processes and petroleum production, and which can arise from gas stations, urban storm water runoff, pesticide and septic system.

- Radioactive contaminants, which can be naturally occurring or resulting from waste disposal.
- Microbial contaminants, such as viruses and bacteria from sewage treatment plants, underground septic systems, agricultural livestock operations. The microbial contaminants of greatest concern in drinking water are usually of faecal origin

Table 3.2: Sources of possible marker contaminant species (modified from Barrett et al., 1999)

	Atmosphere	**Geological Material**	**Agriculture**	**Mains Water**	**sewage**	**Industrial & Commercial Sites**
Majors	✓	✓	✓	✓	✓	✓
N species	✓		✓	✓	✓	✓
B & PO4		✓			✓	✓
Other minors	✓	✓		✓	✓	✓
Metals		✓			✓	✓
CFCs	✓			✓	✓	✓
THMs				✓	✓	✓
Faecal					✓	
Detergent					✓	✓
Industrial					✓	✓
Microbiological					✓	
Colloidal					✓	✓

3.3.3. Hydrochemical data presentation.

Over the past years, a number of techniques for graphical representation of hydrochemical analysis have been developed. Some of these are useful principally for display purposes i.e. to illustrate water quality, compare analysis or to emphasize differences and similarities. Graphical procedures have been devised to help detect and identify the mixing of waters of different composition and to identify some chemical processes that may take place as natural waters circulate (Hem, 1985).

The chemical properties of water are presented by various methods, including the Piper trilinear diagram (Piper, 1944), which is the most commonly used method for illustrating hydrochemical facies. The Piper diagram is useful for screening and filtering large volumes of chemical data sets making interpretations easier. It can be used to define the patterns of spatial changes in water chemistry within the geological units, along the groundwater flow paths. The major ions

concentrations are plotted in milli-equivalent percentages (Hem, 1985). The Schoeller diagram consists of vertical axes on which concentration of ions are plotted in mg/l. The diagram displays the ion ratios between points of each ion joined by straight lines. The diagram allows for the classification of water samples.

3.4. Environmental Isotopes

Stable and radioactive environmental isotopes have been used for more than four decades to study hydrological systems and have proved useful particularly for understanding groundwater systems. Understanding the groundwater system is necessary for sustainable resource development without adverse effect on the environment (Clark and Fritz, 1997). Environmental Isotopes, both stable and unstable occur in the atmosphere and the hydrosphere in varying concentrations. Frequently used environmental isotopes include those of the water molecule, hydrogen (^{2}H and ^{3}H) and oxygen (^{18}O), as well as carbon (^{13}C and ^{14}C) occurring in water as constituents of dissolved inorganic and organic compounds. Isotopes techniques are effective for fulfilling information needs, such as determining (Kendall and McDonnell, 1998);

- The origin of groundwater
- Groundwater age, velocity, and flow directions
- The interconnection between aquifers
- Interconnection between surface water and groundwater, and
- Aquifer characteristics i.e. porosity, transmissivity, and dispersivity.

3.4.1. Stable isotopes

Stable isotopes of different elements are used in hydrology; however, the most commonly used are those of oxygen and hydrogen. Variations in stable isotope ratios of natural compounds are governed by chemical reactions and phase changes due to energy difference between chemical bonds involving different isotopes of an element. The isotopic composition of water is expressed in comparison to the isotopic composition of the ocean water. For this purpose, an internationally agreed upon sample of ocean water has been selected, called Standard Mean Ocean Water (SMOW) (Craig, 1961a, 1961b).

The isotopic composition of water, determined by mass spectrometry, is expressed in per mil ‰ deviation from the SMOW standard. These deviations are written δD for deuterium and δ^{18}O for ^{18}O:

$$\delta(‰) = \frac{R_{sample} - R_{SMOW}}{R_{SMOW}} * 1000 \quad (3.9)$$

Where R is isotope concentration ratio ($^{2}H/^{1}H$, $^{13}C/^{12}C$, $^{15}N/^{14}N$, $^{18}O/^{16}O$, $^{34}S/^{32}S$) of a sample or a SMOW. Water with less deuterium than SMOW has a negative δD; water with more deuterium than SMOW has positive δD. The same is true for δ^{18}O.

Most application of stable isotopes of hydrogen and oxygen in groundwater studies use the variation in isotopic ratios in atmospheric precipitation, that is, in the input to a hydrogeological system. These variations result from a variety of physical processes, the most important being evaporation and condensation (Mazor, 2004). During evaporation, the light molecule of water, $H_2{}^{16}O$, is more volatile than heavier molecules ($^{1}H^{2}H^{16}O$ or $H_2{}^{18}O$). Therefore, vapor that evaporates from the ocean is depleted on the order of 10‰ in ^{18}O and 80 to 120‰ in deuterium with respect to the ocean water. As the degree of condensation of vapor mass depends on temperature, a relation between isotope composition of precipitation and its temperature of formation that should be expected is that; as the formation temperature decreases, the δ-value of precipitation decreases (Mazor, 2004).

When precipitation infiltrates to recharge groundwater, mixing in the unsaturated zone and selective infiltration of precipitation result in attenuation of seasonal isotopic variations in precipitation. In most aquifers, isotopic composition of water does not change further unless exchange with the oxygen of rocks occurs (Cook and Herczeg, 2000). The isotopic composition of groundwater is thus related to that of precipitation in the recharge area of an aquifer at the time of recharge. Groundwater may be of a very old age, and climatic conditions of the region at the time of recharge may have been different from those of today. This implies that the isotopic composition of precipitation could have been different from the present one, due to the correlation between δ-values and temperature (Mazor, 2004).

3.4.2. Radioactive Isotopes

Radioactive isotopes or radioisotopes, such as tritium and carbon-14 have been used in groundwater studies. Radioisotopes occurring in groundwater originate from natural and/or artificial nuclear processes. Cosmogenic radioisotopes are produced in nuclear reactions between the nucleonic component of cosmic radiation and the atmosphere. Anthropogenic radioisotopes are produced in nuclear bomb testing and in nuclear reactors. The concentration of radioisotopes in groundwater are very low and usually measured by estimating the rate of decay, *A,* in a given sample (Kendall and McDonnell, 1998):

$$A = \lambda * N \tag{3.10}$$

Where λ, the decay constant, related to half-life $T_{1/2}$ by equation $\lambda = \ln 2 / T_{1/2}$. The decay rate becomes immeasurably small for long-lived radioisotopes such as ^{36}Cl and ^{129}I. In these cases, the number of atoms need to be measured using the Accelerator Mass Spectrometry (AMS) technique (Mazor, 2004).

Tritium

Tritium, ^{3}H, is the radioisotope of hydrogen with unstable and radioactively disintegrating atoms, forming ^{3}He atoms. The radioactive decay is accompanied by emission of β^- particles:

$$T \rightarrow \beta^- + {}^{3}He \tag{3.11}$$

Tritium content in water is expressed in tritium units (TU), Where 1 TU is equal to 1 atom of ^{3}H per 10^{18} atoms of ^{1}H which is equivalent to 0.118Bq and has it half-life fixed as 12.43a. In natural water the concentration of tritium is generally low. Environmental tritium occurs in precipitation from both natural and anthropogenic sources. The natural production results interaction of cosmic ray produced neutrons in the upper atmosphere with nitrogen atoms.

$$^{14}_{7}N + {}^{1}_{0}n \rightarrow {}^{3}_{1}H + {}^{12}_{6}C \tag{3.12}$$

Tritium oxidizes rapidly to HTO and enters the hydrological cycle with the estimated natural content, in precipitation, estimated to be in the order of 5 TU. In the saturated zone, water is isolated from the atmosphere and the concentration of tritium drops due to radioactive decay; the original concentration of 5 TU drops to 2.5 TU after 12.3 years.

3.5. Statistical analysis of groundwater data

3.5.1. Multivariate Statistical analysis

Multivariate statistical analysis techniques serve an important purpose, as the initial tools to evaluate large and multi-variable hydro-geochemical data sets into manageable classifications with similar characteristics in order to reveal the hidden similarities within the data sets (Suk and Lee, 1999). The most commonly used techniques are the Pearson's correlation, Factor and Cluster analysis.

a) Pearson's correlation is used to measure the relationship between the various hydrochemical parameters. Pearson correlation reveal statistical relationships between variables with Pearson's product-moment correlation (R) as a measure of linear dependence between two variables that is expressed as the covariance of the two variables divided by the product of their standard deviation. The resultant dimensionless R value ranges between +1 and -1, where 1 is perfect positive linear (Borradaile, 2003). Correlation among variables with $r \geq 0.5$ are regarded as practical and meaningful. Correlation strength of variables are described as very strong (r = 0.8-1), strong (0.70-0.79), moderate (r = 0.5-0.69), weak (r = 0-0.49).
b) The Factor analysis is commonly used in hydrochemistry to interpret groundwater quality and relating it to changes in hydrogeochemical processes. Factor analysis can be used for explaining the variations with the data by using common dimension known as factors (Hair et al., 1992). This analysis is used to identify the underlying variables and provides and empirical classification scheme of grouping into factors. Two modes are widely used, Q-mode that correlates the sample site and R-mode that describes the similarities amongst variables in data.
c) Cluster Analysis is a multivariate method which aims to classify a sample of objects on the basis of a set of measured variables into a number of different groups. Cluster Analysis is usually performed to classify observations into groups having similar characteristics. Clustering algorithms assume that the groups or clusters are not known before analysis. Cluster analysis is carried out using Hierarchical and Non-Hierarchical methods.

3.6. Previous hydrogeological studies within the Durban Metropolitan Region.

A regional hydrogeological investigation was conducted by Bell and Maud (2000) at a smaller scale and covered the eastern central part of the Durban Metropolitan area, formerly known as the Greater Durban area. Six hydrogeological units were recognized, namely; dunes, alluvial and estuarine deposits, sandstones, dolerites, tillite, granite-gneiss, and mudstone-shale. The alluvial and estuarine deposits, referred to as Durban Harbour Beds, forms part of primary aquifers and have reported borehole yields from 16 to 35 L/s. the hydraulic conductivity ranges from 3.6×10^{-6} to 6.3×10^{-7} m/s and the electrical conductivity ranges from 83 to 115 mS/m. The dunes and beach sands have a thickness ranging from 25 to 60 m with good groundwater yields, however, the groundwater within these units is often found to be brackish. The aeolian, alluvial and estuarine deposits generally yield fresh to slightly saline groundwater where EC can be over 300 mS/m with a slightly alkaline groundwater pH. Chloride content in these deposits can be as high as 80 mg/l (i.e 16% of TDS).

The Berea Formation, also known as Berea Red Sand, occupies the upper and inner portions of the Durban bluff with a thickness of up to 100 m frequently representing an aquifer of considerable significance. Shallow wells drilled in the sand provided yields of 5.5 l/s with a good water quality. The basement granites complex of the Mapumulo Group has groundwater occurrence in association with fractured and weathered zones (Bell and Le Roux, 1998). Most springs and seasonal seepage emanate between the weathered regolith and intact rock and Moderate to good groundwater yields of up to 2.7 l/s and contains a mean EC and pH of 80 mS/m and 7.7, respectively. The sandstones of the Natal Group represent the best and most consistent secondary aquifer of the area with yields in the range of 0.5 l/s to above 2 l/s with mean EC and pH values of 71 mS/m and 7.1, respectively. The Dwyka Group tillite and diamictite are the poorest secondary groundwater aquifer in the Durban area. However, in some areas yield of up to 3 l/s can be obtained. The average yield of this unit is 0.13 l/s with over 30% boreholes producing yields of between 0.2 and 0.25 l/s with a relatively higher percentage of dry boreholes (Bell and Maud, 2000).

Bicarbonate groundwater type predominates the area and represents recently recharged groundwater. Higher salinity of groundwater is found in proximity to the coastal areas when compared to those of the same hydrogeological units further inland and this is attributed to the

influence of rainfall associated with prevailing winds of the Indian Ocean. Groundwater quality in granites are usually fresh with TDS and EC values of less than 500 mg/l and 50 mS/m, respectively. Calcium/magnesium bicarbonate is the common water type found in granitic rocks. The Natal Group has a very good TDS value of less than 500 mg/l most of which is coming from temporary bicarbonate hardness and values of EC in the coastal areas vary from 23 to 185 mS/m, while inland it rarely exceeds 45 mS/m. The pH is slightly acid to alkaline with bicarbonate character (Bell and Maud, 2000; King, 2002).

CHAPTER 4

METHOD AND MATERIALS

The methods and materials employed during the course of this research for data collection, analyses and interpretation are described in the following sections.

4.1. Desktop Study

The research project was started by reviewing existing data and literature on the Durban Metropolitan district's geological, hydro-meteorological, hydrological and hydrogeological information. As part of the secondary data collection, hydro-meteorological data, which include rainfall, humidity, temperature and wind speed was sourced from the South African Weather Services (SAWS). Groundwater data, such as location of monitoring sites, depth to groundwater, pumping test data, hydrochemistry data and borehole logs were obtained from the Department of Water and Sanitation (DWS), private consulting companies and from the eThekwini Municipality's Durban Solid Waste Department. All of the data and information collected are collated systematically into a hydrogeological database for analysis and interpretation.

4.1.1. Filling of missing rainfall data

Assessing the spatial distribution of rainfall is frequently required for water resource assessment, management, hydrologic and recharge studies. Rainfall is one of the most important variables that are used to define the climate of a region (Mair and Fares, 2011). The normal ratio method has been used to fill in missing rainfall data at one or more stations because of equipment malfunction or operator absence. According to the normal ratio method, the missing precipitation is calculated using the following equation (Fetter, 2001):

$$P_x = \frac{1}{n} \sum_{i=1}^{i=n} \frac{N_x}{N_i} P_i \qquad (4.5)$$

Where, Px is the missing precipitation at the interpolation station 'x', Pi is the precipitation for the same period at the "ith" station of a group of index stations. Nx is the Normal annual precipitation value for the "x" station and Ni is the Normal annual precipitation value for the "ith" station.

4.1.2. Selecting of weather stations for rainfall analysis

Thiessen polygon and isoyhtal methods were used to compute the areal precipitation of the study region from weather observation station. The Thiessen method is based on assumption that the measured rainfall at any station can be applied halfway to the next station at any direction (Thiessen, 1911). This method allows to interpolate rainfall from non-uniform distribution of gauges by providing a weighting factor for each gauge. The Thiessen polygon method has been used for selecting rainfall station used for the interpolation of rainfall distribution within the study area (Raghunath, 2006). This method assumes that an average value over the same area of the polygon is equivalent to the point value located at the centroid of the polygon. The areal rainfall over the basin is expressed by (Taesombat and Sriwongsitanon, 2009):

$$P_T = \sum_{i-1}^{n} T_i P_i \quad (4.6)$$

Where, P_T is the areal rainfall, Pi is the observed rainfall at the centroid of ith polygon and T_i is the Weighing factor.

The weighing factor is given by:

$$T_i = \frac{A_i}{A_T} \quad (4.7)$$

Where A_T is the total area of the basin and A_i is the area defined by the intersection of the Thiessen polygon and the basin boundary.

The isohyetal method was used to calculate the distribution of rainfall over an area. Annual rainfall for eight meteorological stations was used. The isohyetal method is considered as the most accurate method for computing mean rainfall. Rainfall gauge locations are plotted and the contours of equal amount of rainfall is drawn. The mean rainfall, P, is calculated using equation 4.8 (Linsley *et al*., 1975):

$$P = \frac{\sum [A_n(P_n + P_{n+1})/2]}{\sum A_n} \quad (4.8)$$

Where, P_n is the isohyet values and A_n is the area between two isohyets

4.2. Fieldwork

A total of 63 samples were collected from groundwater and surface water sources, with 26 of the samples collected from standalone points (Figure 4.1) and 37 samples collected from around 6 landfill sites, namely; Lovu (Figure 4.2), Bul-Bul Drive (Figure 4.3), Bisasar Road (Figure 4.4), Marianhill (Figure 4.5), La Mercy (Figure 4.6) and Buffelsdraai (Figure 4.7) Landfill sites, during August 2017 and July 2018 sampling campaigns, respectively. Water samples were collected from active and inactive boreholes, springs and up-stream and down-stream of major rivers. Each sample was tested in the field with respect to its electrical conductivity (EC), Total Dissolved Solids (TDS), Dissolved Oxygen (DO), Redox potential (Eh), pH and salinity using the Hanna multi-parameter probe. Groundwater levels were measured using the Solinst Temperature, Level and Conductivity (TLC) dip meter. Samples were collected according to standard procedures for major ions, minor ions, trace elements and environmental Isotopes ($\delta^{18}O$, $\delta^{2}H$ and ^{3}H) analysis. Tritium samples were only collected for groundwater samples. Onsite hydrochemical testing for total alkalinity, carbonate and bicarbonate content of groundwater and surface water was undertaken through titration of water sample using 0.02M HCl acid.

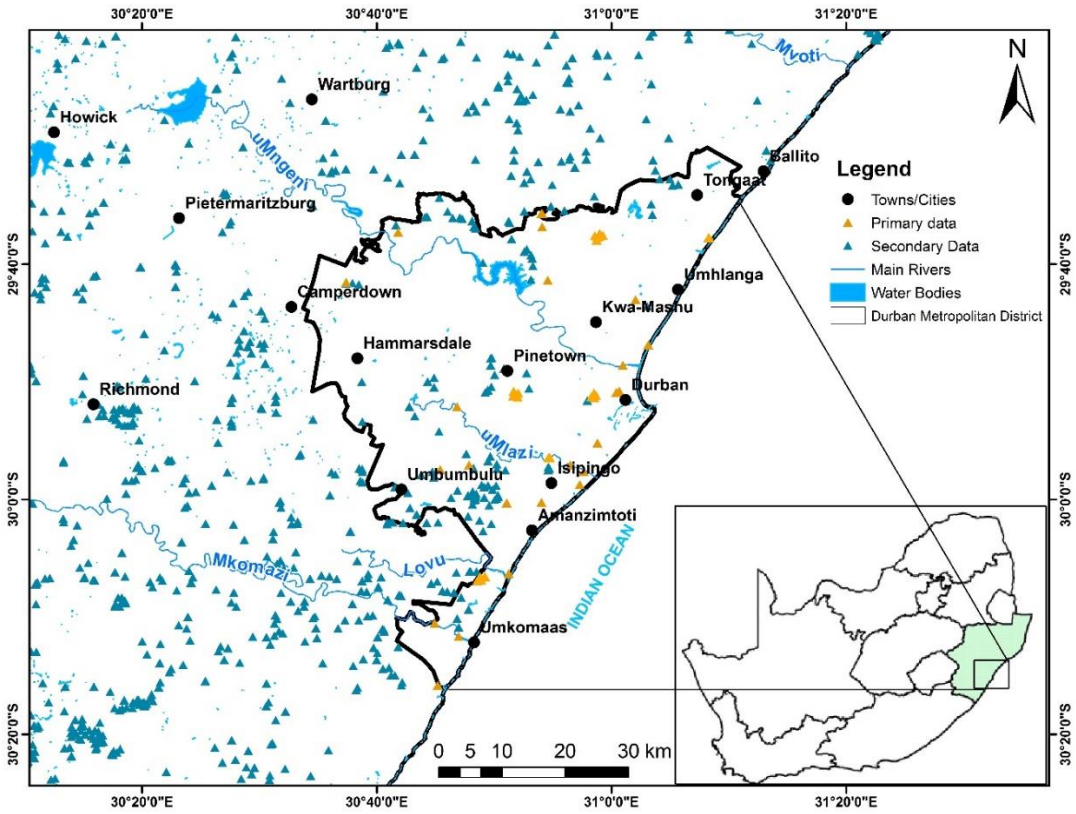

Figure 4.1: Spatial distribution of secondary and primary collected data across the study area.

Figure 4.2: Spatial distribution of groundwater and surface water monitoring points at Lovu landfill site.

Figure 4.3: Spatial distribution of groundwater and surface water monitoring points at Bul Bul Drive landfill site.

Figure 4.4: Spatial distribution of groundwater and surface water monitoring points at Bisasar Road landfill site

Figure 4.5: Spatial distribution of groundwater and surface water monitoring points at Marianhill landfill site.

Figure 4.6: Spatial distribution of groundwater and surface water monitoring points at La Mercy landfill site

Figure 4.7: Spatial distribution of groundwater and surface water monitoring points at Buffelsdraai landfill site.

4.2.1. Detailed field water sampling procedure.

The following standard procedures for water sampling were followed during groundwater and surface water sampling:

- All field sampling and testing equipment were cleaned and calibrated before use.
- Groundwater levels were measured on site, where possible, using the Solinst TLC dip meter.
- Groundwater samples were collected from monitoring boreholes using the Solinst bailer sampler and field measurements of EC, pH, TDS, DO, Eh and temperature were conducted.
- 100 ml sample water at each site was titrated using 0.02M HCl acid solution to determine the total alkalinity and bicarbonate content. In samples with pH > 7.5, few drops of phenolphthalein indicator were added into the samples until water turns colorless and the volume of acid used was noted. Few drops of Bromocresol indicator were added to the samples and titrated with 0.02M HCl acid until the color changed from blue to yellow (4.5 pH end point) and the volume of acid used was noted.

- Cations and anion samples were filtered into 50 ml polyethylene bottles using 0.45 µm filters and were capped using the polyseal capping and the screw lid. Cations samples were acidified using ultrapure acid (30% HNO_3) to pH < 2. Addition of acid prevents adsorption of metals thereby minimizing ion exchange effects.
- Unfiltered environmental isotope samples were collected for tritium and stable water isotope in 1 liter and 50 ml polyethylene bottles, respectively.
- Samples were stored in cooler boxes during transportation and stored in the fridge before lab analysis.

4.3. Laboratory Work

4.3.1. Hydrochemical and Environmental isotope analyses

Hydrochemical data gives information about the nature of the aquifer system and can be used along with isotope data to identify recharge processes. It can also be used to regionally differentiate between deep and shallow aquifers, dating and estimating the mean groundwater residence time (Banks *et al*., 2009). Major cation and trace metal samples were analyzed using Inductively Coupled Plasma Atomic emission spectrometer (ICP-AES) and Mass Spectrometer (ICP-MS), respectively at the University of Stellenbosch analytical laboratory. Major anions were analyzed using a Dionex® Ion Chromatography (IC) within the Department of Geological Sciences, University of KwaZulu-Natal. Environmental isotopes (δ^2H and $\delta^{18}O$ and tritium) were analyzed at the laboratory of the Environmental Isotope Group (EIG) of iThemba Labs, in Johannesburg, South Africa. The measured stable isotopes (δ^2H, $\delta^{18}O$) concentration in sampled water is reported with respect to Standard Mean Ocean Water (SMOW) and tritium is reported in tritium units (TU).

4.4. Data Interpretation and Analysis tools.

A systematic hydrogeological database was developed for the study area, where all hydrological, hydro-meteorological, hydrogeological, hydrochemical and environmental isotope data was collated for further analysis using various software and tools described below:

- Geographical Information System (ArcGIS 10.4) was used for displaying and representing spatial and temporal data. GIS is software system for capturing, storing, checking and displaying spatial data.

- AquaChem was used for hydrochemical data analysis, plotting and visualization. AquaChem is a software developed for graphical and numerical analysis and modelling of water quality data. It provides calculations and graphs for interpreting water quality data. Many data plotting options are available in AquaChem including correlation plots, X-Y scatter and Wilcox plots, Piper Trilinear plots, Thematic Map Plots such as Pie, Bubble and Stiff plots, summary plots, Schoeller, Box and Whisker, and Frequency Histogram.
- SPSS version 24 statistical software package was applied for descriptive statistics, bivariate correlation, factor analysis, and hierarchical cluster analysis of the hydrochemical data collected. It was also applied in borehole data analysis, such as borehole yield, transmissivity and water level.
- Surfer 14 of Golden Software® was used for counting, modeling and visualization of groundwater level and depth to groundwater across the study area.
- Corel Draw Suite X8 was used to reproduce and improve figures from various sources by redrawing and modification. The hydrogeological cross section was also produced with this software.

4.4. Data analysis and interpretation

Data sourced during desktop study and those generated in the 2017 and 2018 field campaigns was processed, analyzed and interpreted towards developing a regional conceptual hydrogeological model of the Durban Metropolitan District and the surrounding areas

4.4.3. Water budget analysis

According to Anderson and Woessner (2002), water budget is an essential step in the development of a conceptual model as it forms the basis of investigating a hydrogeological system and is also used to quantify the flow of water in and out of a system by directly measured and estimated parameters. Evapotranspiration has been estimated for each month of the year using the FOA Penman-Montheith Method (Allen et al., 1998) that describes the reference evapotranspiration, based on several parameters which include precipitation, temperature, relative humidity and wind speed. Actual evapotranspiration was estimated using the Turc Method. The Turc method

considers precipitation and temperature as the dominant factors controlling evapotranspiration. Runoff was estimated using the SCS Runoff curve number described in section 3.2.3.

Mechanism of recharge in urban areas is different from undeveloped area mechanism of recharge. In urban areas Simmers (1998); Garcia Fresca (2004) described four types of recharge, direct recharge, indirect recharge, localized recharge. These combined recharge mechanisms generally increase recharge volumes in urban areas, but the categories can overlap and are not mutually exclusive.

The water balance based direct rainfall recharge across the study area is given by:

$$R_p = P - (Et + R_s + Gw_{abs}) \quad (4.9)$$

Where, R_p is direct rainfall recharge, P is precipitation, Et is the total actual evapotranspiration, R_s is the surface runoff and Gw_{abs} is the total registered groundwater abstraction within the study area.

4.4.5. Groundwater level and Hydrochemical analysis

Groundwater level contour maps were developed based on the secondary and original data collected in the course of this research using Surfer 14 software. The groundwater level maps assisted in defining the flow direction of groundwater and identifying recharge and discharge areas. Depth to groundwater maps were interpolated using Inverse Weighed Distance (IDW) method. Groundwater chemistry data both from secondary sources and primary data were processed and presented. Hydrochemical data is presented in the form of Durov and Piper-trilinear plots. Electrical conductivity contour map is interpolated in ArcGIS using IDW method as well. For each sampling point, hydrochemical facies is determined to understand the hydrochemical evolution of groundwater from recharge to discharge areas.

4.4.6. Hydrogeological conceptual model development

The first step in the modelling protocol is to establish the purpose of the model and thereby the governing equations to be used. A conceptual model is then developed where the hydrostratigraphic units and system boundaries are identified. Field data, including information on the water balance, aquifer properties, and hydrologic stresses, are also included. Collection and interpretation of field data is essential in understanding the natural system and identifying the

groundwater problem. The conceptual model includes: all the different types of aquifers, their thicknesses, hydraulic conductivity, and transmissivity; groundwater levels; hydrometeorological parameters such as precipitation, evapotranspiration and runoff; groundwater abstraction volume; water types; and surface water bodies (Figure 4.8).

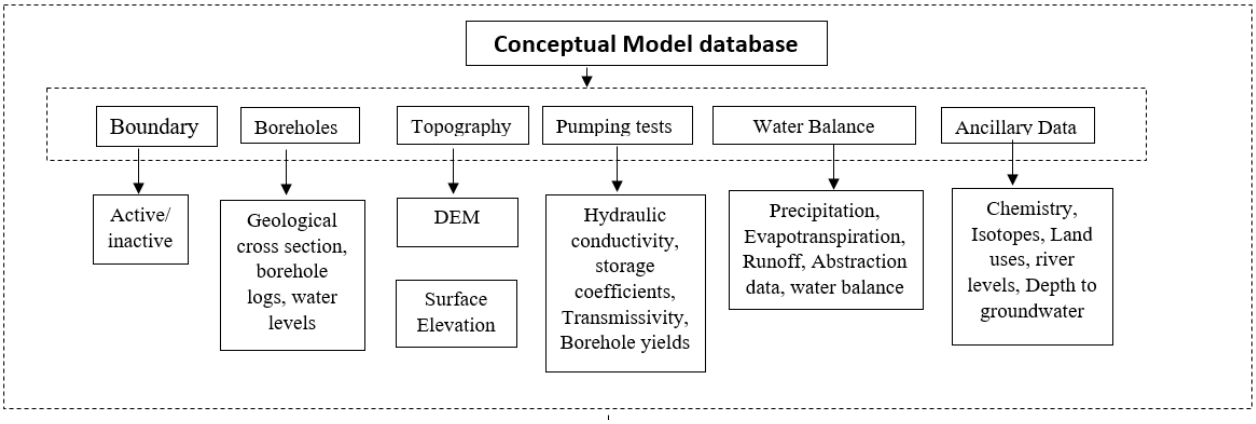

Figure 4.8: Database used for developing the conceptual model.

CHAPTER 5

HYDROGEOLOGICAL CONCEPTUAL MODELLING AND CHARACTERIZATION OF THE DURBAN METROPOLITAN REGION

5.1 Introduction

The development of a conceptual hydrogeological model through hydrogeological and hydrogeochemical characterization is the most important step towards understanding the hydrogeological conditions and groundwater resource management. The level of detail of the conceptual hydrogeological model is determined by the modelling purpose, the size of the area and available field data. The knowledge from the hydrological, hydrogeological and hydrochemical assessment described in this chapter provides a conceptual understanding of the occurrence of groundwater and its hydrochemistry and quality. These in turn could assist groundwater managers with better decision making on groundwater exploration targets, improved aquifer hydraulic parameter estimation and higher confidence in groundwater resources development.

5.2. Hydrometeorological characteristics of the Durban Metropolitan District

5.2.1. Precipitation

Rainfall data for the study area have been sourced from the South African Weather services (2017), recorded from 8 weather stations, namely; Durban South, Durban Botanical Gardens, Virginia, Mount Edgecombe, Stanger, Richmond, Pietermaritzburg and Allerton stations. Average annual rainfall values were calculated across a 30-year meteorological record (1987-2017). The 30 year mean annual rainfall over the study area has been interpolated based on the 8 rainfall stations (Figure 5.1) and estimated at 934.46 mm/year. The isohyetal areal rainfall map of Figure 5.1 shows that rainfall decreases from the coast towards the central region, then increases from the central region towards the west due to topographic effects. The same pattern can be observed from the northern region to central region and from central region towards the southern region (Figure 5.1).

5.2.2. Evapotranspiration

A mean annual potential evapotranspiration (PET) of 985 mm/year was estimated using the FAO56 Penman-Motheith method (Allen *et al*., 1998) and was found to be substantially greater

than the mean annual precipitation. The actual evapotranspiration was estimated at 740 mm/year using the Turc method. Figure 5.2 shows that highest evapotranspiration occurs in December as a result of high temperatures and that during winter evapotranspiration exceeds the amount of rainfall received.

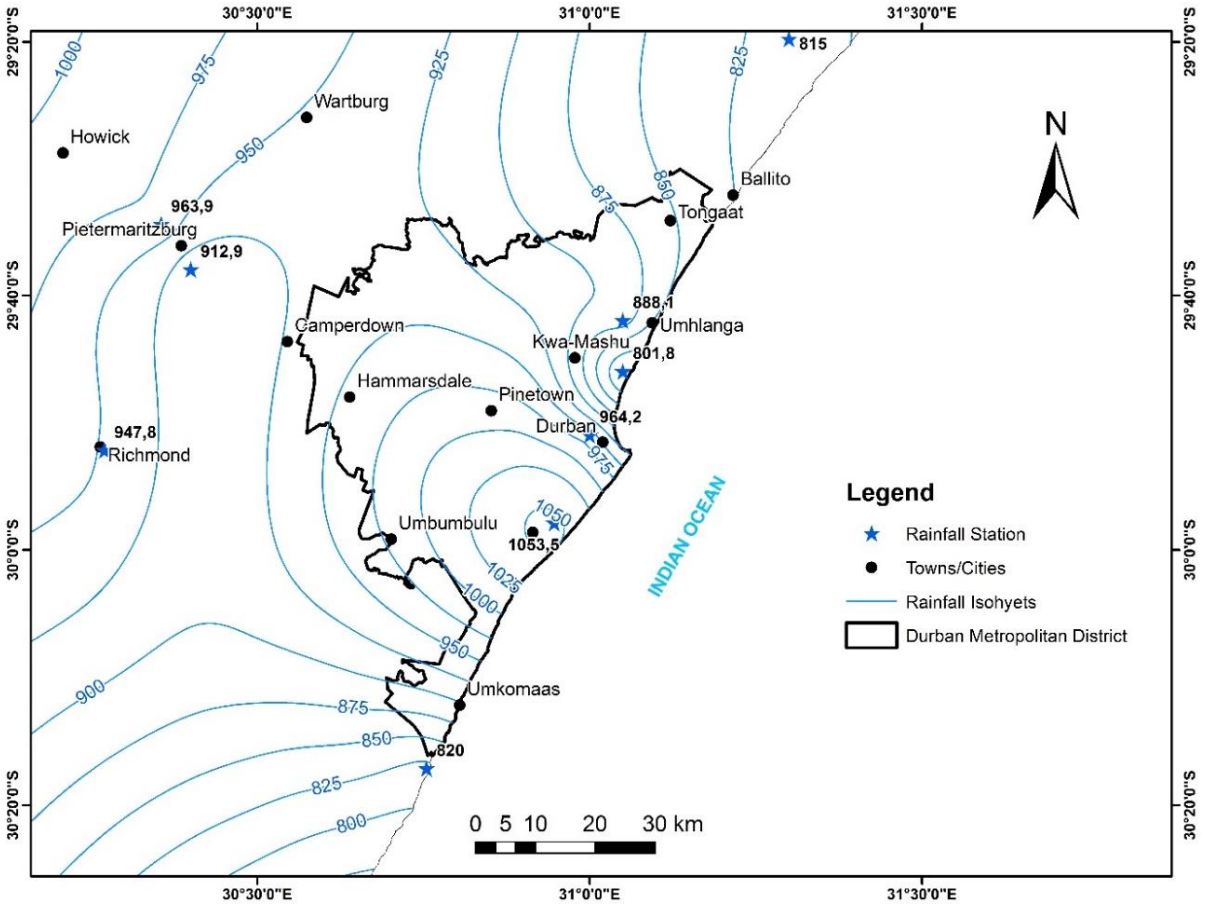

Figure 5.1: Spatial distribution of rainfall across the study area

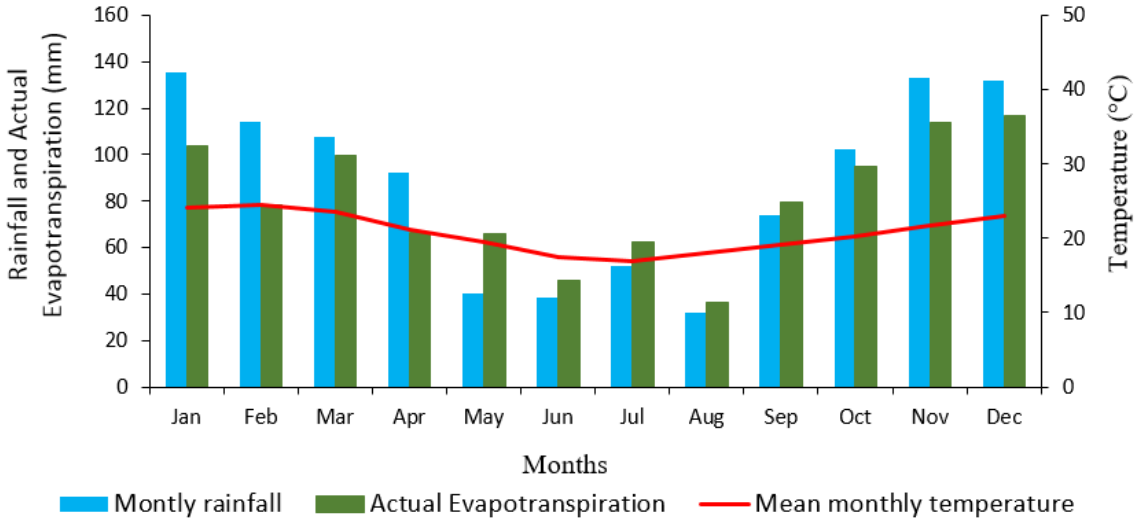

Figure 5.2: Graph of average monthly rainfall and actual evapotranspiration for the study area (rainfall data sourced from SAWS, 2017)

5.2.3. Surface Runoff

Surface runoff is the function of rainfall intensity and duration, soil type, soil moisture, land use/cover and slope and it forms part of the hydrological cycle. The SCS Runoff Curve Number (CN) method (SCS, 1986) has been applied in this study to estimate monthly and annual runoff, which involved the estimation of hydraulic condition for each land use depending on hydrologic soil group (HSG). The curve numbers are estimated based on hydraulic conditions and soil type (Figure 5.3). The estimated monthly runoff for the study area is presented in Table 5.1 and the mean annual estimated runoff rate is 132.76 mm/year or 14.2% of mean annual precipitation (MAP). Runoff is high during the rainy season from October to March and low during the dry season due limited water supply from rainfall (Figure 5.4). Highest runoff occurs in built up areas, whereas low runoff occurs in grassland and forest.

Table 5.1: Summarized monthly runoff (mm) estimated using the SCS curve number method.

Month	**Jan**	**Feb**	**Mar**	**Apr**	**May**	**Jun**	**Jul**	**Aug**	**Sep**	**Oct**	**Nov**	**Dec**
Runoff (mm)	22.57	10.89	13.65	6.5	0.037	0.019	0.703	0.015	6.05	14.78	28.06	29.51

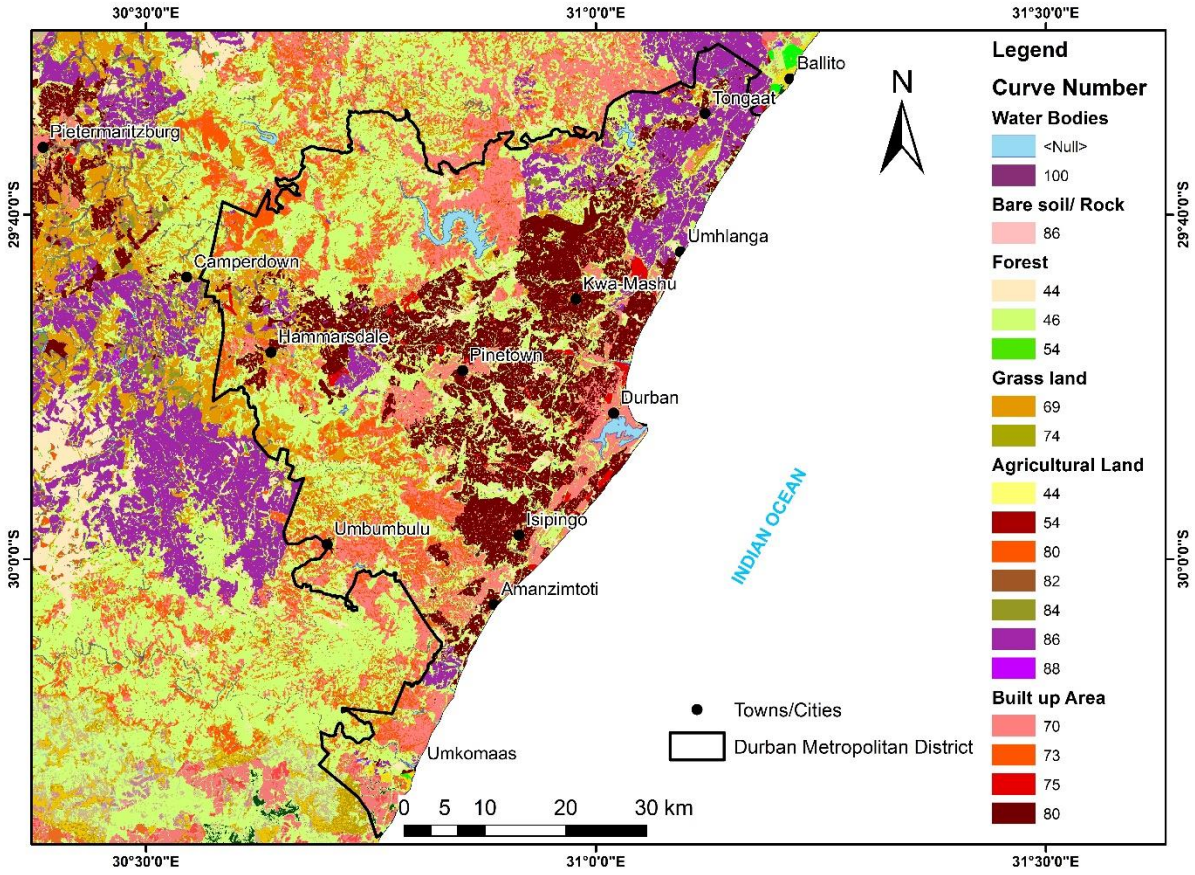

Figure 5.3: Map showing runoff curve number for each land use/cover depending on the hydrologic soil group.

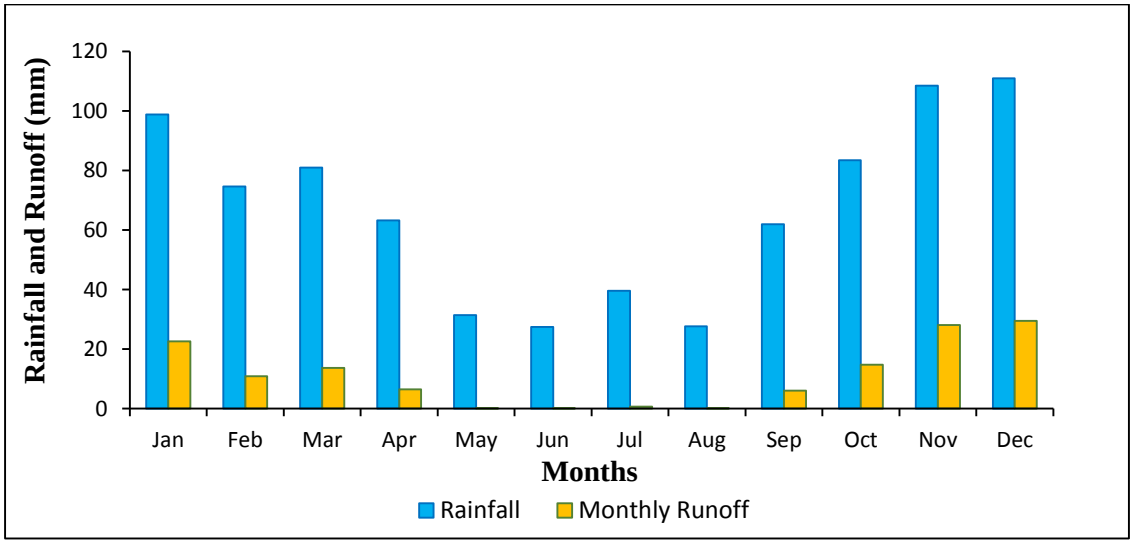

Figure 5.4: Graph of average monthly rainfall and average monthly runoff estimated using the Curve number Method.

5.3.4. Groundwater abstraction and recharge

The quantification of natural groundwater recharge and groundwater abstraction rates are prerequisites for efficient and sustainable groundwater resource management. Groundwater abstraction data was sourced from the Department of Water and Sanitation (2017). The total registered abstraction across the Durban Metropolitan region is 9.24 $x10^6$ m^3/yr and it is mainly used for irrigation of golf courses and for industrial uses. The CMB and water budget method was used to estimate groundwater recharge. The average chloride concentration in rainfall of 7.38 mg/l was used during the estimation of recharge (DWAF, 2006). The estimated recharge indicated that the recharge rate for the study area ranges from 35.8 mm/year to 241.8 mm/year with an average recharge rate of 110 mm/year or 11.78% of MAP (Table 5.2).

Table 5.2: Results of groundwater recharge estimated using the chloride mass balance

Site ID	Latitude	Longitude	Groundwater Cl (mg/L)	Recharge (mm/year)	Recharge (%MAP)
ETM1	-29.92	30.98006	78.32	88.06	9.42
ETM3	-30.0047	30.85111	28.52	241.78	25.87
ETM5	-29.7809	31.05207	44.62	154.56	16.54
ETM6	-29.846	31.01085	36.45	189.18	20.24
ETM8	-29.9786	30.95503	33.14	208.07	22.27
ETM11	-30.1087	30.82026	108.98	63.28	6.77
ETM15	-29.7169	31.03404	69.47	99.28	10.62
ETM19	-29.5943	30.90064	52.95	130.25	13.94
ETM21	-29.6892	30.90943	54.57	126.38	13.52
ETM25	-29.8684	30.78066	102.90	67.02	7.17
148131	-29.7333	30.53333	62.00	111.23	11.90
148239	-29.8333	30.78333	40.00	172.41	18.45
148246	-29.5167	31.03333	94.00	73.37	7.85
149041	-29.775	30.675	86.00	80.19	8.58
171723	-30.2283	30.68472	67.80	101.72	10.88
171725	-30.2581	30.74722	192.60	35.81	3.83
171738	-30.1872	30.67694	86.00	80.19	8.58
172904	-30.3028	30.73611	192.00	35.92	3.84
172927	-29.5153	31.18333	82.60	83.49	8.93
184031	-29.9553	30.97527	65.59	105.14	11.25
184033	-29.9403	30.96777	105.60	65.31	6.99
Mean			80.20	110.13	11.78

The spatial distribution of CMB recharge estimated across the study area is shown in Figure 5.5. The CMB recharge along the coastal areas is underestimated due to maritime influences and possible urban chloride sources in the form of pollution.

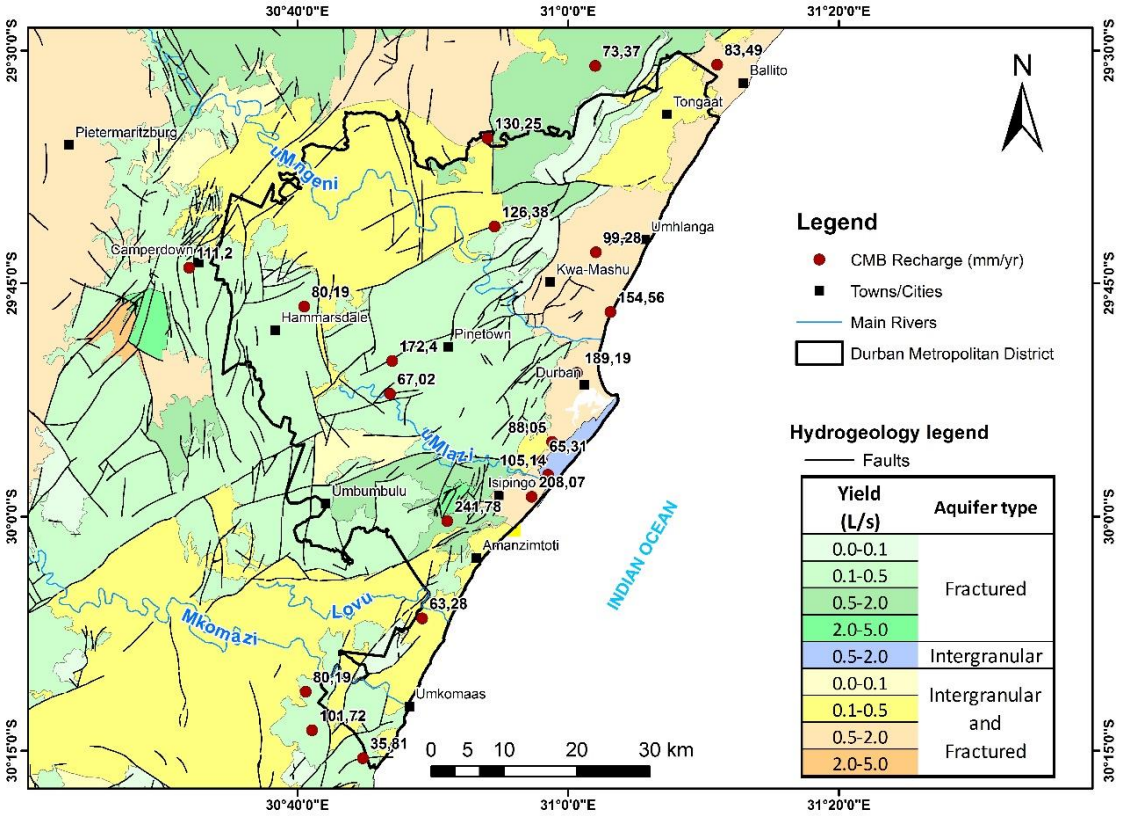

Figure 5.5: Spatial distribution of groundwater recharge estimated using CMB method.

The water balance method of groundwater recharge estimation (equation 4.9) which considers precipitation, evapotranspiration, surface runoff and groundwater abstraction gave recharge volume of 1.32 x10^8 m^3/year or 62 mm/year (6.6% MAP) (Table 5.3). Thus, the average groundwater recharge, combining both methods, is about 86 mm/year or 1.97 x10^8 m^3/year (9.2% MAP).

Table 5.3: Annual estimated water balance for the Durban Metropolitan District

Study Area	Precipitation	Evapotranspiration	Surface Runoff	Groundwater abstraction	Recharge
km^2	x10^9 m^3		x 10^8 m^3	x10^7 m^3	x 10^8 m^3
2295.43	2.15	1.7	3.09	9.24	1.32

5.3. Hydrogeological setting and hydraulic characteristics

With aid of borehole data and pumping test data, geological and hydrogeological reports, the hydrogeological setting of the Durban Metropolitan region has been redefined based on hydraulic conductivity, transmissivity and borehole yields sourced from 701 boreholes. Hydraulic properties have been defined for each geologic unit according to Groups and Formations (Table 5.4). Three modes of groundwater occurrence characterize the study area, namely; intergranular, fractured, and weathered and fractured aquifers.

5.3.1. Intergranular aquifers

Intergranular aquifers of the Maputaland Group comprises the following formations: a) Alluvium and estuarine deposits (locally called Harbour Beds Formation) have an average thickness of 15 m and in some place can be up to 60 m extending just from south of Isipingo to north of Durban and is characterized by borehole yields of 6-36 l/s (Figure 5.6); b) Berea Formation covers most of the coastal area having varying thickness from 0.5 to 45 m and is characterized by borehole yields of 2.5 - 45 l/s; c) The Bluff Formation outcrops mainly at the Bluff ridge just south of Durban City center. It has average thickness of 53 m and borehole yield range from 0.1 to 16 l/s. Groundwater in these intergranular aquifers occurs in shallow depths mainly ranging from 2 to 7 m bgl.

5.3.2. Fractured aquifers

The fractured aquifers in the study area are represented by the Natal Group sandstone, Dwyka Group tillite and the Vryheid Formation sandstone of the Ecca Group. The Natal Group is one of the best lithology for groundwater prospect characterized by average transmissivity of 8.32 m^2/day with maximum borehole yield and thickness of 18 l/s and 350 m, respectively within the study area. (Table 5.4). Groundwater in this unit is found along faults and fractures and is usually in a confined to semiconfined condition. Dwyka Group diamictite is characterized by very low hydraulic conductivities and very low-yielding boreholes (0.1-3.2 l/s) (Figure 5.6). According to Van Wyk (1963), favorable borehole yields in the tillite are found in low-lying sites on faults and major joints. The fractured Vryheid Formation sandstone is characterized by hydraulic conductivity, transmissivity and average borehole yield of 0.17 m/day, 6.3 m^2/day and 16 l/s,

respectively (Figure 5.8). This fractured sandstone forms relatively aquifer when compared to formations of the Ecca Group.

5.3.3. Weathered and fractured aquifers

The weathered and fractured rock units in the study area are minor aquifers made up of Jurassic dolerite intrusions, the Pietermaritzburg Formation shale of the Ecca Group and the granitic basement rocks. Groundwater in these units occur in intergranular interstices in the saturated weathered zone as well as in joints and fractures. The Karoo dolerites acts mostly as barriers to groundwater movement with boreholes drilled in this unit yielding from 0.5 to 3.2 l/s (Figure 5.8) with a maximum hydraulic conductivity of 0.5 m/day. The Pietermaritzburg Formation mainly comprises shale which normally act as an aquitard rather than aquifer with most of the groundwater circulate along the fracture zones. It is characterized by very low average hydraulic conductivity and transmissivity of 0.03 m/day and 0.28 m^2/day, respectively. The granitic basement units of the Mapumulo Group, Oribi Gorge and Mzumbe Suites are characterized by average hydraulic conductivity of 0.56 m/day and transmissivity of 3.9 m^2/day with borehole yields ranging from 0.2 - 8.3 l/s (Figure 5.6). These units have groundwater stored in weathered zones near the surface with very low storage capacity and the clay content from weathering of feldspars results into high porosity, but with low hydraulic conductivity.

Table 5.4: Mean hydraulic characteristics of the geological unit within the study area.

Geological Unit		**No of data sets**	**Thickness (m)**	**Hydraulic Conductivity (m/day)**	**Transmissivity (m^2/day)**	**Borehole Yield (l/s)**
Group/ Suite	**Rock type/ Formation**					
Maputaland Group	Alluvium & Estuarine deposits	11	2-73	6.5	32	6-36
	Berea Formation	7	0.5-45	5	406	2.5-45
	Bluff Formation	12	10-75	3.2	9.6	0.1-26
Ecca Group	Pietermaritzburg shale	36	15 - 105	0.03	0.28	0.02-2.4
	Vryheid Sandstone	96		0.17	6.3	0.01-16
Dwyka Group	Diamictite & Tillite	148	5-135	0.8	1.3	0.1-3.2
Natal Group	Sandstone & Siltstone	250	20-350	2.8	8.32	0.2-18

Mapumulo, Oribi and Mzumbe suite	Granitic Basement	177	-	0.56	3.9	0.02-8.3

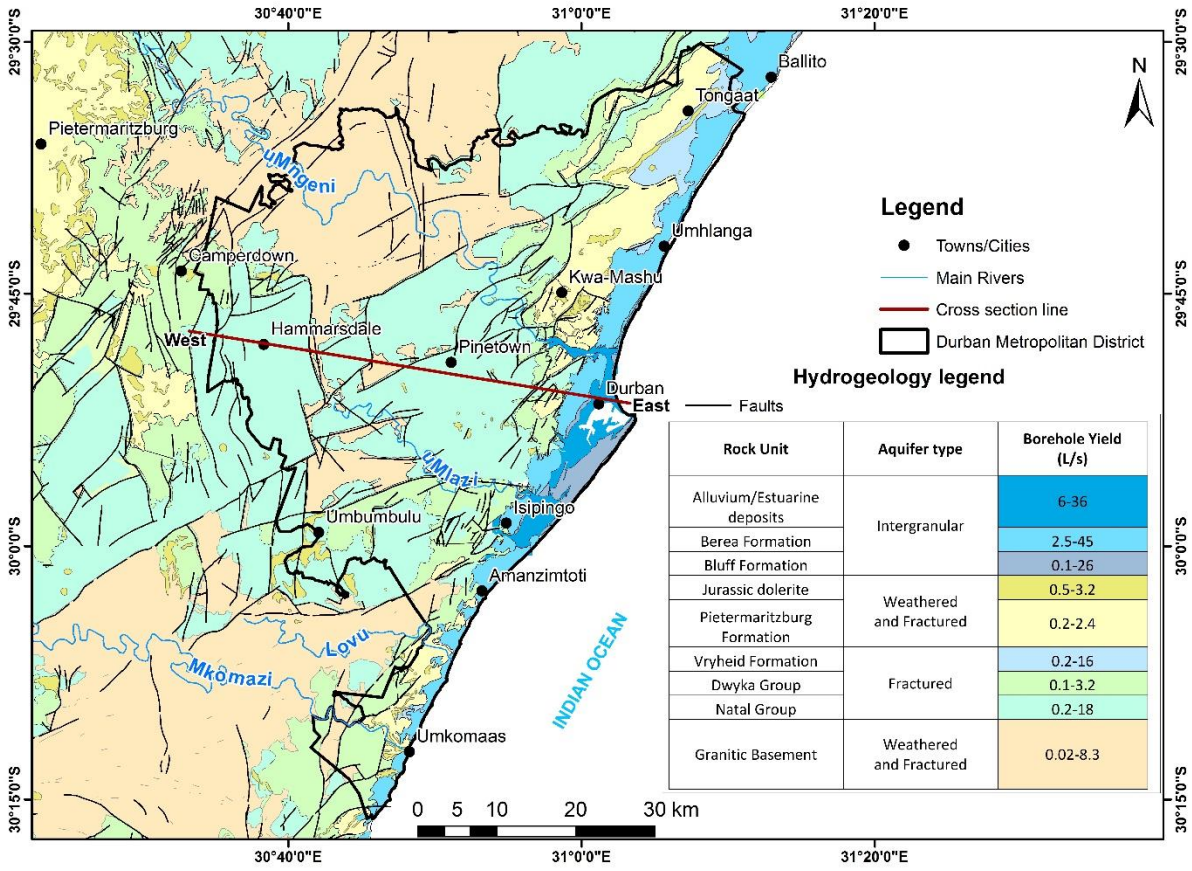

Figure 5.6: Hydrogeological map of the Durban Metropolitan region based on groundwater occurrence and borehole yields.

5.3.4. Groundwater levels and depth to groundwater

Depth to groundwater and groundwater level maps were developed from 716 historical borehole data sourced from the Groundwater Resource Information Project (GRIP), Durban Solid Waste (DWS) and various consultant databases. Depth to groundwater in the study area vary spatially, controlled by the local geology and topography. Groundwater occurs at shallow depths along the eastern coastal area and valley bottoms. The depth to groundwater is shallow in the coastal sediments of the Maputaland Group with average depth of 6 m below ground level (bgl). In the Natal Group, groundwater can be incepted at an average depth of 20 m bgl, while in the granitic

basement is characterized by deep water level, exceeding 45 m bgl. Generally, the depth to groundwater increase from east to west, following the topography (Figure 5.7).

Groundwater levels above mean sea level (amsl) have been used in constructing groundwater level contour map along with groundwater flow direction (Figure 5.8). The definition of groundwater flow direction is an essential component to water management plan as it is used to identify regions within which the groundwater is recharged and identifies potential contaminant flow paths (Saraf and Choudhary, 1998). The general groundwater flow direction in the study area is from west to east towards the Indian Ocean. Localized groundwater flow directions vary, indicating a complex flow pattern which is influenced by topography and geology. Groundwater flow gradient is steep within the granitic basement and gentle in the sediments. It can be observed that groundwater flow direction vectors converge at major rivers indicating that groundwater discharges into streams and surface water bodies. This can also be observed at Albert Falls dam, northwest of the study area, where groundwater is flowing into the dam/reservoir from all direction (Figure 5.8). According to the groundwater flow vectors, regional groundwater recharge occurs in the west and discharges into the Indian Ocean along the coast in the east, as expected.

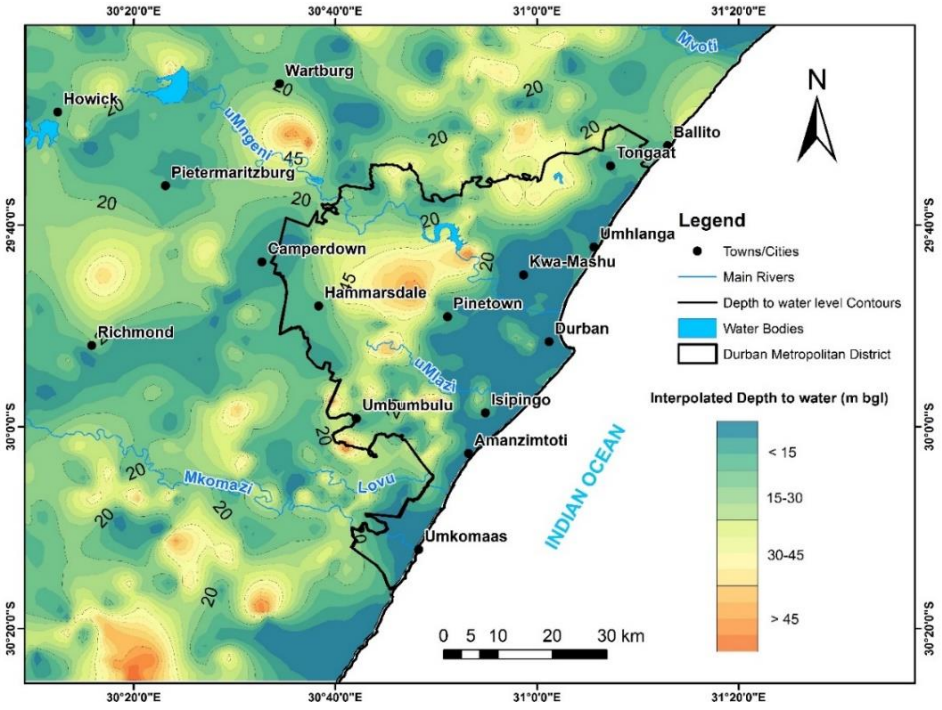

Figure 5.7: Depth to groundwater level map of the study area.

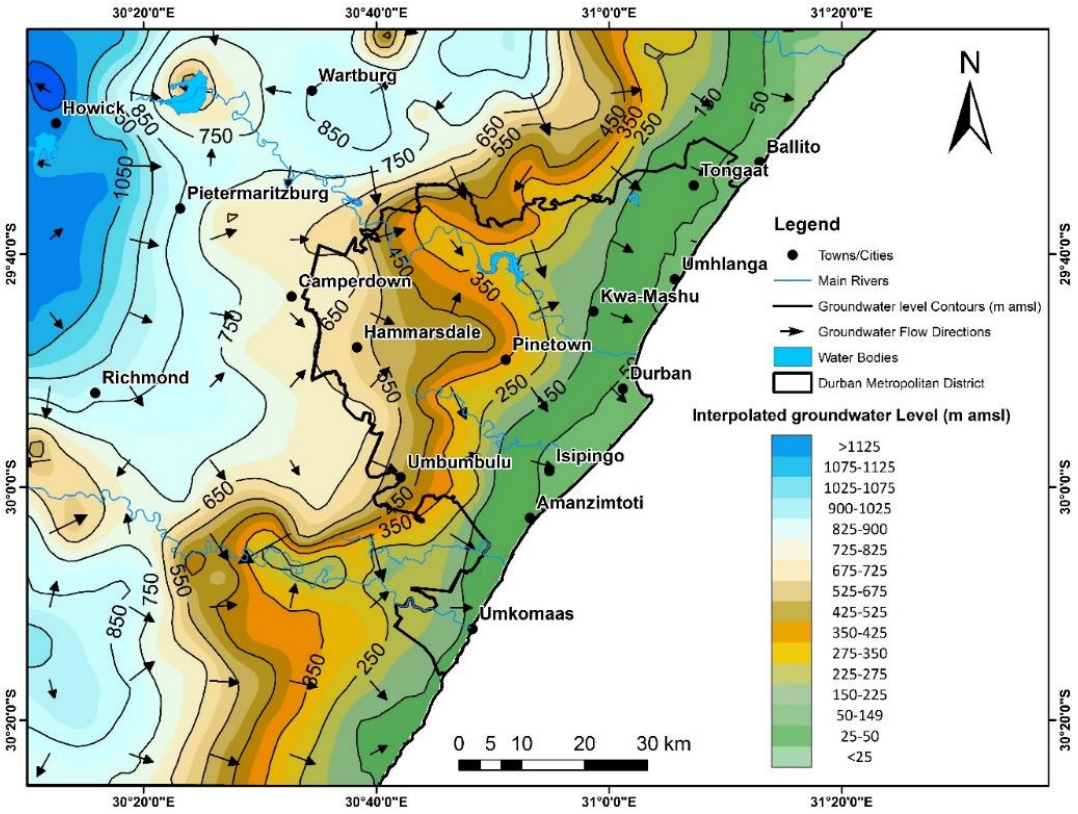

Figure 5.8: Contour map of groundwater levels with groundwater flow vectors across the study area

5.4. Hydrochemical Characteristics of the Durban Metropolitan Region

The chemistry of groundwater is generally governed by nature of geochemical reactions, solubility and availability of minerals, groundwater flow and anthropogenic influences (Drever, 1982; Howari and Banat, 2002). Hydrogeochemical processes within aquifers control the chemistry of groundwater and are commonly used to identify the source of groundwater, its circulation history and quality. Understanding the characteristics of groundwater hydrochemistry is essential in identifying the groundwater origins and also the hydrochemical processes occurring in the aquifer. The hydrochemical data generated during the course of this study is presented in Table 5.5 with trace elements presented in appendix 3.2.

Table 5.5: On site and laboratory measured surface water and groundwater physicochemical parameters generated during this research (concentration is in mg/l, EC is in µS/cm).

Sample No.	Sample source	Sample date	Temp	EC	TDS	pH	Eh	Mg	Ca	K	Na	Si	Cl	NO3	SO4	HCO3	Fe	Mn
ETM1	Borehole	18/07/2018	23	807	403	6.78	13.8	14.04	36.12	2.72	113.46	18.54	78.32	19.63	25.79	179.23	0.026	0.001
ETM2	Borehole	18/07/2018	23.2	1191	594	7.2	-10.6	36.32	27.22	20.74	148.54	24.85	93.25	0.68	0.75	348.37	3.630	0.278
ETM5	Borehole	19/07/2018	22.5	736	369	7.65	-35.3	9.45	59.56	7.71	90.01	18.23	44.62	22.86	20.59	229.55	0.010	0.001
ETM6	Borehole	19/07/2018	22.66	501	252	8.07	-55	5.91	11.32	1.66	92.99	19.30	36.45	24.46	18.54	113.35	0.025	0.001
ETM8	Borehole	19/07/2018	21.01	644	323	8.47	-75.5	17.63	77.42	7.21	47.87	13.29	33.14	2.39	15.04	0.00	0.030	0.006
ETM11	Borehole	20/07/2018	22.13	1530	765	8.55	-79	34.79	49.20	2.04	233.41	4.03	108.98	0.70	1.15	331.05	0.020	0.341
ETM15	Borehole	23/07/2018	22.4	661	331	6.89	-48.9	15.60	34.82	3.56	85.30	25.87	69.47	1.05	4.56	213.33	0.036	0.167
ETM17	Borehole	23/07/2018	22.38	226	114	6.88	13.6	8.66	15.93	2.44	26.94	22.74	18.47	4.36	10.11	132.88	0.101	0.039
ETM19	Borehole	23/07/2018	21.23	618	312	7.75	-29.7	17.98	42.14	3.03	66.28	21.56	52.95	0.67	1.19	255.98	7.251	0.477
ETM21	Borehole	25/07/2018	23.88	356	180	6.23	17	7.25	5.60	1.67	63.93	27.39	54.57	31.83	-	104.90	0.361	0.029
ETM22	Borehole	25/07/2018	22.02	107	57	6.95	14.9	5.05	3.79	0.71	14.71	5.48	27.91	3.71	3.64	175.52	0.096	0.137
ETM25	Borehole	26/07/2018	22.6	1267	634	7.36	3.4	31.99	32.64	2.71	199.82	15.59	102.90	1.06	30.26	247.09	0.017	0.275
ETM3	Spring	18/07/2018	20.49	204	104	6.94	9.5	8.29	8.24	1.71	27.81	6.68	28.52	2.17	8.30	108.49	7.069	0.080
ETM10	Spring	20/07/2018	18.52	196	99	7.46	-25.1	7.48	7.90	3.85	29.72	4.28	27.92	0.67	3.09	86.37	0.253	0.020
ETM7	Spring	19/07/2018	22.62	566	283	7.93	-50	5.36	6.12	4.07	112.53	16.34	48.14	6.49	34.49	114.92	0.044	0.014
ETM4	stream	18/07/2018	17.72	381	191	7.5	-17.4	11.23	13.11	4.63	51.08	8.10	55.28	2.98	17.73	141.07	0.234	0.083
ETM9	stream	20/07/2018	18.03	169	85	8.91	-94.3	7.04	4.01	1.22	28.80	7.45	42.79	0.96	4.54	47.38	0.500	0.027
ETM12	stream	20/07/2018	21.81	605	303	7.89	-7.8	18.67	13.04	1.34	90.33	9.17	72.42	0.79	7.25	145.27	0.165	0.275
ETM13	stream	20/07/2018	21.28	1500	750	6.92	2.4	32.95	19.75	9.84	229.08	6.31	-	0.65	15.69	76.80	0.042	0.029
ETM14	stream	20/07/2018	21.26	152	76	6.7	10.3	5.75	11.19	0.97	15.72	6.01	14.32	0.73	-	86.58	0.046	0.001
ETM16	stream	23/07/2018	20.13	381	191	7.7	-41.2	13.25	17.28	2.78	51.69	9.16	62.10	1.91	18.40	146.88	0.071	0.157
ETM18	stream	23/07/2018	15.45	119	62	8.85	-83	5.07	6.22	1.67	18.59	11.45	17.85	2.73	4.18	51.26	0.273	0.013
ETM20	stream	25/07/2018	20.36	322	167	8.29	-56	10.63	17.87	3.92	46.12	7.04	52.33	4.55	17.60	159.15	0.264	0.273
ETM23	stream	25/07/2018	18.75	353	177	8.4	-68.7	9.36	17.64	4.95	44.03	5.05	49.24	30.08	28.12	67.83	0.085	0.028
ETM24	stream	25/07/2018	17.44	434	222	8.11	-54.1	12.75	18.71	7.23	61.56	5.05	33.00	3.71	11.92	143.33	0.175	0.131
ETM26	stream	26/07/2018	18.46	478	240	7.55	-24.3	12.17	16.09	8.99	74.36	1.08	40.68	6.31	14.84	132.51	0.093	0.027

5.4.1. Analysis of specific electrical conductivity distributions

Electrical Conductivity (EC) provides useful preliminary information of groundwater quality of the area. The spatial distribution of EC across the study area is given in Figure 5.10 and varies from 40 to 6800 µS/cm with the mean value of 718 µS/cm. The EC of groundwater decreases generally from the coast inland with areas around Camperdown, Durban and Ballito with very high EC values. These high EC values interpreted to be associated to land use activities, such industries, landfills and proximity to the coast. Based on EC the general hydrochemical quality of groundwater within the Durban Metropolitan is good except in areas were EC exceeds 1500 µS/cm (Figure 5.9). The high EC around Camperdown can be associated with the Ferroalloys Landfill.

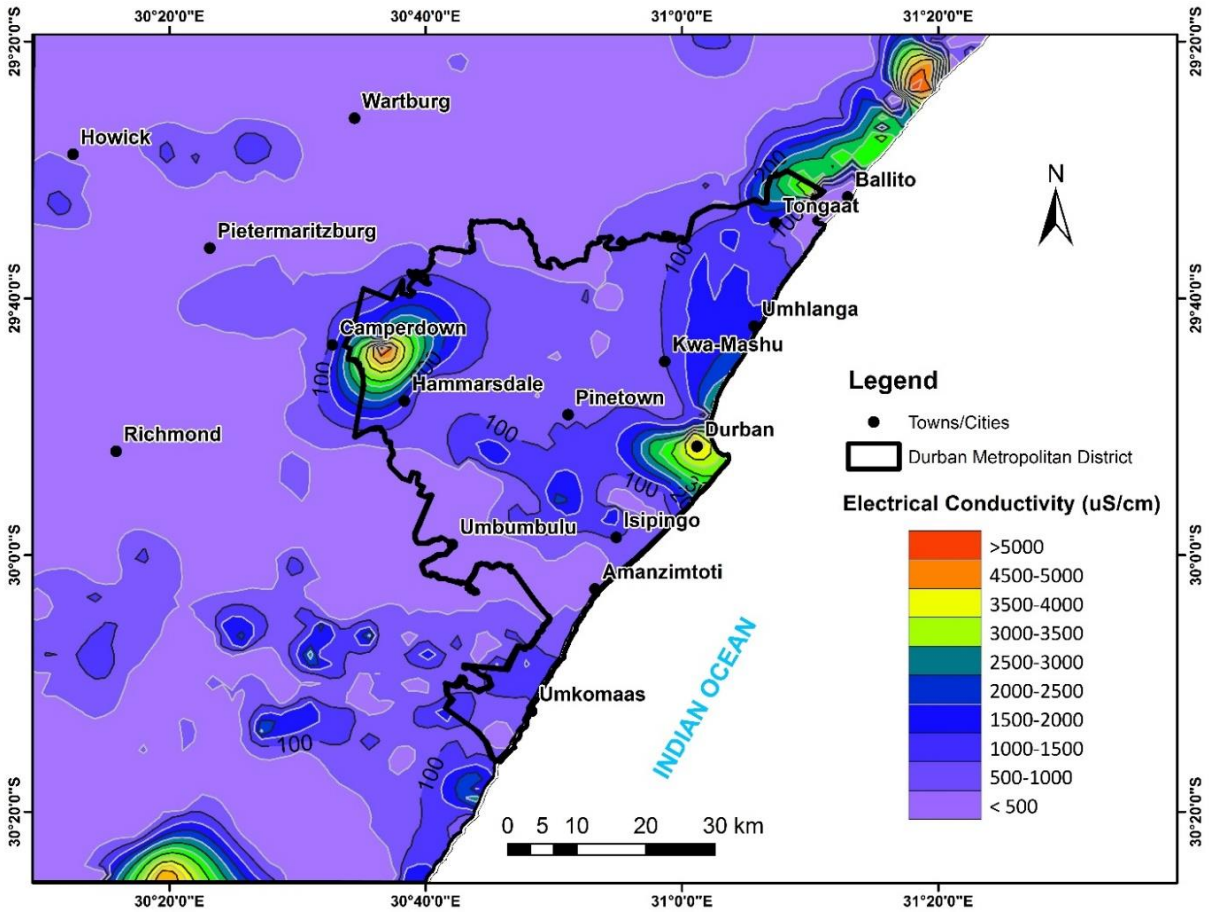

Figure 5.9: Spatial distribution of EC across the study area.

5.4.2. Statistical analysis of hydrochemical data

Statistical analysis of hydrochemical data was undertaken using all the hydrochemical data sets collected from 147 boreholes located across the study area covering all hydrogeological units in order to illustrate the distinctions and similarities between different hydrochemical

parameters. The descriptive statistics (Table 5.6) shows the pH range from 6.3 to 9.9, revealing slightly acidic to alkaline groundwater. The electrical conductivity (EC) varied widely from 40 to 6800 µS/cm. According to the salinity classification of Mondal et al. (2008), the groundwater in the study area falls into the categories of freshwater (< 1500 µS/cm), brackish (1500-3000 µS/cm), and saline (> 3000 µS/cm). Based on this classification, 65% of the borehole were of freshwater quality, 23% were brackish and 12% were saline groundwater. Similar to the EC, total dissolved solids (TDS) also showed a wide variation (34- 4363 mg/l). The variations in EC and TDS reflected a considerable variation in the hydrochemical characteristics in different parts of the study area with different types of hydrochemical facies. Most of the groundwater is characterized by considerable variations in the concentration of Na^+ (3.1- 844 mg/L), K^+ (0.38-30.98 mg/l), Mg^{2+} (1.3 – 274.2 mg/l), Ca^{2+} (1.5 - 294.6 mg/l), Cl^- (1.5 - 1967 mg/l), SO_4^{2-} (2 - 621.9 mg/l) and HCO_3^- (35.3 – 682 mg/l). These variations highlight that the groundwater chemistry is heterogeneous due to variation in aquifer mineralogy, hydrogeochemical processes and proximity to the coast.

Table 5.6: Descriptive statistics of groundwater hydrochemical parameters (all concentrations in mg/l and EC in µS/cm)

Variable	No. Of data sets	Range	Minimum	Maximum	Mean	Std. Deviation
pH	147	3.34	6.25	9.59	7.56	0.51
EC	147	6760.00	40.00	6800.00	718.06	827.55
TDS	126	4329.00	34.00	4363.00	493.03	561.16
Na	127	841.50	3.10	844.60	90.17	120.93
K	126	30.60	0.38	30.98	3.02	4.14
Mg	147	272.90	1.30	274.20	18.83	27.42
Ca	147	293.10	1.50	294.60	31.31	36.52
NH4	127	92.78	0.02	92.80	0.78	8.23
Cl	147	1966.10	1.50	1967.60	124.52	218.64
SO4	128	619.90	2.00	621.90	33.25	72.41
HCO3	147	682.00	35.30	682.00	132.34	97.32
Si	147	42.08	1.20	42.08	4.17	7.15

To understand the relationship between the various hydrochemical parameters, a bivariate Pearson's correlation matrix of the measured variables was undertaken (Table 5.7). Pearson correlation reveal statistical relationships between variables with Pearson's product-moment correlation (r) as a measure of linear dependence between two variables that is expressed as the covariance of the two variables divided by the product of their standard deviation. The resultant dimensionless r value ranges between +1 and -1, where 1 is perfect positive linear. In this study,

correlation among variables with $r \geq 0.5$ are regarded as meaningful. Correlation strength of variables are described as very strong (r = 0.8 - 1), strong (0.70 - 0.79), moderate (r = 0.5 - 0.69), weak (r = 0 - 0.49) (Borradaile, 2003).

A strong to moderate positive correlation was observed between EC and several major ions, which include Na^+, K^+, Mg^{2+}, Ca^{2+}, Cl^-, SO_4^{2-} and HCO_3^-, suggesting the obvious contribution of these major ions to salinity (EC). When compared to each other, excluding HCO_3^-, the ions have a strong significant correlation. The moderate correlation between pH and HCO_3^- could be an indication that groundwater has a high buffering capacity as indicated in Table 5.6. The moderate to strong correlation between sulphate (SO_4^{2-}) and all other major ions (Na^+, K^+, Mg^{2+}, Ca^{2+}, and Cl^-) is observed. A very strong correlation between Na^+ and Cl^- (r = 0.93) is observed and this relationship may be explained by the proximity of the study area to the Indian due to pollution from various land uses across the study area.

Table 5.7: Pearson correlation matrices for groundwater hydrochemical data

Variables	pH	EC	TDS	Na	K	Mg	Ca	NH4	Cl	SO4	HCO_3	Si
pH	1											
EC	.288	1										
TDS	.307	.306	1									
Na	.298	.966	.322	1								
K	.090	.583	.127	.503	1							
Mg	.213	.908	.212	.814	.617	1						
Ca	.263	.884	.231	.793	.572	.890	1					
NH4	-.09	.064	-.051	.016	.088	-.021	.143	1				
Cl	.197	.974	.241	.928	.651	.927	.867	.056	1			
SO4	.112	.851	.069	.823	.600	.846	.847	.299	.867	1		
HCO3	.505	.612	.435	.686	.082	.452	.540	.060	.463	.371	1	
Si	.043	.294	.119	.279	.000	.314	.353	-.032	.240	.245	.123	1

Factor analysis in the form of PCA with varimax rotation was performed on 12 hydrochemical parameters in order to identify the factors responsible for the groundwater chemistry in the study area (Table 5.8). Three components, with eigenvalues greater than 1, were extracted explaining 75% of the hydrochemical variation. These components can therefore be used to explain the hydrochemical processes without losing the most important characteristics. Component 1 contains most of the variance (54.1%), having high positive loading factors for EC, Na^+, K^+, Mg^{2+}, Ca^{2+}, Cl^- and SO_4^{2-} concentrations. The loading of these hydrochemical variables with EC in factor 1 could be interpreted as major parameters contributing to the

groundwater salinity. Industrial effluent, sewer leakage and wastewater could also be source of these constituents as the study area is located in urban to peri-urban environmental setting. High loading of SO_4^{2-} indicates anthropogenic impact on the environment. Component 2 accounts for 12.8% of the explained variance in the hydrochemical data and shows high loading for pH, TDS and HCO_3^-. The HCO_3^- could be the results of weathering and dissolution of carbonate minerals, rootzone hydrogeochemical and redox processes (Freeze and Cherry, 1979; Appelo and Postma, 2005). It also reveals the common dependency of pH on HCO_3 and HCO_3^- contribution to groundwater salinity in the form of TDS. 8.8% of the variance is explained in component 3, with high loading for NH_4^+ and Si.

The relationship of various hydrochemical variables relative to the dominant components determined in Table 5.8 for the principal component analyses PCA is illustrated in Figure 5.10. The presence of NH_4 in in groundwater is most likely related to recharge from industrial and domestic wastewater leakage, sewage sludge and agricultural return flow. Si is derived from the weathering of granite, sandstone and conglomerates from the study area.

Table 5.8: results of principal components factors analysis of hydrochemical data for all groundwater samples

Variable	Communalities		Component (Factors)		
			1	2	3
pH	1.000	0.578		0.754	
EC	1.000	0.977	0.963		
TDS	1.000	0.507		0.710	
Na	1.000	0.892	0.899		
K	1.000	0.585	0.714		
Mg	1.000	0.922	0.953		
Ca	1.000	0.889	0.918		
NH4	1.000	0.537			0.723
Cl	1.000	0.963	0.979		
SO4	1.000	0.887	0.939		
HCO3	1.000	0.772		0.851	
Si	1.000	0.565			0.733
Initial Eigenvalues	**Total Explained**		6.488	1.535	1.052
	% of Variance		54.066	12.794	8.771
	Cumulative %		54.066	66.861	75.631

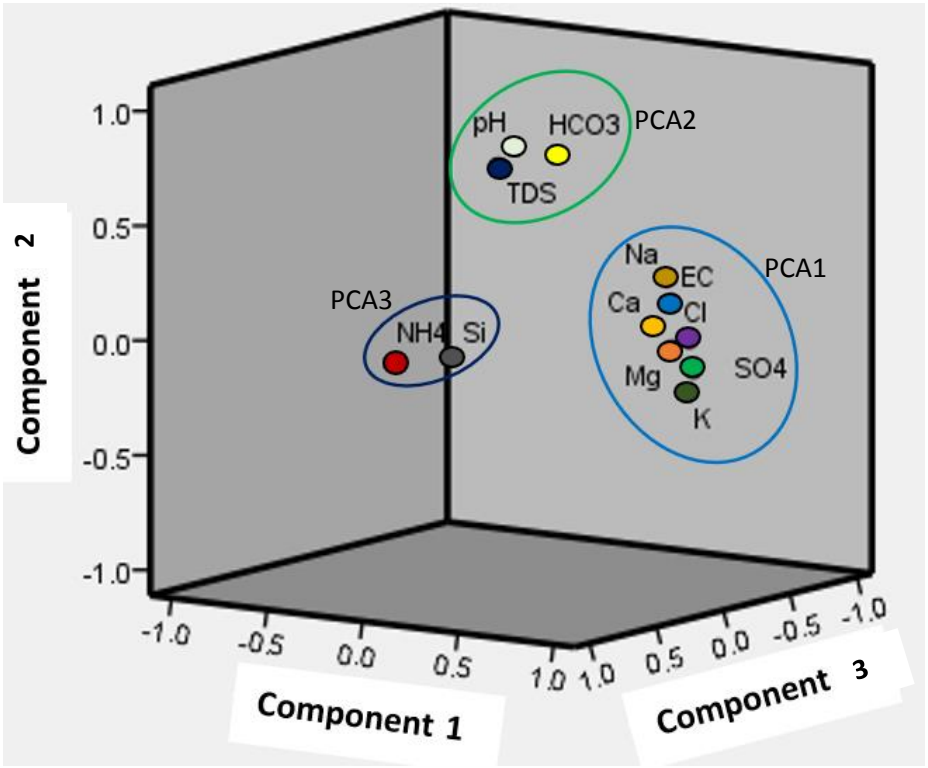

Figure 5.10: Principal component plot of the variables in rotated space.

Furthermore, hierarchical cluster anlysis was undertaken on the hydrochemical data of 23 variables using Ward linkage method in Q-mode and based on the squared Euclidean distance between groups). Cluster analysis classifies the set of observed hydrochemical data within two or more groups based on combination of interval hydrochemical variables (Brown, 1998). The results of the cluster analysis is shown in Figure 5.11. The variables cluster in 2 major groups (C1 and C2), the first group (C1) shows the similarity between the trace elements (Ni, Cu, As, Cr, Li, Al, Zn, Mn, Fe) and the Major ions (Mg, K, NO_3, SO_4, Ca, Na, HCO_3, and Cl), including pH and Eh. Group 2 (C2) shows a cluster of EC and TDS indicating their obvious linear relationship. The minor group C1-1 shows a cluster of trace elements with pH and Eh. These metal ions are generally immobile under neutral to alkaline groundwater conditions. Thus, the relationship with pH and Eh indicates the mobility and solubility of these metals is dependent on pH and Eh conditions. The presence of strong acids (NO_3^- and SO_4^{2-}) within the group indicates some sort of anthropogenic impacts as well. Group C1-2 indicates that Na, Cl and HCO_3 contribute relatively more to the salinity of groundwater when compared to other ions.

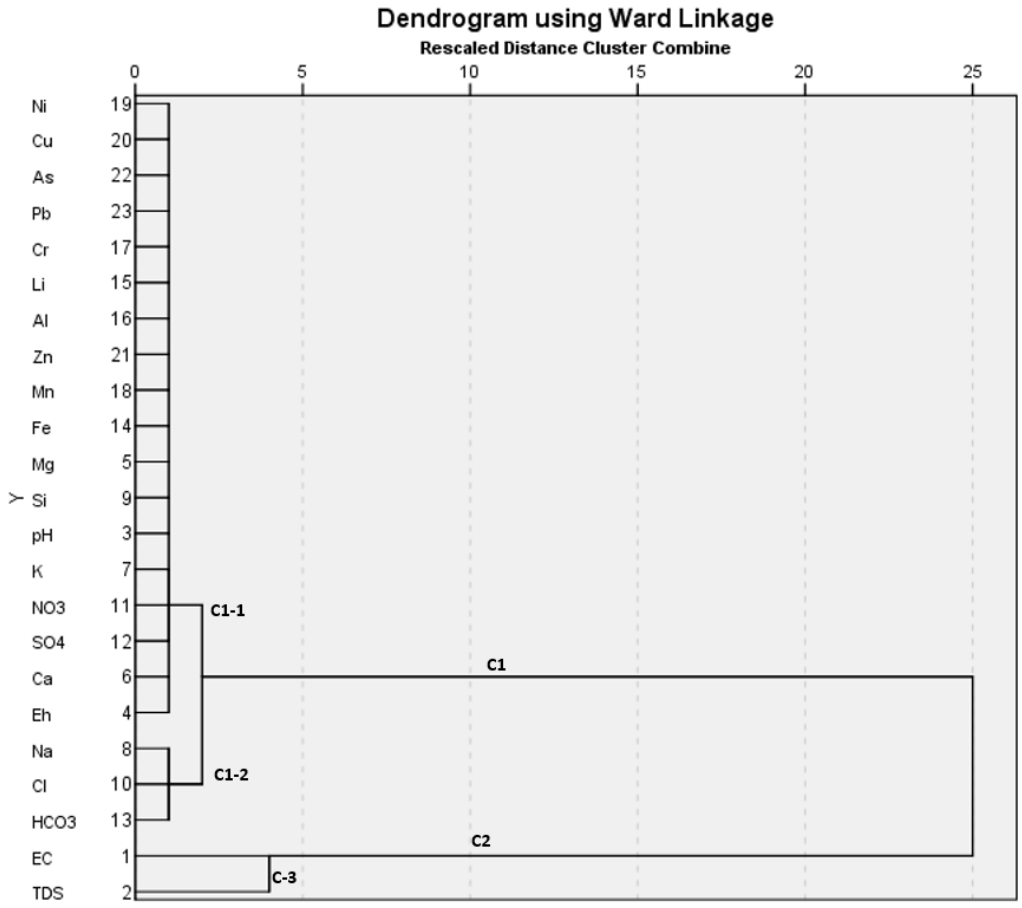

Figure 5.11: Dendogram for 23 hyrochemical variables across the study area

5.4.3. Hydrogeochemical processes controlling groundwater chemistry and hydrochemical facies

To identify the dominant mineral in the rock weathering process across the aquifers of the study area, molar ratio were plotted (Figure 5.12). According to Meybeck (1987), the milligram equivalent ratio of $(Na^+ + K^+)/Cl^-$ can be an indicator of the sources of cations and of the occurrence of silicate weathering, where a ratio greater than 1 implies Na^+ released from silicate weathering and a ratio of 1 indicates halite dissolution. In fact, the primary effect of silicate weathering on the groundwater chemistry is the addition of cations and silica (Appello and Postma, 2005). The scatter plot of Cl^- versus $Na^+ + K^+$ (Figure 5.12a) shows that most samples are distributed along but below the 1:1 line with only a few above, implying that (Na^+ and K^+) are mainly released into solution from the weathering of silicate minerals. It also indicates that silicate weathering is the primary hydrochemical process occurring within the aquifers. Additionally, the excess of $(Na^+ + K^+)$ over Cl^- indicates cation exchange processes occurring within the aquifers.

The plot of (HCO_3^- + SO_4^{2-}) versus (Ca^{2+} + Mg^{2+}) (Figure 5.12b) shows that most samples fall above and along the 1:1 line and that some of the granitic basement plot below the 1:1 line, indicating that the dissolution of silicate is again the main sources of Ca^{2+} and Mg^{2+}. According to Masindi and Abiye (2018), such plots are useful in revealing the likely chemical reactions in groundwater, particularly the extent to which ion exchange reactions influence groundwater quality. The excess of Na^+ + K (Figure 5.12a) and deficiency of Ca^{2+} + Mg^{2+} (Figure 5.12b) indicate the occurrence of cation exchange hydrogeochemical processes within the aquifers (Garrels and McKenzie, 1971; Holland, 1978).

The cluster of granitic basement samples along either side of the 1:1 line indicates that both ion exchange and reverse ion exchange are occurring within aquifer (Figure 5.12b). Groundwater samples from the Primary aquifers and Ecca Group rocks plot close and on either side of the 1:1 line (Figure 5.13). According to Hem (1985), this trend indicates some halite dissolution. However, there is no known source of halite across the study area. This indicates that the groundwater chemistry within these aquifers is controlled by the marine depositional environment of the sediments. A good linear relationship between the concentrations of Cl^- and Na^+ with a slope of about 1 is explained by the proximity of the study area to the Indian Ocean. Na/Cl ratio greater than 1 can be linked to silicate weathering with the increase in Na ions suggesting ion exchange and reduction in Na indicating reverse ion exchange.

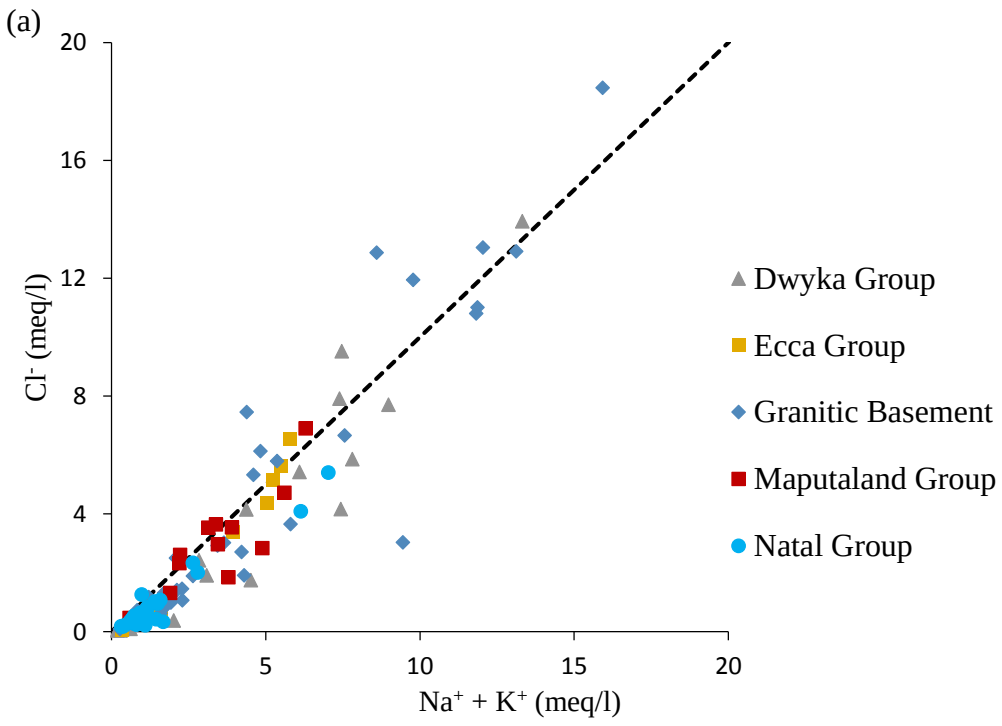

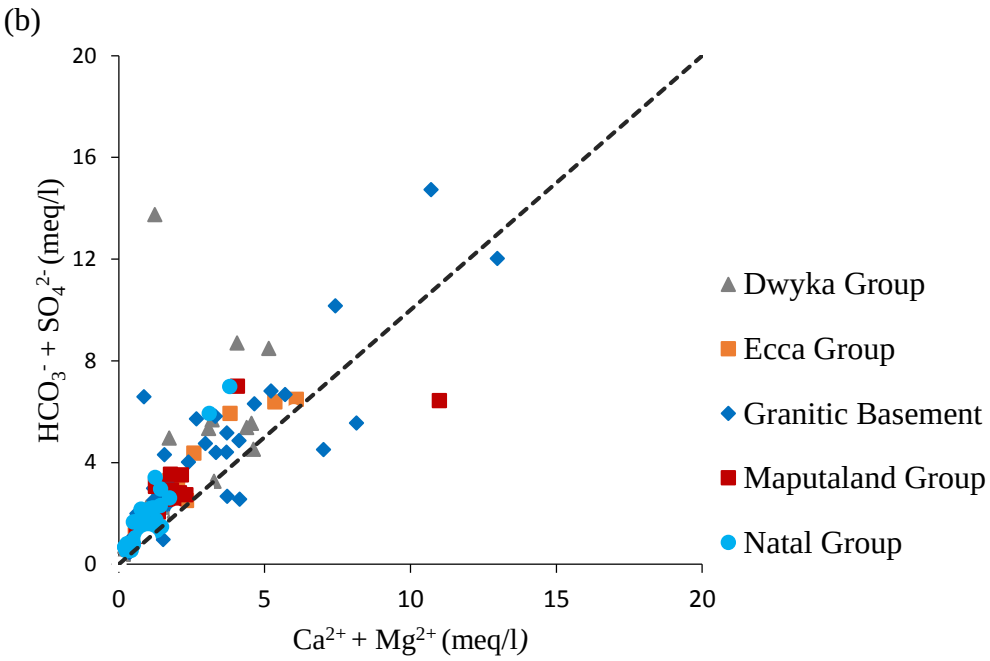

Figure 5.12: Bivariate plot of ionic relation. (a) Cl^- versus $(Na^+ + K^+)$. b) $(HCO_3^- + SO4^{2-})$ versus $(Ca^{2+} + Mg^{2+})$.

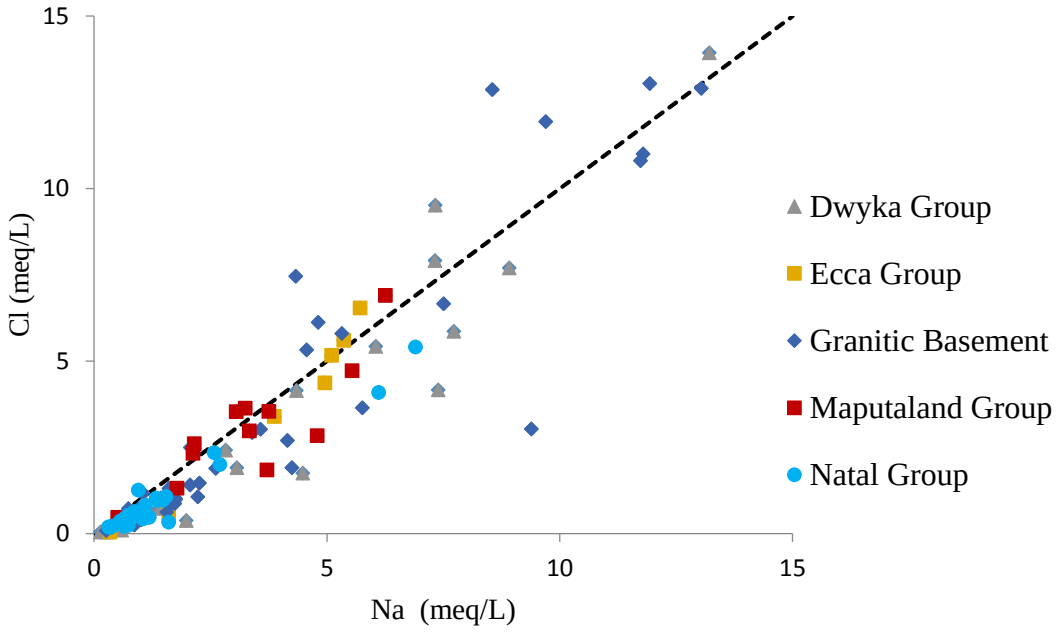

Figure 5.13: Bivariate plot of Na^+ versus Cl^- (mg/l).

The Piper diagram (Piper, 1944) was used to understand the influence of saline and non-saline sources on groundwater chemistry in the study area. Water samples were classified as various chemical types on the Piper diagram based on each geological unit in which the boreholes were drilled (Figure 5.14). Based on the classification of Langguth (1966), the plots demonstrate that

groundwater in the study area is dominated by alkalis (Na and K) over alkaline earths (Ca and Mg) and that weak acids (HCO_3) exceed strong acid (SO_4). The dominant hydrochemical facies present in the study area have the following order: Na-Cl (39% of boreholes) > mixed Ca-Na-HCO_3 (36% of boreholes) > Ca-HCO_3 (20.5 % of boreholes) > Ca-Mg-Cl (3 % of boreholes) > Na-HCO_3 (1.5% of boreholes) (Figure 5.14). This indicated that groundwater was enriched with chloride and sodium followed by calcium and bicarbonate then magnesium. Thus, sea water influence along the coast, dissolution of mineral and ion exchange reactions with clay minerals play a major role in controlling groundwater chemistry in the study area. The Na-Cl-HCO_3 facies are mainly dominant in boreholes drilled in the Maputaland Group primary aquifers and Dwyka Group fractured aquifers. The mixed Ca-Na-HCO_3 facies is dominated in boreholes drilled in the granitic basement (Figure 5.14).

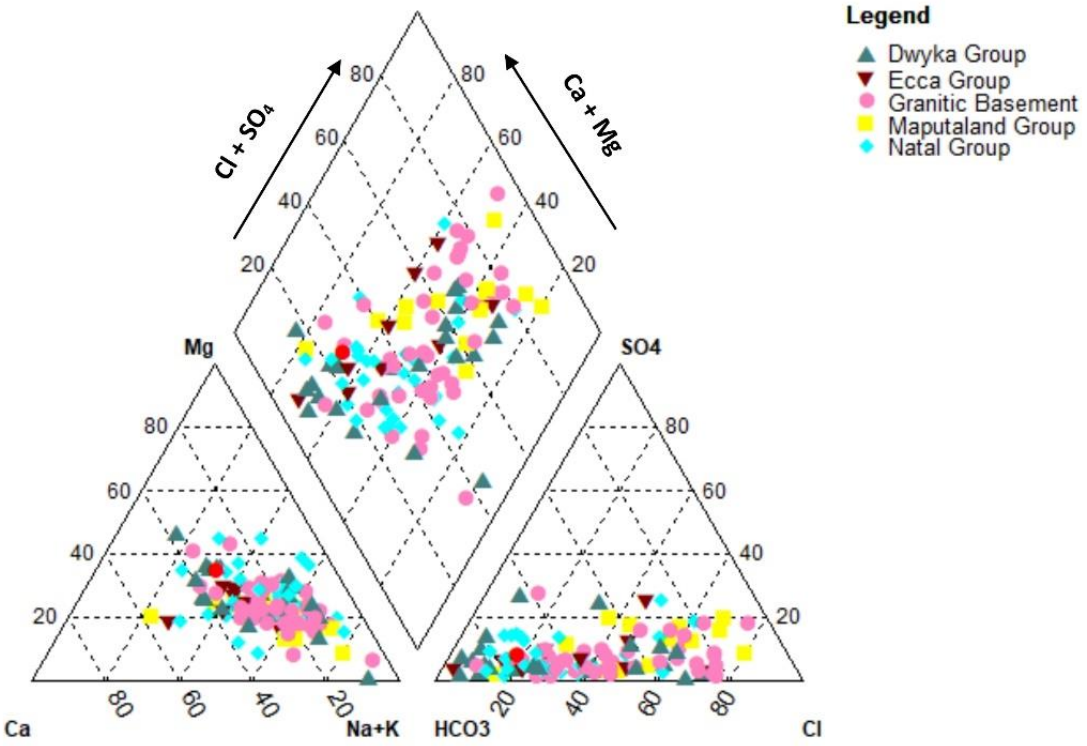

Figure 5.14: Piper diagram showing groundwater hydrochemical facies in the study area.

Figure 5.15 further illustrate the spatial distribution of hydrochemical facies across the study area. The Maputaland Group primary aquifers, because of their location and depositional history, are characterized by a mainly Na-Cl type water. This indicates marine influences, leaching of minerals during regional groundwater circulation and impacts from anthropogenic sources such as sewage leakage in the urban setting of the study area. The fact that mixed groundwater hydrochemical type prevails in the study area is supported by data plotted on

Durov diagram (Durov, 1984) (Figure 5.16), where 75% of boreholes plot along the dissolution or mixing line. Based on the classification of Lloyd and Heathcoat (1985), this trend can be attributed to fresh recent groundwater recharge exhibiting simple dissolution and mixing processes.

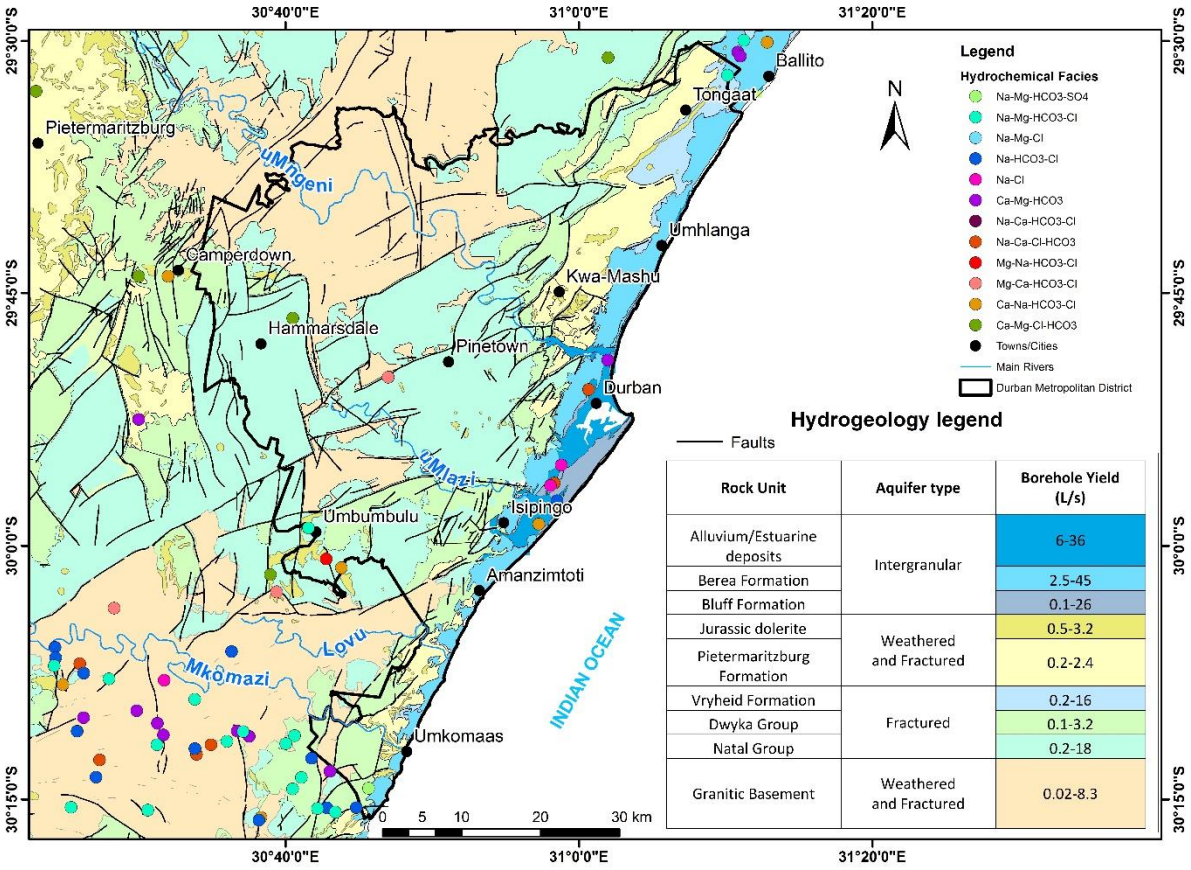

Figure 5.15: Spatial distribution of hydrochemical facies across the study area.

5.4.4. Environmental isotope characteristics

Stable and radioactive environmental isotopes have been used for more than half a century to study hydrological systems and have proved useful particularly for understanding groundwater systems. The most frequently used environmental isotopes include heavy isotopes of the water molecule, hydrogen (^{2}H and ^{3}H) and oxygen (^{18}O). The stable isotope ratios of oxygen and hydrogen in groundwater studies are useful tools to differentiate between saline origins and to help understand various sources of recharge processes to groundwater due to their sensitivity to physical processes such as atmospheric circulation, groundwater mixing and evaporation (Dansgaard, 1964; Clark and Fritz, 1997; Edmunds *et al*., 2003; Butler, 2007). In semi-arid regions, like South Africa, evaporation could be an important process influencing groundwater chemistry (Li et al., 2016). A total of 26 groundwater and surface water samples distributed

across the study area were analyzed for stable isotopes (Table 5.9). The stable isotope plot of Figure 5.17 shows that these water samples plot within a narrow range along the local meteoric water line (LMWL) indicating that

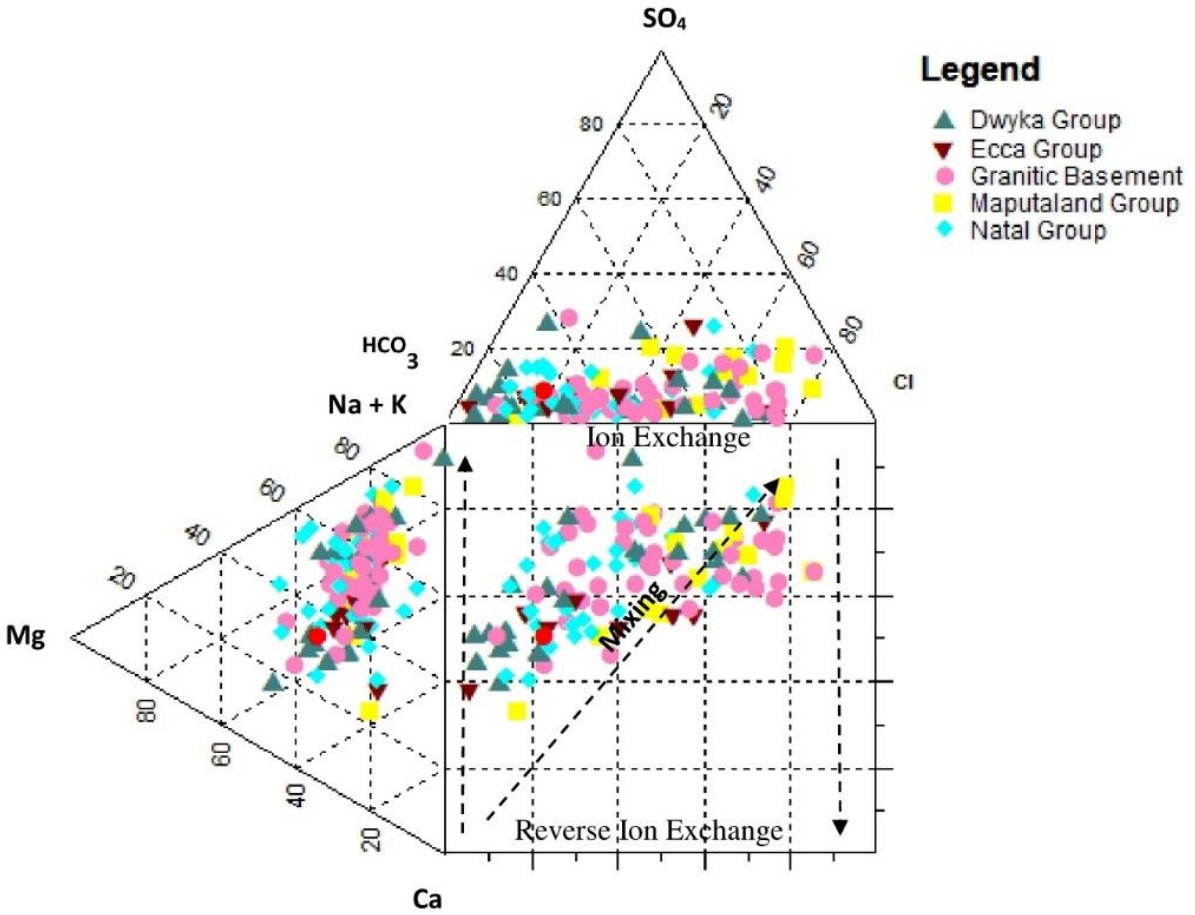

Figure 5.16: Durov diagram depicting hydrochemical processes influencing groundwater chemistry.

groundwater and surface water samples have the same rainfall source. The scattering of samples into groups along the LMWL (Figure 5.17) indicate that group I samples are relatively depleted in the heavy isotopes because of the fact that the groundwater was recharged from local precipitation without evaporation prior to recharge; Group II samples includes both surface and groundwater samples, where the groundwater samples may have been recharged from these surface water sources revealing surface water-groundwater interactions; Group II samples are surface water samples that are characterized by a relatively enriched isotopic signal compared to Group I and Group II samples, indicating evaporation.

The detectable groundwater tritium signatures were observed throughout the study area, with tritium activity values ranging from 0.1 TU to 1.9 TU (Figure 5.18). This is indicative of active recharge of the various aquifers given that the background tritium activity in the South Africa

rainfall is 2 TU (IAEA, 2012). Further comparison of the measured tritium activity with the classification reported by Clark & Fritz (1997), indicate that the majority of the groundwater samples show a mixture between sub-modern and recent recharge signature. This active recharge means that the groundwater in the study area is vulnerable to pollution unless proper landuse management is put in place.

Table 5.9: Environmental isotope data generated during the study.

Sample No.	source	Sample date	EC (µS/cm)	pH	Eh (mV)	δ D (‰)	δ ^{18}O (‰)	Tritium (TU)
ETM1	Borehole	18/07/2018	807	6.78	13.8	-10	-3.51	0
ETM2	Borehole	18/07/2018	1191	7.2	-10.6	-11.2	-3.75	1.5
ETM3	Spring	18/07/2018	204	6.94	9.5	1.4	-1.17	1.9
ETM4	stream	18/07/2018	381	7.5	-17.4	-2.4	-1.9	
ETM5	Borehole	19/07/2018	736	7.65	-35.3	-7.4	-2.83	1.5
ETM6	Borehole	19/07/2018	501	8.07	-55	-5.7	-2.47	1
ETM7	stream	19/07/2018	566	7.93	-50	-0.8	-1.56	1.2
ETM8	Borehole	19/07/2018	644	8.47	-75.5	-8.6	-3.32	0.7
ETM9	stream	20/07/2018	169	8.91	-94.3	-6.3	-2.73	
ETM10	Spring	20/07/2018	196	7.46	-25.1	15.6	2.22	1.8
ETM11	Borehole	20/07/2018	1530	8.55	-79	-9.3	-3.45	0.8
ETM12	stream	20/07/2018	605	7.89	-7.8	-2.6	-2.21	
ETM13	stream	20/07/2018	1500	6.92	2.4	-7.2	-2.59	
ETM14	stream	20/07/2018	152	6.7	10.3	-7.8	-2.39	
ETM15	Borehole	23/07/2018	661	6.89	-48.9	-10.8	-3.5	0.1
ETM16	stream	23/07/2018	381	7.7	-41.2	-3.4	-1.9	
ETM17	Borehole	23/07/2018	226	6.88	13.6	-11.6	-3.4	0.9
ETM18	stream	23/07/2018	119	8.85	-83	-8.9	-2.86	
ETM19	Borehole	23/07/2018	61.8	7.75	-29.7	-10.8	-3.01	0.5
ETM20	stream	25/07/2018	322	8.29	-56	-0.1	-1.21	
ETM21	Borehole	25/07/2018	356	6.23	17	-12.9	-3.64	1.1
ETM22	Borehole	25/07/2018	107	6.95	14.9	-15.8	-3.79	1.9
ETM23	stream	25/07/2018	353	8.4	-68.7	-2.1	-1.4	
ETM24	stream	25/07/2018	434	8.11	-54.1	-0.2	-1.38	
ETM25	Borehole	26/07/2018	1267	7.36	3.4	-9.4	-3.59	0.6
ETM26	stream	26/07/2018	478	7.55	-24.3	-1.5	-1.58	

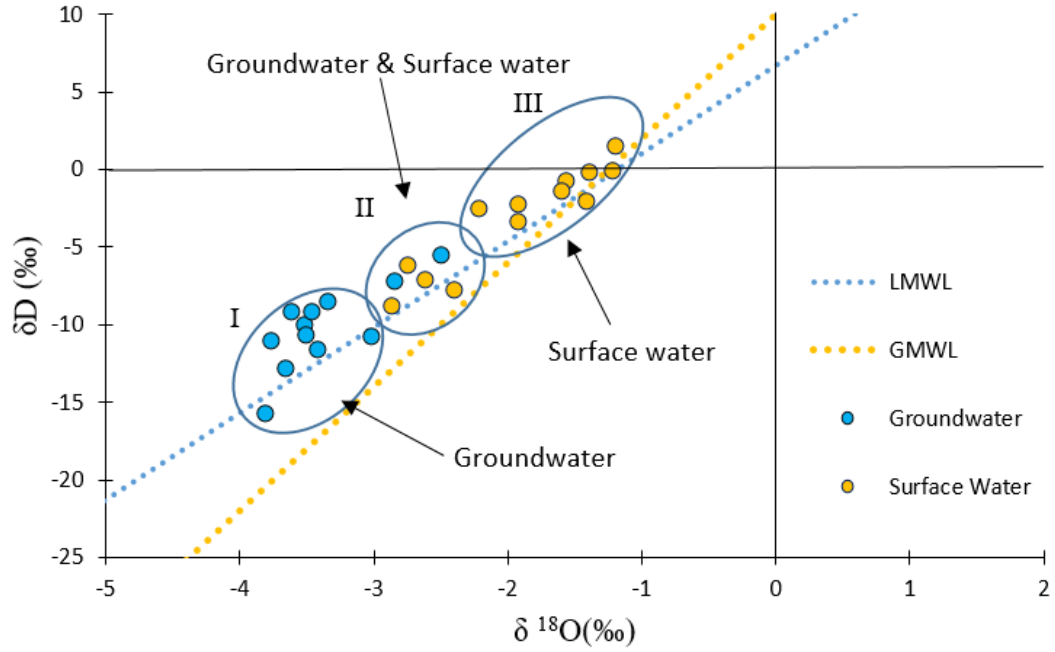

Figure 5.17: Stable isotopes, Oxygen-18 and deuterium plot for samples across the study area (note that GMWL stands for global meteoric line (Craig, 1961a)).

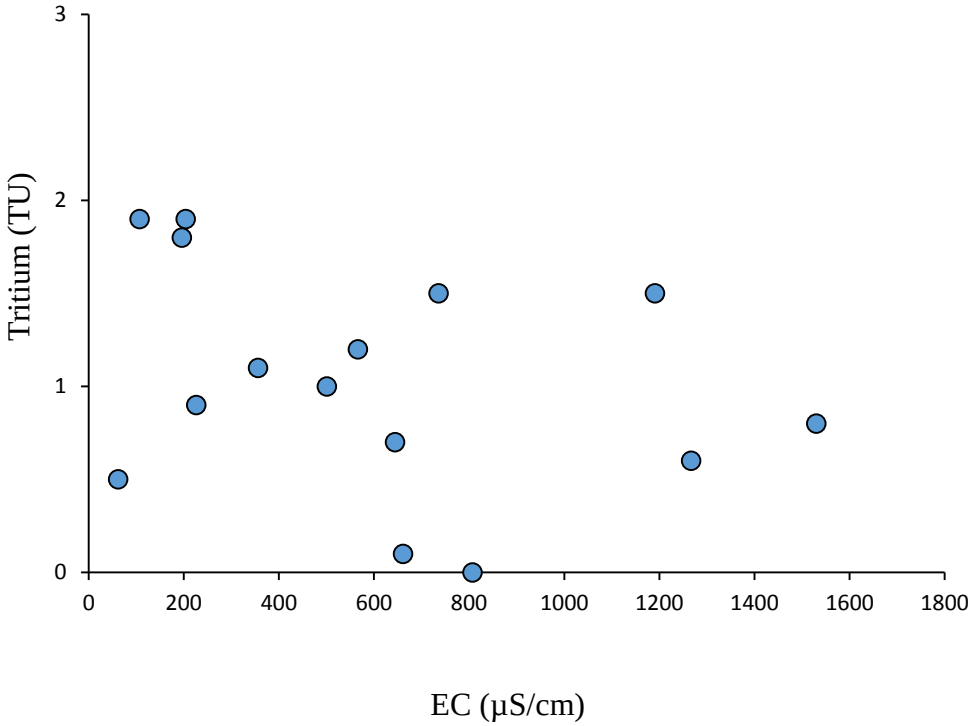

Figure 5.18: Tritium versus EC plot for groundwater samples across the study area.

5.4.5. Trace element composition of surface and groundwater

Heavy metals are among the most persistent pollutants in groundwater and surface water systems under natural conditions (Arnason and Fletcher, 2003). High concentration of these metals can be released into the water environment as a result of leaching from bedrocks, atmospheric deposition and discharge of urban and industrial waste water (Soars et al., 1999; Yang and Rose, 2005). The results of trace elements descriptive analysis for 26 samples collected across the study area during the July 2018 field campaign are presented in Table 5.10. All trace metals except Fe and Mn have concentration within the permissible limits of drinking water. The concentration of iron from the collected samples ranged from 9.98 to 7250.4 µg/l, with mean concentration of 804.48 µg/l, which is above the permissible limit (300 µg/l or 0.3 mg/l, WHO, 2017; SANS 2014). Mean concentration is above the maximum permissible limits for Mn (111.931 µg/l). This indicates that in some areas there is a possibility of Fe and Mn toxicity for the respective water sources and needs attention.

Table 5.10: Discriptive statistics for trace elements across the study area (concentration in µg/l).

Variables	No of data sets	Minimum	Maximum	Mean	Std. Deviation
EC	26	107	1530	557.85	407.831
TDS	26	57	765	280.15	203.200
pH	26	6.23	8.91	7.6127	0.71305
Fe	26	9.979	7250.939	804.479	1996.520
Li	26	3.000	33.253	7.611	9.426
B	26	41.375	536.537	126.492	103.080
Al	26	14.472	391.050	55.477	70.806
V	26	0.040	4.094	0.914	1.009
Cr	26	0.108	12.137	1.643	3.021
Mn	26	0.590	476.868	111.931	131.081
Co	26	0.046	0.873	0.228	0.192
Ni	26	1.565	8.190	3.389	1.400
Cu	26	0.585	5.303	2.234	0.965
Zn	26	13.766	153.429	61.107	46.295
Rb	26	0.216	15.281	3.115	3.250
Mo	26	0.040	1.885	0.389	0.420
Hg	26	0.017	0.107	0.047	0.022
Pb	26	0.071	0.801	0.282	0.171

CHAPTER 6

HYDROCHEMICAL CHARACTERISTICS OF WATER RESOURCES AROUND LANDFILL SITES WITHIN THE STUDY AREA

6.1. Introduction

95% of South Africa's waste is disposed of in landfills producing leachate which infiltrates to the groundwater and runoff to surface water (Strachan *et al*., 2002). It is, therefore, necessary to assess the hydrochemistry of water resources around landfills so as determine the state and quality of the water resources around these sites (Appelo and Postma, 2005). According to various sources (Christensen *et al*., 1994; Bjerg *et al*., 2014; Lu *et al*., 2012), water soluble pollutants from municipal landfill can be divided into four groups: 1) water soluble organic substances and volatile fatty acids; 2) inorganic macro nutrients such as Ca^{2+}, Mg^{2+}, Na^{+} , K^{+} NH_4^{+}, Fe^{2+}, Mn^{2+}, Cl^{-}, SO_4^{2-}, HCO_3^{-} and 3) heavy metals: Cadmium (Cd^{2+}), Chromium (Cr^{3+}), Copper (Cu^{2+}), Lead (Pb^{2+}), Nickel (Ni^{2+}), Zinc (Zn^{2+}) and others; 4) Radionuclides including ^{3}H, Ra, U, Be, Co, Sr.

Landfill sites across the Durban Metropolitan region were investigated to understand the effectiveness of leachate containment, treatment and monitoring operations and assess possible impact on local groundwater and surface water resources. The analysed groundwater quality data are compared to the South African National Standards for Drinking Water (SANS 241, 2014) and World Health Organisation standards (WHO, 2017). The results are based on interpretation of primary data collected during the course of this research (Table 6.1). The results and discussions are presented for the landfill sites investigated, namely; Lovu, Bul-Bul Drive, Bisasar Road, Marianhill, La Mercy and Buffelsdraai Landfill sites.

6.2. Analysis of hydrochemical data around the landfill sites

Statistics of 37 samples collected around six landfill sites located within the Durban Metropolitan District have been analyzed. Table 6.2 shows the descriptive statistics of the basic hydrochemical data and reveals a pH ranging from 6.08 to 8.16 and EC varies greatly from, 394 to 3339 µS/cm, indicating that fresh to brackish water is present in areas around landfill sites (Mondal et al., 2008). The TDS also shows a wide range of variation (from 295.5 to 2504.3 mg/l) reflecting considerable variation in the hydrochemical characteristics of the water resources around landfill sites.

Table 6.1: On site and laboratory measured surface water and groundwater chemical parameters for landfill sites generated during the course of this research.

*Sample No.	source	Sample date	EC (µS/cm)	pH	Eh (mV)	Mg mg/l	Ca mg/l	K mg/l	Na mg/l	Si mg/l	Cl mg/l	NO3 mg/l	SO4 mg/l	HCO3 mg/l	Fe mg/l	Mn mg/l
BB1	Borehole	7/8/2017	1273	6.08		38.67	43.31	15.21	179.20	15.29	156.21	2.21		78.07	0.021	1.843
BB2	Borehole	7/8/2017	522	7.45		36.26	18.27	2.83	118.21	2.98	137.34	0.28		198.30	0.008	0.001
BB3	Borehole	7/8/2017	671	7.6	27.9	39.24	33.59	5.04	163.49	6.76	180.23	1.26		351.18	0.009	0.004
BB6	Borehole	7/8/2017	755	6.86	16.9	34.59	54.45	2.46	156.24	12.18	80.81	1.71	18.65	122.40	0.343	0.499
BB7	Borehole	7/8/2017	2032	7.23	-3.9	62.24	73.51	3.14	274.15	15.42	109.37	5.41		382.43	0.013	0.001
BB8	Borehole	7/8/2017	1234	7.31	-9.1	23.10	16.30	2.47	387.49	13.28	161.40	5.66	10.18	432.22	0.01	0.002
BB9	Borehole	7/8/2017	637	6.2	51.5	9.78	2.71	4.52	124.68	30.33	176.84	4.49		84.17	0.027	0.200
LBH1	Borehole	8/8/2017	1531	7.65	-29.1	34.34	47.44	2.08	238.58	3.69	73.10	0.78	0.87	326.72	0.013	0.307
LBH2	Borehole	8/8/2017	1214	7.29	-7.1	42.39	52.26	2.37	313.36	13.79	252.80	0.92	7.26	326.32	0.16	0.234
LBH4	Borehole	8/8/2017	587	7.1	3.5	24.93	17.86	1.88	154.32	26.86	160.56	29.97	27.56	286.34	0.032	0.002
LBH6	Borehole	8/8/2017	835	7.52	22.6	41.14	84.19	2.58	150.62	7.52	150.66	1.57	11.97	340.47	0.095	0.001
BS1	Borehole	8/8/2017	2144	6.97	11	137.89	182.02	5.66	482.50	7.15	230.76	1.19	18.15	497.30	0.02	1.910
BS2	Borehole	8/8/2017	1905	7.25	-5.2	129.25	124.62	17.68	429.63	16.68	143.67		4.33	546.81	0.015	0.801
BS3	Borehole	9/8/2017	425	7.5	-20.5	171.11	22.33	8.96	665.38	2.02	189.10	2.07	6.20	182.42	0.016	0.128
BS4	Borehole	9/8/2017	394	7.2	-2.1	19.94	27.16	0.96	41.96	19.75	41.29	2.89	1.50	215.60	0.013	0.096
BS5	Borehole	9/8/2017	555	7.38	-12.9	19.57	20.15	1.10	121.81	34.01	52.53	9.82	20.77	245.85	0.017	0.002
BB5	stream	7/8/2017	1273	6.22	48.6	50.16	6.43	3.24	196.53	31.82	85.36			89.05	0.014	0.438
BB10	stream	7/8/2017	507	7.03	7.7	12.12	17.55	7.18	63.60	4.73	31.47	2.63	16.02	134.06	0.021	0.001
L2	stream	8/8/2017	1032	7.48	-19	35.34	38.59	39.87	251.46	10.47	180.12	17.19	6.28	357.60	0.065	0.001
L3	stream	8/8/2017	597	7.38	-12.8	14.44	10.02	1.45	84.84	11.28	64.41		9.16	94.93	0.228	0.001
BS6	stream	9/8/2017	492	7	9.5	11.92	61.44	10.53	65.61	15.64	78.91		1.11	219.38	11.415	1.296
BS7	stream	9/8/2017	3339	7.97	-48	51.50	50.06	162.21	474.88	16.79	52.06	17.22	1.67	852.13	0.659	0.337

MH1	Borehole	11/8/2017	674	8.16	-59.6	4.56	40.81	3.72	140.26	7.84	43.47	1.42	32.63	324.70	0.148	0.007
MH2	Borehole	11/8/2017	428	6.14	54.7	13.47	15.49	3.47	52.57	11.37	74.65	7.97	35.00	62.21	0.065	0.048
MH3	Borehole	11/8/2017	610	7.16	0.2	17.31	53.54	3.19	44.94	11.96	49.29	3.06	8.10	277.76	0.013	0.002
MH4	stream	11/8/2017	1043	7.16	-7.8	30.89	32.59	27.56	123.72	11.89	140.85	48.02	15.38	293.60	1.203	1.825
MH5	Borehole	11/8/2017	467	7.18	-1.5	15.78	19.98	2.14	49.51	11.01	77.02	6.73	21.37	104.76	0.08	0.006
MH6	Borehole	11/8/2017	3317	6.97	10.5	14.45	9.12	1.76	36.33	11.19	37.88	14.05	26.81	75.57	0.021	0.001
BF1	Borehole	11/8/2017	688	6.38	18.7	48.83	40.65	2.60	132.86	12.21	294.75	10.11	12.12	207.26	0.04	0.004
BF2	Borehole	14/8/2017	601	7.49	16.5	25.34	26.39	2.75	78.93	16.16	88.37	1.06	8.74	256.01	0.017	0.835
BF3	Borehole	14/8/2017	546	6.82	-54.3	22.80	9.71	5.14	76.38	2.67	95.95	1.57	1.58	174.84	0.018	0.019
BF4	Borehole	14/8/2017	660	6.86	-1.4	22.42	27.40	1.05	84.15	19.35	37.98	22.54	10.90	311.85	0.01	0.001
BF5	stream	14/8/2017	562	8.07	-11.5	17.54	12.09	0.72	77.22	16.67	89.96		9.33	166.77	0.02	0.001
BF6	stream	14/8/2017	1113	7.18	4.9	4.38	2.75	2.12	26.34	8.15	36.46		2.89	34.12	0.189	0.001
BF7	stream	14/8/2017	2317	7.35	-27.1	127.39	77.94	9.62	273.81	8.15	455.10	15.17	7.53	719.30	0.017	0.019
LM1	Borehole	10/8/2017	466	7.08	42.4	3.36	23.78	3.59	10.95	5.69	11.00	2.47	134.81	71.96	0.116	0.105
LM2	Borehole	10/8/2017	686	7.61	-19.5	3.26	4.55	8.18	130.47	6.00	47.17	3.39	1.93	250.54	0.087	0.053

*BB samples are from Bul Bul Drive landfill; LBH and L samples are from Lovu landfill, BS samples are from Bisasar Road landfill, MH samples are from Marianhill and BF samples are from Buffelsdraai landfill site.

The water samples taken around the landfill sites are characterised by high variation in concentration of Na^+ (10.9-665.4 mg/L), Cl^- (11-455.1 mg/l), SO_4^{2-} (0.87 – 134.8 mg/l), HCO_3^- (34.1 -852.1 mg/l) and NO_3^- (0.28-48 mg/l). The maximum concentrations of Na^+, Cl^-, NO_3^- and TDS exceed the limits for drinking water, making it unsuitable for domestic use (SANS, 2014). According to Panno et al. (2001), sodium and chloride are the most important indicators of groundwater contamination from leaking landfill sites due to their high mobility and persistence in aqueous environment. Thus, the high concentration in these parameters indicate that some of the landfill sites are polluting the water resources posing a threat to human health. This is further supported by high tritium activity of 92.2 TU in groundwater resource indicating the presence of luminescent materials within the landfills (Table 6.2).

Factor analysis in the form of PCA with verimax rotation was performed on 14 hydrochemical parameters in order to identify the factors responsible for the groundwater chemistry around landfill sites (Table 6.3). Four components explaining 71% of the hydrochemical data variation were extracted. Component 1 contains the most hydrochemical variance (31.1%) and shows positive loading for EC (0.663), Mg^{2+} (0.683), Ca^{2+} (0.584), K^+ (0.610), Na^+ (0.793), Cl^- (0.532) and HCO_3^- (0.573). The loading of these hydrochemical parameters with EC indicates that this parameter are the main contributors to the groundwater salinity. Component 2 accounts for 17% of the explained variance showing a positive loading for K^+ (0.559), NO_3 (0.550) and Fe (0.511). Component 3 accounts for 14% of the total variance and shows loading of Eh (0.604), NO_3^- (0.550), Fe (0.511) and Mn (0.682). The loading of these variables in component 3 indicate clear pollution impact from the landfill leachate leakage. Loading of SO_4^{2-} in component 4 also indicates release from the landfill sites into groundwater resources. The principle component plot (Figure 6.1) also signifies the anthropogenic inputs into groundwater as NO_3^-, SO_4^{2-}, Fe and Mn cluster together. The plot also reveals that the main contributors to groundwater salinity are Na^+, HCO_3^-, Mg^{2+}, Ca^{2+}, Cl^- and K^+.

Table 6.2: Descriptive statistics of hydrochemical data for landfill sites within the Durban Metropolitan District (Concentrations in mg/l, EC in µS/m).

Variables	No. of data sets	Minimum	Maximum	Mean	Std. Deviation
EC	37	394.00	3339.00	1030.59	756.24
TDS	37	295.50	2504.25	772.95	567.18
pH	37	6.08	8.16	7.17	0.50
Eh	35	-59.60	54.70	-0.15	26.94
Hardness	37	24.75	1020.40	251.10	230.40
Mg	37	3.26	171.11	38.15	39.69
Ca	37	2.71	182.02	37.87	35.81
K	37	0.72	162.21	10.30	26.84
Na	37	10.95	665.38	175.05	149.50
Si	37	2.02	34.01	12.94	7.87
Cl	37	11.00	455.10	118.08	88.61
NO_3	31	0.28	48.02	7.90	10.41
SO_4	31	0.87	134.81	15.83	24.00
HCO_3	37	34.12	852.13	262.03	179.37
Fe	37	0.01	11.42	0.41	1.87
Mn	37	0.00	1.91	0.30	0.55
δD	37	-14.91	3.13	-5.82	5.26
$\delta^{18}O$	37	-4.00	-0.62	-2.54	0.95
Tritium	14	0.40	92.20	11.20	25.35

Table 6.3: Results of PCA for groundwater samples around landfill sites

Variables	Communalities		Components			
	Initial	Extraction	1	2	3	4
EC	1.000	0.475	0.663	0.149	0.054	0.103
pH	1.000	0.719	0.472	0.314	-0.564	0.281
Eh	1.000	0.732	-0.520	-0.310	0.604	0.028
Mg	1.000	0.822	0.683	-0.582	0.097	-0.086
Ca	1.000	0.709	0.584	-0.493	0.308	0.176
K	1.000	0.720	0.610	0.559	-0.063	0.175
Na	1.000	0.725	0.793	-0.279	-0.133	0.024
Si	1.000	0.600	-0.108	0.436	0.140	-0.615
Cl	1.000	0.769	0.532	-0.502	0.179	-0.449
NO_3	1.000	0.816	0.210	0.582	0.550	-0.361
SO_4	1.000	0.511	-0.437	-0.020	0.299	0.480
HCO_3	1.000	0.813	0.873	0.150	-0.118	-0.121
Fe	1.000	0.822	0.362	0.615	0.511	0.227
Mn	1.000	0.737	0.434	-0.028	0.682	0.289
Eigenvalues	Total		4.351	2.374	1.995	1.249
	% of Variance		31.080	16.954	14.249	8.925
	Cumulative %		31.080	48.034	62.283	71.207

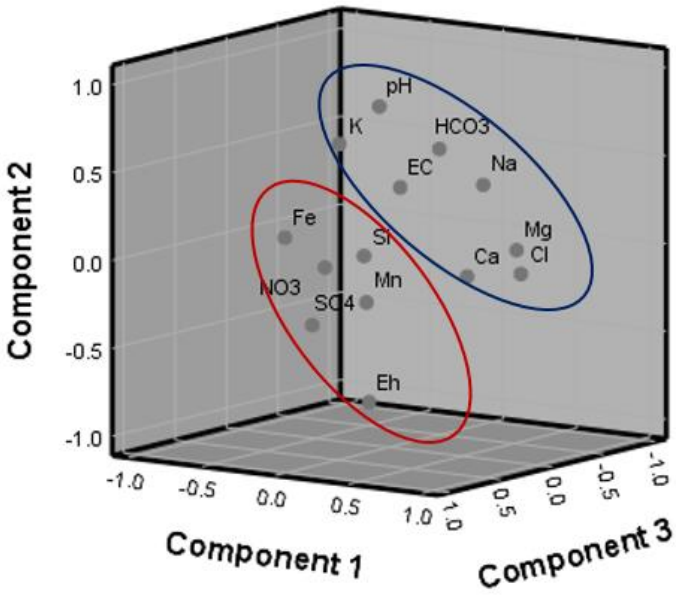

Figure 6.1: Principle component plot showing distribution of hydrochemical parameters around landfill sites.

The hydrochemical data collected aroun the landfill sites was further classified using HCA and is presented as a dendogram (Figure 6.2). Two broad groups (C1 and C2) with large linkage distance in between are presented. The first group (C1) is futher classified into 2 sub-groups presenting different hydrochemical facies and antropogenic influences. Sub-group C1-1 contains samples characterised by freshwater (EC < 1000 µS/cm) and have relatively low inputs form the landfills. They are either characterised by Na-Ca-Cl-HCO_3 and Na-Mg-HCO_3-Cl hydrochemical facies. Sub-group C1-2 is characterised by EC values between 1000 and 1550 µS/cm. According to their Cl, NO_3 and SO_4 concentrations, it appears that this group is not signifficantly affected by lecheate leakage. However, when compared to sub-group C1-1, it is slighly polluted. Group 2 show samples with EC > 1550 µS/cm indicative of brackish water and all samples sites are located downgradient of the respective landfill site. Group 2 is divided into 2 sub-groups (C2-1 and C2-2). Sub-group C2-1 is characterised by EC values of 2144 and 2317 µS/cm for BS1 and BF7 samples, respectively. It is also caracterised by Na and Cl concentrations > 200 mg/l and Mg > 100 mg/l. Sub-group C2-2 is characterised by EC values greater than 3000 µS/cm indicating high influence from the landfills and contains acidic water, indicating leachate leakage into the groundwater. The clusters show the following order of increasing landfill impact: C1-1 > C1-2 > C2-1 > C2-2.

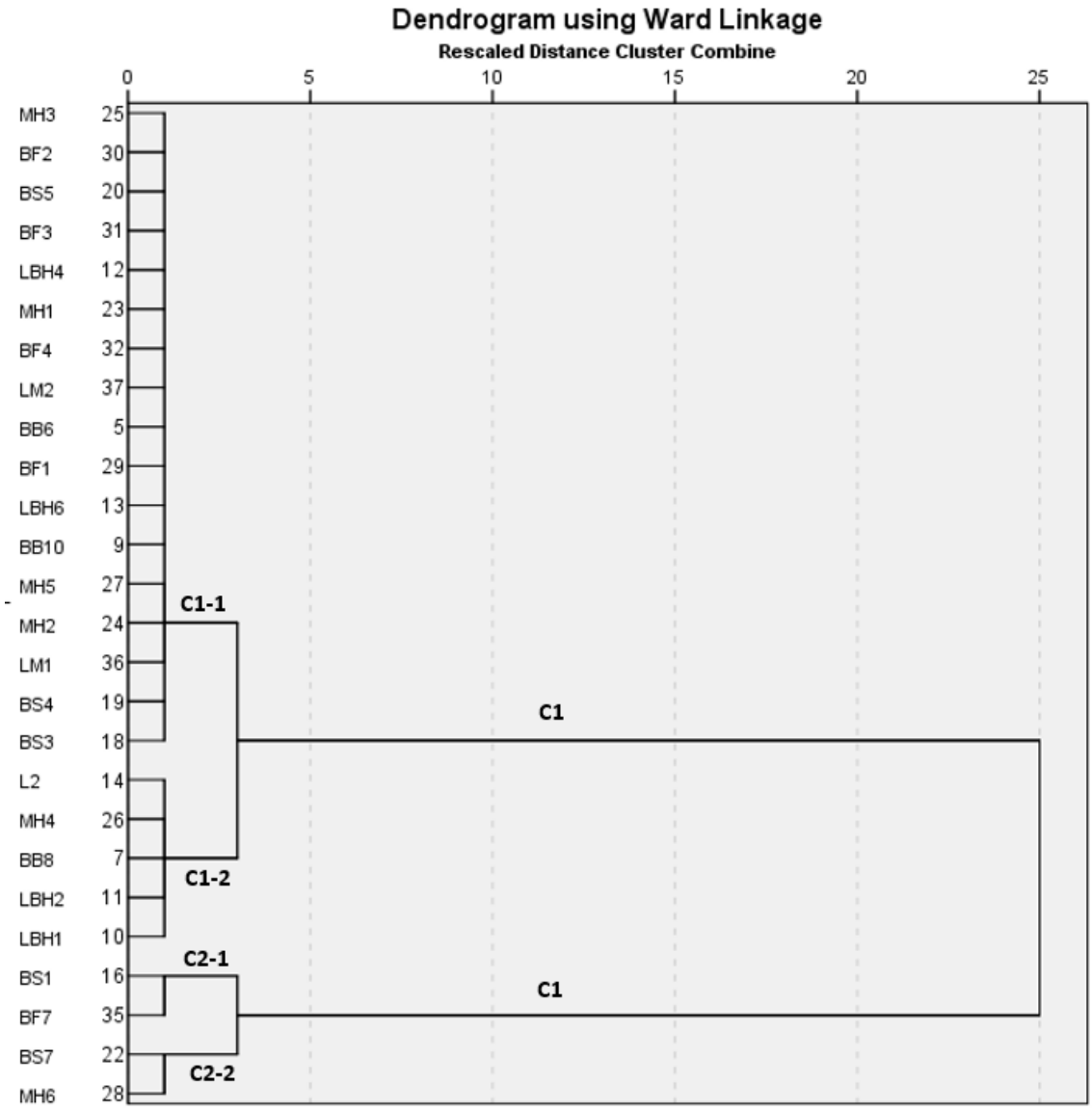

Figure 6.2: Dendogram of hydrochemical samples collected around landfill sites across the study area.

Piper trilinear diagrams have been used to understand groundwater and surface water types around the landfill sites, identify potential controlling hydrochemical processes and to further understand the geochemical evolution of groundwater in the vicinity of landfill sites. The piper diagram (Figure 6.3a) illustrates that groundwater around the landfill sites is dominated by alkalis (Na and K) over alkaline earths (Ca and Mg) and that week acid (HCO_3) exceeds strong acids (SO_4) (Langguth, 1966). The plot indicates that most of the groundwater samples represent mixed Na-Mg-Cl-HCO_3 hydrochemical facies. At Bul Bul Drive landfill fill site, up-gradient samples (BB1

and BB2) are characterized by Na-Mg-Ca-Cl and down gradient samples (BB6 and BB8) are characterized by Na-Mg-Ca-HCO_3-Cl hydrochemical facies. This indicates an increase in alkalinity from up-gradient to down gradient of the landfill site. At Buffelsdraai and Marianhill landfill sites, there is no major changes in hydrochemical facies between up-gradient and down-gradient samples.

At Bisasar road landfill site both surface and groundwater hydrochemical vary from up-gradient to down-gradient, with down gradient samples showing an increase in HCO_3^-. High variation in water types at La Mercy landfill site from up-gradient sample (LM2 = Na-HCO_3-Cl) to down-gradient sample (LM1= Ca-SO_4-HCO_3) is shown in Figure 6.3a. The variation of hydrochemistry at the various landfill sites indicates that groundwater around landfill sites has been polluted by landfill leachate. Figure 6.3b reveals that ion exchange process may have resulted into the observed changes in water type from up-gradient to down-gradient samples due to the mixing and dissolution processes.

6.3. Analysis of trace metals

Trace elements are contributed to groundwater and surface water from various natural and anthropogenic sources (Ramessur, 2000). Various anthropogenic activities under the shadow of urbanization and industrial development result in effluent disposal and introduce high concentration of trace metals into groundwater resources. In general, the concentration of heavy metals in landfills is fairly low and is generally higher at earlier stages due high metal solubility as a result of low pH caused by production of organic acids (Kulikowska and Klimiuk, 2008; Christensen *et al*., 2001).

The range in concentration of trace metals across all landfill sites in ppb is, Fe (8.43 – 11415), Cr (0.1- 13.67), Mn (0.64 – 1910), Cu (0.89 – 40.7), Zn (10 - 80.5), As (0.01 – 12.33), Hg (0.04 - 0.21) and Pb (0.08 - 7.02) (Appendix 4.1). Fe and Mn exceed the permissible limit in drinking water, whereas the trace metals are within permissible limit. However, when comparing up-gradient samples with down-gradient samples there appears to be an increase in the concentration of these metals. This trend is observed mainly at the Bul Bul Drive, Bisasar Road, Marianhill and La Mercy landfill sites. At the Bisasar Road and Marianhill landfill sites high concentration of Fe and Mn is shown by the downstream surface water sample BS7 and MH4, respectively. This is also observed in down-gradient groundwater samples at Bul Bul Drive landfill site (BB6).

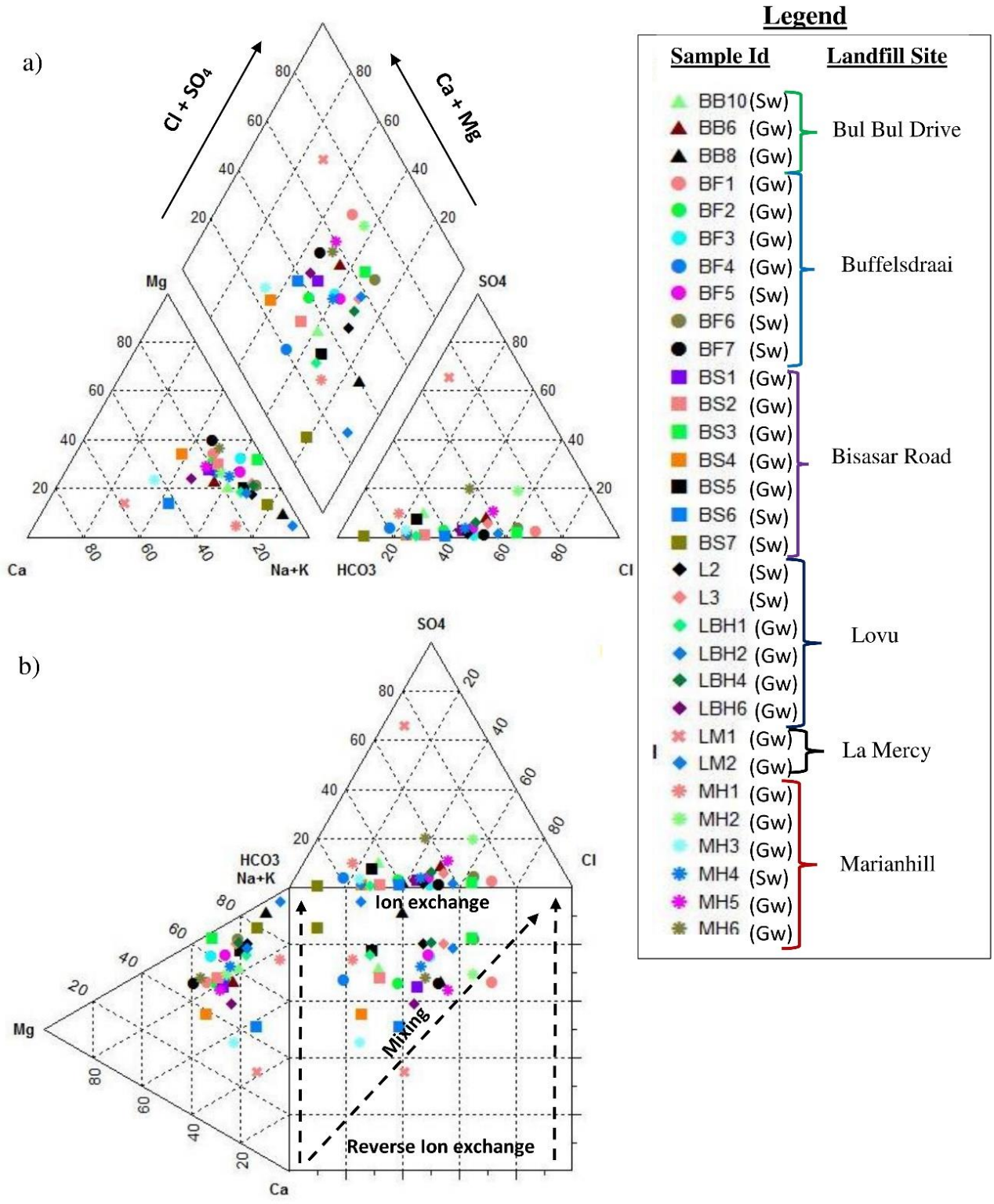

Figure 6.3: Hydrochemical composition plots for groundwater and surface water resources around landfill sites (a) Piper diagram showing hydrochemical facies. b) Durov diagram showing hydrochemical processes.

This indicates that both surface water and groundwater has been polluted by landfill leachate. The major source of Fe in water resources around the landfill sites is mainly from the industrial waste disposed at the sites from steel industry which dump effluents at the landfill. These trace metals increase with increasing concentration of inorganic compound such as HCO_3^-, SO_4^{2-}, Cl^- and NO_3^-. This also indicated influence from landfill sites.

6.4. Environmental isotope characteristics

Environmental isotopes samples were collected around landfill sites during the August 2017 field campaign and analyzed for ^2H, ^{18}O and ^3H (Table 6.4). Environmental isotopes have used as a tracer in determining the source, age, mixing of surface water and groundwater systems. Environmental isotopic are used in pollution studies as well to understand the extent of a pollution plume by monitoring the tritium levels (Baedecker and Back, 1979).

Figure 6.4 shows isotopic composition of groundwater and surface water samples from monitoring points around the landfill sites investigated. Samples lie within a narrow range along the local meteoric water line (LMWL) indicating that groundwater samples had the same recharge source. Scattering of samples along the LMWL indicates that the recharge into aquifers originates from recent precipitation. The lower group shows groundwater samples with relatively depleted isotopic values indicating that non-evaporated water is rapidly infiltrated to the saturated zone. The central group contains both surface and groundwater samples demonstrating that the water is affected by evaporated open water or soil water and the third group demonstrates highly evaporated samples. It is observed that more than 80% of the samples plotted above the LMWL showing the preferential hydrogen isotope fractionation within the landfill.

At the Bul Bul Drive landfill site the isotopic composition of oxygen-18 ranges from -11.9 to 2.4 ‰ and for deuterium the range is -3.7 to -0.9 ‰. At the Bisasar landfill site, isotopic compositions range from -3.30 to -0.73 ‰ for Oxygen-18 and -10 to +3.1 ‰ for deuterium. All samples plot above the meteoric water lines. At the Marianhill landfill site, isotopic compositions range from -4 to -1.31 ‰ for Oxygen-18 and -13.8 to +0.6 ‰ for deuterium. At the La Mercy landfill site the down-gradient sample plots above the LMWL, and the up-gradient sample plots below both the LMWL and GMWL (Figure 6.4) indicating some degree of evaporation before recharge. The down-gradient sample is enriched in δD but depleted in $\delta\ ^{18}O$, when compared to the up-gradient

Table 6.4: Environmental isotope data from samples around landfill sites

*Sample No.	source	Sample date	EC (µS/cm)	pH	Eh (mV)	δD (‰)	δ ^{18}O (‰)	Tritium (TU)
BB1	Borehole	7/8/2017	1273	6.08	-	-11.9	-3.68	0.5
BB2	Borehole	7/8/2017	522	7.45	-	-4.3	-2.53	13.4
BB3	Borehole	7/8/2017	671	7.6	27.9	-7.9	-2.88	3.8
BB6	Borehole	7/8/2017	755	6.86	16.9	-11	-3.2	37.4
BB7	Borehole	7/8/2017	2032	7.23	-3.9	-9.4	-3.41	-
BB8	Borehole	7/8/2017	1234	7.31	-9.1	-8.8	-3.46	-
BB9	Borehole	7/8/2017	637	6.2	51.5	-8.7	-3.43	-
LBH1	Borehole	8/8/2017	1531	7.65	-29.1	-9	-3.31	-
LBH2	Borehole	8/8/2017	1214	7.29	-7.1	-6.4	-2.77	0.5
LBH4	Borehole	8/8/2017	587	7.1	3.5	-8.5	-3.02	0.4
LBH6	Borehole	8/8/2017	835	7.52	22.6	-9.2	-3.22	-
BS1	Borehole	8/8/2017	2144	6.97	11	-10.03	-3.3	-
BS2	Borehole	8/8/2017	1905	7.25	-5.2	-3.204	-2.489	92.2
BS3	Borehole	9/8/2017	425	7.5	-20.5	-9.601	-3.205	1.1
BS4	Borehole	9/8/2017	394	7.2	-2.1	3.1267	-0.734	-
BS5	Borehole	9/8/2017	555	7.38	-12.9	-1.864	-1.797	0.9
MH1	Borehole	11/8/2017	674	8.16	-59.6	-13.76	-4.002	0.4
MH2	Borehole	11/8/2017	428	6.14	54.7	-1.597	-1.635	2.7
MH3	Borehole	11/8/2017	610	7.16	0.2	-12.68	-3.811	-
MH5	Borehole	11/8/2017	467	7.18	-1.5	0.1957	-1.437	-
MH6	Borehole	11/8/2017	3317	6.97	10.5	0.5214	-1.321	-
BF1	Borehole	11/8/2017	688	6.38	18.7	-10.1	-3.263	0.4
BF2	Borehole	14/8/2017	601	7.49	16.5	-3.084	-1.633	1.9
BF3	Borehole	14/8/2017	546	6.82	-54.3	-9.305	-3.147	-
BF4	Borehole	14/8/2017	660	6.86	-1.4	-10.16	-3.232	-
LM1	Borehole	10/8/2017	466	7.08	42.4	-14.91	-2.95	-
LM2	Borehole	10/8/2017	686	7.61	-19.5	-11.78	-3.595	1.2
BB5	stream	7/8/2017	1273	6.22	48.6	-8.2	-2.92	-
BB10	stream	7/8/2017	507	7.03	7.7	2.4	-0.92	-
L2	stream	8/8/2017	1032	7.48	-19	0.3	-1.86	-
L3	stream	8/8/2017	597	7.38	-12.8	-2.9	-2.31	-
BS6	stream	9/8/2017	492	7	9.5	-0.06	-1.934	-
BS7	stream	9/8/2017	3339	7.97	-48	2.9415	-1.383	-
MH4	stream	11/8/2017	1043	7.16	-7.8	0.6037	-1.305	-
BF5	stream	14/8/2017	562	8.07	-11.5	1.5955	-0.615	-

BF6	stream	14/8/2017	1113	7.18	4.9	-7.697	-2.87	-
BF7	stream	14/8/2017	2317	7.35	-27.1	-0.926	-1.489	-

*BB samples are from Bul Bul Drive landfill; LBH and L samples are from Lovu landfill, BS samples are from Bisasar Road landfill, MH samples are from Marianhill and BF samples are from Buffelsdraai landfill site.

sample. Deuterium enrichment may be due to decomposition of material at the landfill with different isotopic compositions, or from bacterial processes that consume the lighter hydrogen isotope (Baedecker and Back, 1979). The analysed samples at Buffelsdraai follow the trend of the LWML with $\delta^{18}O$ ranging from -3.26 to -0.61 and δD ranging from -10.2 to 1.6. Groundwater isotopic signatures indicate that the up-gradient samples are relatively depleted with ^{2}H and ^{18}O as compared to the down-gradient samples, which display isotopic enrichment. This is a result of the evaporation process occurring within the landfill, indicating leachate migration.

According to Abiye (2013), tritium can be used as a landfill leachate tracer and can be used to trace and identify sensitive tritium containing spillages or leakages. It is possible to identify the recharge period of recent groundwater by comparing its tritium content with those of present-day rainfall as rain-water in South Africa contains natural tritium at concentrations of about 3 Tritium TU (Hackley *et al*., 1996). In this study tritium was used to identify groundwater contamination around the landfill sites from leachate leakage

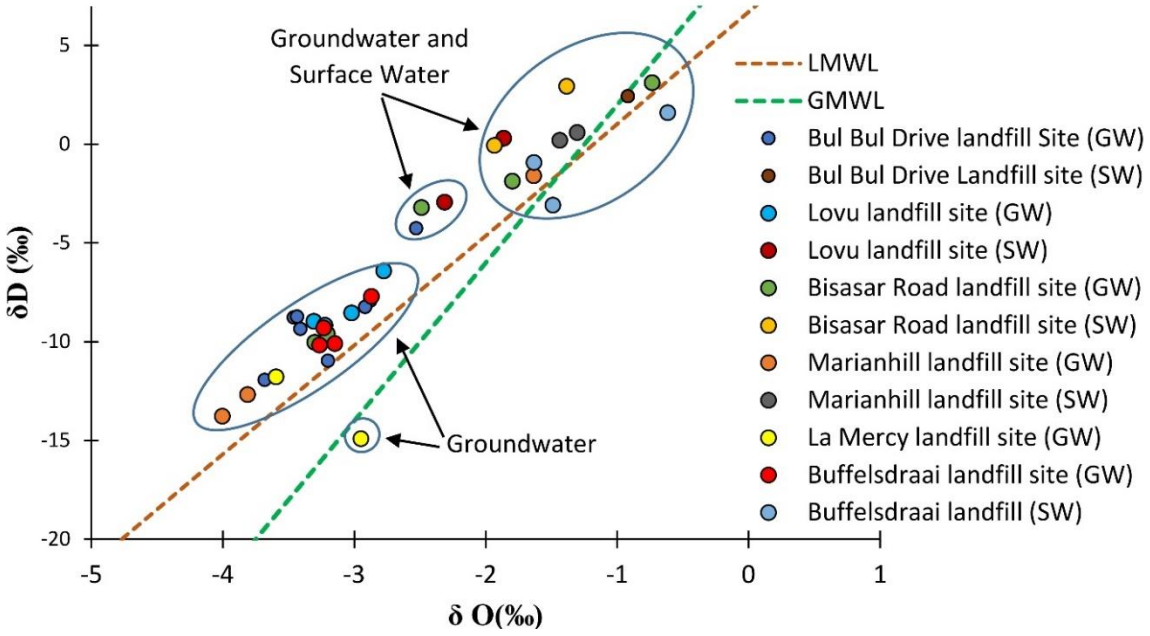

Figure 6.4: $\delta^{18}O$ versus δD plot of groundwater and surface samples from monitoring points around the landfill sites (note that GMWL stands for global meteoric line (Craig, 1961a).

At Lovu Landfill, low but measurable tritium activity is observed at BH2 (0.5 TU) and BH4 (0.4 TU). The tritium signal at Lovu Landfill is relatively low and generally the same at both the up-gradient and down-gradient monitoring points, indicating no pollution from the landfill. BH1 and BH6 indicate zero tritium activity indicating either very low recharge and or long residence times in excess of 50 years. At Bul Bul landfill site, down-gradient monitoring point samples BB2 and BB6 have high tritium signals of 13.4 and 37.4 TU, respectively, indicating pollution from leachate migration into the groundwater. At the Bisasar Road landfill site, tritium activity ranges from 0.9 to 92.2 TU. The up-gradient borehole revealed a tritium activity of 0.9 TU, whereas the down-gradient borehole BS2 has a tritium activity of 92.2 TU. This is clear evidence that groundwater down gradient of the Bisasar Road landfill site is contaminated by landfill leachate. The sources of tritium found in groundwater around landfills may be from medical and scientific waste and luminescent waste including paint (Tazioli, 2011). The activity at the groundwater monitoring sites around the Marianhill landfill site range from 0.4 TU to 2.7 TU indicative of active groundwater recharge than pollution but shows the vulnerability of groundwater to pollution. The tritium activity around the La Mercy and Buffelsdraai landfill sites is low and show no indication that the landfills are leaking leachate into the groundwater. The EC-tritium activity scatter plot of Figure 6.5 shows that groundwater polluted from landfill sites leachate leakage indicates increase in EC and tritium activity simultaneously at least for some of the samples.

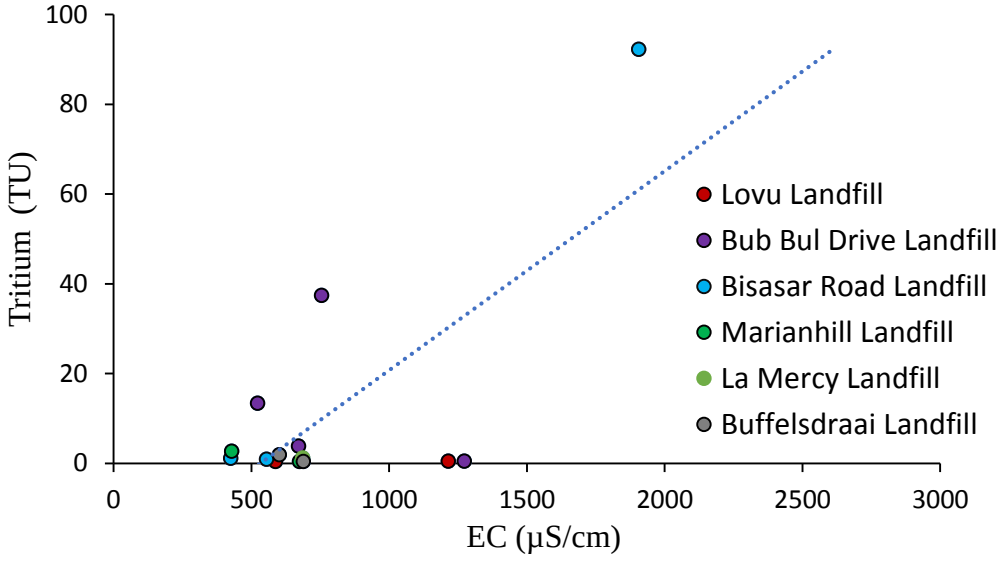

Figure 6.5: Tritium versus EC plot for groundwater samples around landfill sites.

CHAPTER 7

CONCLUSIONS AND RECOMMENDATIONS

Geological, hydrogeological, hydrochemical, hydrometeorological and environmental isotope data were integrated and interpreted to conceptualize the hydrogeological setting of the Durban Metropolitan Region. The main aim of the research was to contribute towards better understanding of the groundwater occurrence, circulation, hydrochemical evolution and related quality issues in the region. The region receives an annual areal precipitation of 936 mm/yr of which 79 % is lost to evapotranspiration, 14% runs off through surface water drainage channels to the Indian Ocean. The average of CMB and water balance method estimated groundwater recharge of 86 mm/yr or 9.2% MAP infiltrating to recharge the various aquifers across the Durban Metropolitan region. Environmental isotopes (^{2}H, ^{18}O and ^{3}H) supports modern active recharge across the study area. Stable environmental isotope information further indicates surface water recharging the aquifer. Compared to the annual rate of recharge, groundwater abstraction across the region is very limited.

The hydrogeological and hydrochemical characterization identified five main hydrostratigraphic units that vary in their hydraulic and hydrochemical characteristics. According to stratigraphic order, these are: 1) weathered and fractured granitic basement aquifers of the Mapumulo Group and Oribi Gorge Suite characterized by average borehole yield and transmissivity (T) of 1.2 l/s and 3.9 m^2/day, respectively and Ca-Mg-HCO_3 hydrochemical water type; 2) fractured Natal Group sandstone aquifer characterized by average borehole yield and hydraulic conductivity (K) of 5.6 l/s and 2.8 m/day, respectively and Na-Mg-HCO_3-Cl dominant hydrochemical water type; 3) fractured aquifers of the Dwyka Group diamictite and tillite that are characterized by average borehole yield of 0.4 l/s and T of 1.3 m^2/day and Na-Cl-HCO_3 dominant hydrochemical water type; 4) the Vryheid Formation sandstone of the Ecca Group, which is characterized by average borehole yield of 2.5 l/s, T of 4.9 m^2/day, K of 0.17 m/day and Na-Cl-HCO_3 hydrochemical water type; 5) the intergranular primary aquifers of the Maputaland Group which consists the Bluff, Berea Formations and recent alluvium and estuarine deposits. These primary aquifers have average borehole yield of 14.8 l/s and transmissivity of up to 406 m^2/day with a mainly Na-Cl-HCO_3 hydrochemical signature.

Measured depth to groundwater varies across the aquifers of study area are mainly controlled by the surface topography and geology. In the granitic basement aquifers, depth to groundwater can be as deep as 45 m bgl, whereas in the Natal, Dywka and, Ecca Groups, groundwater is encountered at average depth of 20 m. Groundwater in the Maputaland Group primary aquifers, along the coast, occurs at an average depth of about 6 m. The general groundwater flow direction is from west to east towards the Indian Ocean. However, local groundwater flow directions vary depending on geology and topography.

In order to assess the effectiveness of leachate containment systems and to understand the state of groundwater quality and the water quality monitoring systems around the landfill sites, six landfills sites located across the Durban Metropolitan District were investigated through a combined hydrogeological, hydrochemical and environmental isotope approaches. From the six landfill sites investigated, namely, Lovu, Bul Bul Drive, Bisasar Road, Marianhill, La Mercy and Buffelsdraai Landfill Sites, the results indicate that groundwater downstream of the Bul Bul Drive, Bisasar Road and La Mercy landfill sites have been found to be impacted by leachate leakage. These observed groundwater contaminations are identified through a combined hydrochemical and tritium tracer's data variation from the base line data. At the Bul Bul Drive Landfill, which was decommissioned in 2009, groundwater quality varied from up-gradient to down-gradient with a very poor groundwater quality and high tritium activity (from 13.4 to 37.4TU) observed in the south west downstream direction indicating leachate leakage and migration. At Bisasar Road Landfill site, leachate migration was observed through very high increase in groundwater quality determinants and very high tritium activity (92.2 TU) form upstream to downstream of the landfill. Around the La Mercy Landfill site, shallow aquifer monitoring wells show contamination from leachate generated from the landfill, but the deep aquifer monitoring wells show no sign of pollution. These indications of leakage leachate around the three landfill sites means that immediate corrective action is needed to stop contamination of larger aquifer volumes.

Finally, based on the preceding main hydrogeological, hydrogeochemical and environmental isotope findings and conclusions, a regional hydrogeological conceptual model that characterises the hydrogeological and hydrochemical conditions of the Durban Metropolitan region is proposed (Figure 7.1).

Following are recommendations emanating from the present study:

- Groundwater monitoring network is required to monitor the changes in groundwater levels and chemistry across the Durban Metropolitan District.
- It recommended that vandalised and destroyed boreholes, previously used for water supply, be converted into monitoring borehole as they spatial distribution is even.
- The proposed conceptual model is recommended for large scale studies, as local features were not accounted for.
- For better understanding of the groundwater flows situation a regional numerical model should be developed as data becomes available.
- To prevent plume advancement and to assess the effectiveness of the bioremediation technology at the Bul Bul Drive Landfill Site, the new on-site treatment plant should be utilized as soon as possible.
- The extent of contaminant plume at Bisasar Road landfill sites need to be defined so as to take appropriate remediation measures.
- It is recommended that surface water be monitored at the La Mercy landfill site
- Water resources should be analysed for environmental isotopes at least twice a year to fully understand the impact of landfill.

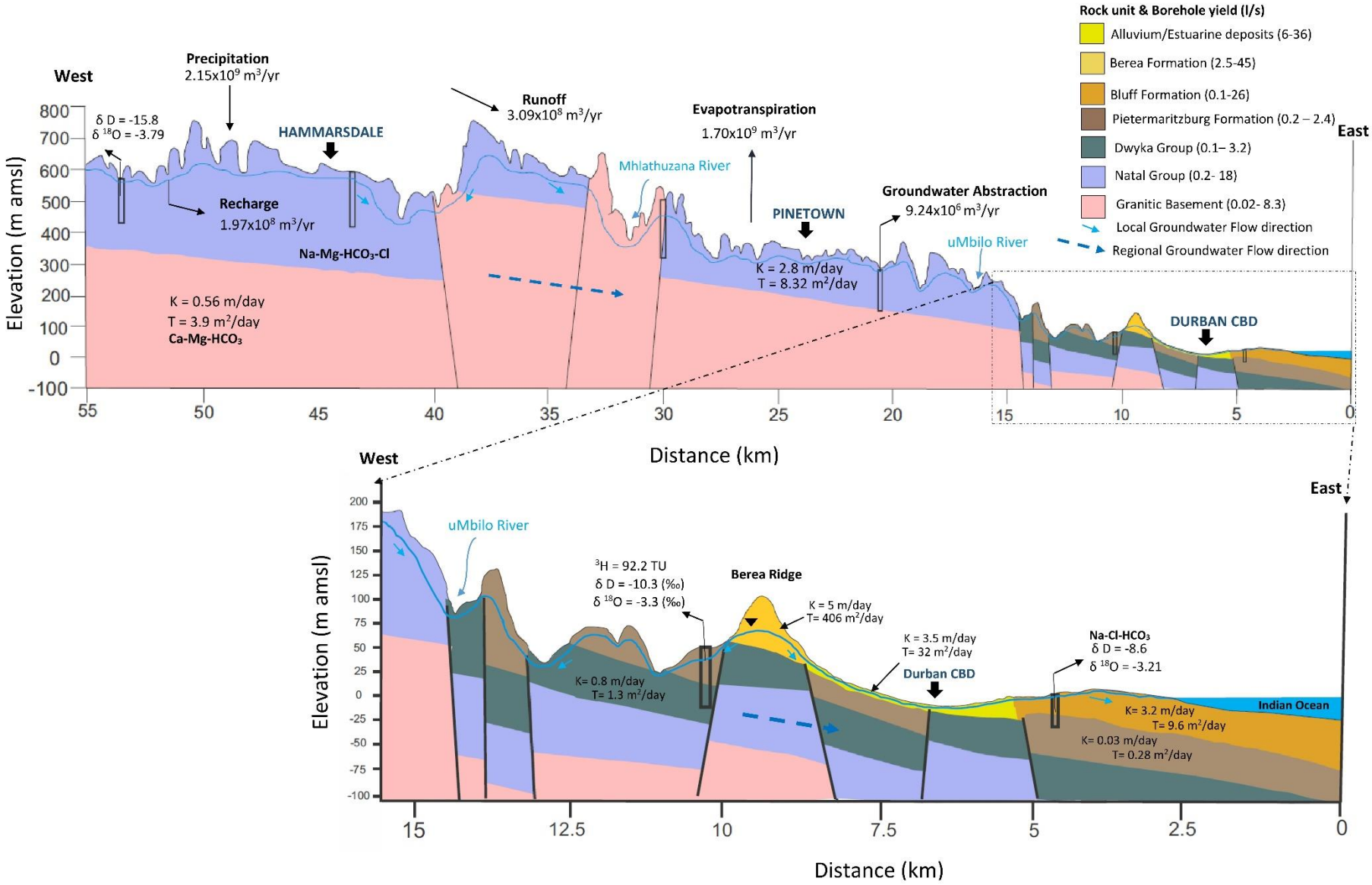

Figure 7.1: Regional hydrogeological conceptual model of the Durban Metropolitan region based on and a west-east X-section

REFERENCES

Abiye, T. (2013). The use of Isotope Hydrology to Characterize and Assess Water Resources in South(ern) Africa. Report for the Water Research Commission Report No. TT 570/13, 211p.

Allen, R.G., Pereira, L.S., Raes, D. and Smith, M. (1998). Crop evapotranspiration: guidelines for computing crop water requirements. Irrigation and Drainage Paper, No. 56. Rome: Food and Agriculture Organization of the United Nations, 300p

Alley, W.M., Reilly, T.E., Franke, O.L. (1999). Sustainability of Ground-Water Resources. U.S. Geological Survey Circular 1186, 79p

Allison, G.B., Barnes, C.J., Hughes, M.W. and Leaney, F.W.J. (1984). Effect of climate and vegetation on oxygen-18 and deuterium profiles in soils. In: Isotope Hydrology 1983, IAEA Symposium 270, September 1983, Vienna, 195-123. In: Clark, I.D. and Fritz, P. 1997. Environmental isotopes in hydrogeology. Lewis Publishers, New York, 328p.

Anderson, M.P. and Woessner, W.W. (2002). Applied Groundwater Modelling; Simulation of Flow and Advective Transport. Academic Press, London, 381p

Anderson, M.P., Woessner, W.M. and Hunt, R.J. (2015). Applied Groundwater Modelling: Simulation of Flow and Advective Transport. Academic Press, San Diego, CA. 720p

Appelo, C. A. J. and Postma, D. (2005). Geochemistry, Groundwater and Pollution, 2nd Edition. Balkema, Amsterdam, 649p

Arnason, G and Fletcher, B. A. (2003). A 40+year record of Cd, Hg, Pb, and U deposition in sediments of Patroon reservoir, Albany Country, NY, USA, *Environmental Pollution*, 123(3): 383-391

Baedecker, M.J. and Back, W. (1979). Hydrogeological processes and chemical reactions at a landfill. *Groundwater*, *17*(5): 429-437.

Baier, K., Schmitz, K.S., Azzam, R., and Strohschon, R. (2014). Management tools for sustainable ground water protection in mega urban areas-small scale land use and ground water vulnerability analyses in Guangzhou, *China International Journal of Environmental Research*, *8*: 249-262

Banks, E.W, Simmons, C.T, Love, A.J, Werner, A.D, Bestland, E.A, Wood, M. and Wilson, T. (2009). Fractures bedrock and Saprolite hydrogeologic control on groundwater/surface water interaction: a conceptual model (Australia). *Hydrogeology Journal*, 17(8): 1969- 1989

Barnett, B., Townley, L.R., Post, V., Evans, R.E., Hunt, R.J., Peeters, L., Richardson, S., Werner, A.D., Knapton, A. and Boronkay, A. (2012). Australian groundwater modelling guidelines, Waterlines report, National Water Commission, Canberra. 203p

Barrett, M.H., Hiscock, K.M., Pedley, S., Lerner, D.N., Tellam, J.H. & French, M.J. (1999). Marker species for identifying urban groundwater recharge sources: A review and case study in Nottingham, UK. *Water Research, 33(14)*: 3083–3097

Barrett, M.H., Johal, K., Howard, G., Pedley, S. and Nalubega, M. (2000). Sources of faecal contamination of shallow groundwater in Kampala. Accepted for publication at IAH Congress, Cape Town.

Beekman, H.E., Selaolo, E.T. and De Vries, J.J. (1999). Groundwater recharge and resources assessment in the Botswana Kalahari. GRES II Executive summary and technical reports, 48p

Bell, F.G. and Le Roux, K. (1998). The chemical and engineering properties of weathered granite in the Valley of One Thousand Hills, Natal, South Africa. In: Proceedings Eighth Congress International Association Engineering Geology, Vancouver A.A. Balkema, Rotterdam, 1,267-274

Bell, F.G., and Maud, R. (2000). A groundwater survey of the greater Durban area and environs, Natal, South Africa. *Environmental Geology, 39(8):* 925-936.

Berg, A., Byrne, J. and Rogerson, R. (1996). An urban water balance study, Lethbridge Alberta: estimation of urban lawn overwatering and potential effects on local water tables. *Canadian Water Resources Journal, 21(4)*: 17–27

Betts, A.K. (2004). Understanding hydrometeorology using global models. *Bulletin of the American Meteorological Society*, *85*(11): 1673-1688

Beven, K. (1983) Surface water hydrology-runoff generation and basin structure. *Revision Geophysics*, 21(3): 721–730

Bhuyan, S.J., Mankin, K.R. and Koelliker, J.K. (2003). Watershed-scale AMC selection for hydrologic modelling. *Trans ASAE*, 46: 237–244

Bjerg, P. L., Albrechtsen, H.-J., Kjeldsen, P., Christensen, T. H., and Cozzarelli, I.M. (2014). The Biogeochemistry of Contaminant Groundwater Plumes Arising from Waste Disposal Facilities. *Treatise on Geochemistry*, 2: 573–605

Bornstein, R. and Lin, Q. (2000). Urban Heat Islands and Summertime Convective Thunderstorms in Atlanta: Three Case Studies. *Atmospheric Environment* 34(3): 507-516

Borradaile, G. (2003). Statistics of Earth Science Data: Berlin, Springer-Verlag, 351 p

Botha, G. A., Bristow, C. S., Porat, N., Duller, G. A. T., Armitage, S. J., Roberts, H. M., Clarke, B. M., Kota, M. W., and Schoeman, P. (2003). Evidence for dune reactivation from ground penetrating radar (GPR) profiles on the Maputaland coastal plain, South Africa. In: Bristow, C.S. and Jol, H.M. (Eds.), Ground Penetrating Radar: Applications in Sedimentology. Geological Society, London, Special Publications 211: 26-46

Brown, C.E. (1998). Applied multivariate statistics in geohydrology and related sciences. Springer, Berlin, 248p

Butler, J.J. and Lui, W.Z. (1991). Pumping tests in non-uniform aquifers- the linear strip case. *Journal of Hydrology*, 128 (1): 489-273

Butler, T.W. (2007). Application of multiple geochemical indicators, including the stable isotopes of water, to differentiate water quality evolution in a region influenced by various agricultural practices and domestic wastewater treatment and disposal. *Science of the Total Environment*, 388(1–3): 149–167

Changnon, S.A. (1976). Inadvertent weather modification 1. *Journal of the American Water Resources Association*, 12 (4): 695-715.

Christensen, T.H., Kjeldsen, P. and Kjeldsen, P. (2001). Biogeochemistry of landfill leachate plumes. *Applied Geochemistry*, 16(7-8): 659–718

Christensen,H., Peter, K., Hans-Jo, H., Gorm, H., Per, H.N., Poul, L.B. and Peter, E.H. (1994) Attenuation of landfill leachate pollutants in aquifers. *Critical Revision in Environmental Science Technology*, 24(2): 119-202

Clark, I.D. and Fritz, P. (1997). Environmental Isotopes in Hydrogeology, Lewis Publishers, New York, 328p

Clarke, B.M. (2008). The geology of the Natal Metamorphic Province in the Durban area. *South African Journal of Geology*, 111(1): 1–20

Coldewey, W.G. and Meber, J. (1997). The effects of urbanization on groundwater recharge in the Ruhr region of Germany. In Chilton J et al., (eds) Groundwater in the Urban Environment: Problems, Processes and Management. Balkema, Rotterdam, 115–119.

Conrad, J., Nel, J., and Wentzel, J. (2004). The challenges and implications of assessing groundwater recharge: A case study-northern Sandveld, Western Cape, South Africa. *Water SA* 30(5): 75-81

Cook, P. and Herczeg, A.L. (2000). Environmental tracers in subsurface hydrology. Kluwer, Boston, 529p

Cook, P., Plummer, L.N., Solomon, D., Busenberg, E. and Han, L. (2006). Effects and processes that can modify apparent CFC age. In: Groning, M., Han, L.F., Aggarwal, P. (Eds.), Use of Chlorofluorocarbons in Hydrology. A Guidebook International Atomic Energy Agency, Austria, 31-58.

Cornell, D.H., Thomas, R.J., Bowring, S.A., Armstrong, R.A. and Grantham, G.H. (1996). Protolith interpretation in metamorphic terranes: aback-arc environment with Besshi-type base metal potential for the Quha Formation, Natal Province, South Africa. *Precambrian Research 77*: 243–271.

Council for Geoscience. (1988a). 2930 Durban Geological map series 1: 250 000, South Africa

Council for Geoscience. (1988b). 3030 Port Shepstone Geological map series 1: 250 000, South Africa.

Council for Geoscience. (2015). 2930DD & 2931CC Durban Geological map series 1:50 000. South Africa.

Craig, H. (1961a). Isotopic variations in meteoric waters. *Science* 133(3465): 1702–1703

Craig, H. (1961b). Standard for reporting concentrations of deuterium and oxygen-18 in natural waters. *Science* 133: 1833–1834.

Dansgaard, W. (1964). Stable isotopes in precipitation. *Tellus* 16(4): 436–468

Del Bon, A., Sbarbati1, C., Brunetti, E., Carucci, V., Lacchini1, A., Marinelli1, V. and Petitta1, M. (2015). Groundwater flow and geochemical modeling of the Acque Albule thermal basin (Central Italy): a conceptual model for evaluating influences of human

exploitation on flowpath and thermal resource availability. *Central European Geology,* 58(1–2): 152–170

Demlie, M. and Titus, R. (2015). Hydrogeological and Hydrogeochemical Characteristics of the Natal Group sandstone, South Africa. *South African Journal of Geology* 118 (1): 33-44

Doorenbos, J. and Pruitt, W.O. (1977). Guidelines for predicting crop water requirements. Irrigation and drainage paper 24. 2nd ed. Rome: Food and Agriculture Organization of the United Nations, 156p

Drever, J.I. (1982). The geochemistry of natural waters: surface and groundwater environments (3rd Ed), Prentice- Hall, Upper Saddle River, NJ, 410-411

Durov, S.A. (1948). Classification of natural waters and graphical representation of their composition. *Dokl. Akad. Nauk. USSR*, 59(1): 87-90

DWA, (2010). Strategic planning for water resources In South Africa, Situational analysis. Department of Water Affairs, Pretoria, South Africa.

DWAF. (1998). 1:500 000 hydrogeological map series of the Republic of South Africa. Durban Sheet 2928.

DWAF. (2006). Groundwater Resource Assessment II- Task 3aE Recharge. Department of Water Affairs and Forestry. Pretoria, 129p

DWS. (2017). Department of Water and Sanitation, Durban office, KZN groundwater abstraction and river data

Edmunds, W. M., Guendouz, A. H., Mamou, A., Moulla, A., Shand, P., and K. Zouari. (2003). Groundwater evolution in the Continental intercalaire aquifer of southern Algeria and Tunisia: trace element and isotopic indicators. *Applied Geochemistry 18*(6): 805–822

Erikson, E. (1985). Principles and applications of hydrochemistry. Chapman and Hall, New York, 188p

Eriksson, E. and Khunakasem, V. (1969). Chloride concentration in groundwater, recharge rate and rate of deposition of chloride in the Israel coastal plain. *Journal of Hydrology* 7: 178-197

Evans, M.J., Eglington, B.M., Kerr, A. and Saggerson, E.P. (1987). The geology of the Proterozoic rocks around Umzinto, southern Natal, South Africa. South African Journal of Geology 90: 471–488.

Fetter, C.W. (2001). Applied Hydrogeology. 4th Edition. Prentice-Hall, Inc. Upper saddle River, New Jersey, 598pp.

Foster, S., Lawrence, A. & Morris, B. (1998). Groundwater in urban development: assessing management needs and formulating policy strategies. *World Bank Technical Paper No 390*, 149: 111–135

Foster, S.S.D. (1990). Impacts of urbanization on groundwater. Hydrological processes and water management in urban areas. Wallingford, UK, International Association of Hydrological Sciences – association Internationale des Sciences Hydrologiques (IAHS-AISH) Pub. No. 198.

Foster, S.S.D., Morris, B.L. and Lawrence, A.R. (1994). Effects of urbanization on groundwater recharge. In Wilkinson WB (ed) Groundwater Problems in Urban Areas. Tomas Telford, London, 43–63p

Freeze, R.A. and Cherry, J.A. (1979). Groundwater. Prentice Hall. 604p

Garcia-Fresca, B. (2004). Urban effects on groundwater recharge in Austin, Texas. MS thesis, the University of Texas, Austin, 173p.

Garrels, R.M. and Mackenzie, F.T. (1971). Evolution of Sedimentary Rocks, W.W. Norton and Co., Int., New York, 394p

Hackley, K.C., Liu, C.L. and Coleman, D.D. (1996). Environmental isotope characteristics of landfill leachates and gases. *Groundwater*, *34*(5): 827-836.

Hair, J.T. Anderson, R.E. Tatham, R.L. and Black, W.C. (1992). Multivariate data analysis with readings (3rd Ed), Macmillan. 734p

Hem, J.D. (1985). Study and Interpretation of the Chemical Characteristics of Natural Water (3rd) Ed. U.S Geological Survey Water-Supply Paper 2254

Holland, H.D. (1978). The Chemistry of the Atmosphere and Oceans John Wiley and Sons, New York. 351p

Howard, K.W.F. (2002) Urban Groundwater Issues—An Introduction. In: Howard K.W.F., Israfilov R.G. (eds) Current Problems of Hydrogeology in Urban Areas, Urban

Agglomerates and Industrial Centres. Nato Science Series (Series IV: Earth and Environmental Sciences), vol 8. Springer, Dordrecht

Howari, F.M and Banat, K.M. (2002). Hydrochemical characteristics of Jordan and Yarmouk river waters: effect of natural and human activities *Journal of Hydrology and Hydromechanics*, 50(1): 50-64

Hunt, R.J., Coplen, T.B., Haas, N.L., Saad, D.A. and Borchardt, M.A. (2005). Investigating surface water-well interaction using stable isotope ratios of water. *Journal of Hydrology* 302(1-4): 154-172

Hunt, R.J., Feinstein, D.T., Pint, C.D. and Anderson, M.P. (2006). The importance of diverse data types to calibrate a watershed model of the Trout Lake Basin, northern Wisconsin,

IAEA, 2012. Global Network of Isotopes in Precipitation. The GNIP Database. (http://wwwnaweb.iaea.org/napc/ih/GNIP/userupdate/description/1stpage.html) (Accessed 12.10.18).

IDP. (2017). eThekwini Municipality Integrated Development Plan. eThekwini Municipality. Durban, South Africa. 559p

Ingebritsen, S.E., Sanford, W.E., and Nuezil, C.E. (2006). Groundwater in Geologic Processes. Cambridge University press. New York. 536p

Johnson, M.R., Visser, J.N.J., Cole, D.I., de Wickens, H., Christie, A.D.M., Roberts, D.L. and Bradle, G. (2006). Sedimentary Rocks of the Karoo Supergroup, in "Johnson, M.R., Anhaeusser, C.R., and Thomas., R.J (eds). (2006). The Geology of South Africa. Geological Society of South Africa, Johannesburg/Council for Geoscience, Pretoria, 691p"

Kelbe, B. E., Taylor, R. H., and Haldorsen, S. (2013). Groundwater hydrology. In: Perissinotto, R.,Stretch, D. D., Taylor, R. H. (Eds.), Ecology and Conservation of Estuarine Ecosystems: Lake St Lucia as a Global Model. Cambridge University Press, 486p.

Kendall, C. and McDonnell, J.J. (1998). Isotope tracers in catchment hydrology. Elsevier, Amsterdam

King, G.M. (1997). The Development Potential of KwaZulu-Natal Aquifers for rural water supply. Unpublished MSc. Dissertation. Rhodes University.

King, G.M. (2002). An Explanation of the 1:500 000 General Hydrogeological Map, Durban 2928. Department of water and Forestry. Pretoria, South Africa, 38p

Kolm, K.E. (1996). Conceptualization and characterization of ground-water systems using Geographic Information Systems. *Engineering Geology*, 42(23): 111-118.

Kresic, N. and Mikszewski, A. (2013). Hydrogeological Conceptual Site Models: Data Analysis and Visualization. CRC Press, Boca Raton, 584p

Kulikowska, D. and Klimiuk, E. (2008). The effect of landfill age on municipal leachate composition. *Bioresource Technology*, 99(13): 5981–5985

KZN-PPC. (2016). KwaZulu-Natal Situational Overview. KwaZulu-Natal Provincial Growth and Development Strategy (PGDS). Province of KwaZulu-Natal, South Africa, 345p

Langguth, H. R. (1966). Groundwater verhaltisse in Bereiech Des Velberter. Sattles. Der Minister Fur Eraehrung, Land Wirtsch Forste Duesseldorf: NRW, 127p

Leopold, L.B. (1968). Hydrogeology for urban land planning – A guidebook on the hydrologic effects of urban land use. US Geological Survey Circular 554, 18p.

Lerner, D. N. (2002). Identifying and quantifying urban recharge: A review *Hydrogeology Journal 10*: 143-152

Lerner, D. N., Issar, A. and Simmers, I. (1990). Groundwater Recharge - A guide to understanding and estimating natural recharge, International contribution to hydrogeology, I.A.H. Publ., Vol. 8, Verlag Heinz Heisse, 345p

Lerner, D.N. (1986). Leaking pipes recharge ground water. *Ground Water*, 24(5): 654–662

Lerner, D.N., Burston, M.W. and Bishop, P.K. (1993). Hydrogeology of the Coventry region (UK): an urbanized, multilayer, dual porosity aquifer system. *Journal of Hydrology*,

Li, P., Wu, J., and Qian, H. (2016). Hydrochemical appraisal of groundwater quality for drinking and irrigation purposes and the major influencing factors: a case study in and around Hua County, China, *Arabian Journal of Geosciences* 9(1): 15, 1 -17

Linsley, R. K., Kohler, M.A. and Paulhus, J. L.H. (1975). Hydrology for engineers. McGraw-Hill, New York. 482p

Lloyd, J. A., and Heathcoat, J.A. (1985). Natural inorganic hydrochemistry in relation to groundwater: An introduction. Oxford Uni. Press, New York, 296p

Lu Z., He Z., Parisi V. A., Kang S., Deng Y., Van Nostrand J. D. (2012). GeoChip-based analysis of microbial functional gene diversity in a landfill leachate-contaminated aquifer. Environmental Science Technology 46: 5824–5833

Lunt, I.A. and Bridge, J.S. (2004). Evolution and deposits of a gravelly braid bar, Sagavanirktok River, Alaska. *Sedimentology*, 51(3): 415-432

Mair, A. and Fares, A. (2011). Comparison of Rainfall Interpolation Methods in a Mountainous Region of a Tropical Island. *Journal of Hydrologic Engineering*, 16(4): 371-383

Marshall, C.G.A. (2006). The Natal Group. In: Anhaeusser, C.R., Johnson, M.R., and Thomas, R.J. (Eds), The Geology of South Africa. The Geological Society of South Africa, Johannesburg, South Africa

Masindi, K. and Abiye, T. (2018). Assessment of natural and anthropogenic influences on regional groundwater chemistry in a highly industrialized and urbanized region: a case study of the Vaal River Basin, South Africa. *Environmental Earth Science, 77:22*.

Mather, J. R. (1978). The climatic water budget in environmental analysis, Lexington, US, Lexington Books. 239p

Mather, J. R. (1979). Use of the climatic water budget to estimate streamflow, in Mather, J.R., ed., Use of the climatic water budget in selected environmental water problems: Elmer, N.J., C.W. Thornthwaite Associates, Laboratory of Climatology, *Publications in Climatology*, 32(1): 1–52

Maud, R.R. (1968). Quaternary geomorphology and soil formation in coastal Natal. *Journal of Geomorphology*, 7: 155-199

Mazor, E. (2004). Chemical and Isotopic Groundwater Hydrology. 3rd edition. Marcel Dekker Inc. 470p.

McCuen, R.H. (2003). Hydrologic analysis and design, 3rd Ed. Prentice Hall, Englewood Cliffs

Meybeck, M. (1987). Global Chemical Weathering of Surficial Rocks Estimated from River Dissolved. *American Journal of Science 2*87: 401-428

Mondal, N.C. Singh, V.S. Saxena V.K., Prasad, R.K. (2008). Improvement of groundwater quality due to fresh water ingress in Potharlanka Island, Krishna delta, *India Environmental Geology*, 55 (3): 595-603

Ndlovu, M.S. and Demlie, M. (2018a). Assessment of Meteorological drought and Wet conditions using two drought indices across KwaZulu-Natal Province, South Africa. Submitted to the *South African Geographical Journal*, (RSAG-2018-0046).

Ndlovu, M.S. and Demlie, M. (2018b). Statistical analysis of groundwater level variability across KwaZulu-Natal Province, South Africa. *Environmental Earth Sciences*, 77:739

Panno, S.V., Hackley, K.C., Hwang, H.H. and Kelly, W.R. (2001). Determination of the sources of nitrate contamination in karst springs using isotopic and chemical indicators. *Chemical Geology*, *179*(1): 113-128

Pelton, W.L., King, K.M. and Tanner, C.B. (1960). An evaluation of the Thornthwaite and mean temperature method for determining potential evapotranspiration. *Agronomy Journal*, l52: 387–395

Piper, A.M. (1944). A graphic procedure in the geochemical interpretation of water-analyses," *Eos, Transactions, American Geophysical Union,* 25(6): 914–928

Plummer L. N., Parkhurst D. L. and Wigley T. M. L. (1979). Critical review of the kinetics of calcite dissolution and precipitation. In: Chemical Modeling—Speciation, Sorption,

Pruitt, W.O. (1964). Cycle relation between evapotranspiration and radiation. *Trans ASAE*, 7(3): 271–275

Raghunath, H.M. (2006). Hydrogeology: Principles, Analysis and Design. 2nd Ed. New Delhi. New Age International publisher, 482p

Ramessur, R.T. (2000). Determination of some dissolved trace metals from groundwater in Mauritius using inductively-coupled plasma-mass spectrometry. Science and Technology-Research Journal, University of Mauritius, Réduit, Mauritius, 5: 14p

Ramsay, P. and Cooper, A. (2002). Late Quaternary Sea-Level Change in South Africa. *Quaternary Research*, 57: 82-90

Ramsay, P. J., Smith. A. M., Lee-Thorp, J. C., Vogel, J. C., Tyldsley, M., and Kidwell, W. (1993). 130 000-year-old fossil elephant found near Durban: Preliminary report. *South African Journal of Science* 89**:** 165

Rogers, P. (1994). Hydrology and water quality. Changes in land use and land cover: A global perspective *4*. 231p

Rosenthal, E. (1987). Chemical composition of rainfall and groundwater in recharge areas of the Bet Shean Harod multiple aquifer system, Israel. *Journal of Hydrology*, 89: 329-352.

Rowsell, D.M. and de Swardt. (1976). Diagenesis in Cape and Karoo sediments, South Africa and its bearing on the hydrocarbon protentional. *Transitional geological Society of South Africa*, 84-145

Roy, J.W., Van Stempvoort, D.R. and Bickerton, G. (2014). Artificial sweeteners as potential tracers of municipal landfill leachate. *Environmental Pollution,* 184: 89-93 USA. *Journal of Hydrology* 321 (1-4): 286-296

SANS. (2014). South African National Standards for Drinking water (2nd Ed).

Saraf, A.K. and Choudhury, P.R. (1998). Integrated Remote Sensing and GIS for Groundwater Exploration and Identification of Artificial Recharge Sites. *International Journal of Remote Sensing*, 19: 1825-1841.

SAWS, (2017). South African Weather Services, Durban Weather Office Climatic data.

Scanlon, B.R., Healy, R.W. and Cook, P.G. (2002). Choosing appropriate techniques for quantifying groundwater recharge. Hydrogeology Journal, 10(1): 18-39

SCS. (1986). Urban Hydrology for Small Watersheds, Technical Release-55 (TR-55). USDA

Shahin, M. A. (1990). Impacts of urbanization of the Greater Cairo area on the groundwater in the underlying aquifer. Hydrological processes and water management in urban areas; Proceedings of the Duisberg Symposium, April 1990, IAHS Publ. 198.

Shaw, E.M. (2005). Hydrology in Practice. 3rd edition, Chapman & Hall, London. 546p

Simmers, I. (1998). Groundwater recharge: an overview of estimation 'problems' and recent developments. In Robins NS (ed) Groundwater Pollution, Aquifer Recharge and Vulnerability. *Geological Society Special Publication*, 130: 107–115

Soares, H.M.V.M. Boaventura, R.A.R., Machado, A.A.S.C., and Esteves da Silva, J.C.G. (1999). Sediments as monitors of heavy metal contamination in the Ave River Basin (Portugal): Multivariate analysis of data. Environmental Pollution, 105(3): 311- 323.

South Africa, (1998). National Water Act 36 of 1998. Notice 19182. *Government Gazette* 1091 (398): 1-101

Statistics Sa. (2011). Mid-year population estimates: Statistics South Africa. P0302. Statistics South Africa, Pretoria.

Strachan, L.B., Pattey, E., and Boisvert, J.B. (2002). Impact of nitrogen and environmental conditions on corn as detected by hyperspectral reflectance. *Remote Sensing of Environment,* 80(2), 213-224

Strohschon, R., Wiethoff, K., Baier, K., Lu, L., Bercht, A.L., Wehrhahn, R., and Azzam, R. (2013). Land use and water quality in Guangzhou, China: A survey of ecological and social vulnerability in four urban units of the rapidly developing megacity. *International Journal of Environmental Research, 7:* 343-358

Suk, H. and Lee, K.K. (1999). Characterization of a groundwater hydrochemical system through multivariate analysis: Clustering into ground water zones. *Groundwater*, 37 (3): 358–366

Taesombat, W. and Sriwongsitanon, N. (2009). Areal rainfall estimation using spatial interpolation techniques. *Science Asia,* 35: 268-275

Taylor, C.J. and Alley, W.M. (2002). Groundwater level monitoring and the importance of long term water level data. US. Geological Survey Circular 1217

Tazioli, A. (2011). Landfill investigation using tritium and isotopes as pollution tracers. *Acquae Mundi, 7*: 89-92.

Thiessen A.H. (1911). Precipitation for Large Areas, Monthly Weather Review, 39:1082-1084.

Thomas, R.J. (1988). The geology of the Port Shepstone area. Explanation of sheet 3030 Port Shepstone. Geological Survey of South Africa, Pretoria, 136p.

Thomas, R.J. (1990). Mzumbe Gneiss Suite. In: Johnson, M.R. (Ed.), Catalogue of South African Lithostratigraphic Units 2, 35–36.

Thomas, R.J. (1991). Mkomazi Gneiss. In: Johnson, M.R. (Ed.), Catalogue of South African Lithostratigraphic Units 3, 27–28.

Thornthwaite, C.W. (1948). An approach toward a rational classification of climate. *Geographical Revision,* 38: 55–94

Tripathi, R.P, and Singh, H.P. (1998). Soil erosion and conservation. New Age International (P) LTD Publishers.

U.S. Environmental Protection Agency. (1983). Results of the Nation-wide Urban Runoff Program, Volume 1 – Final Report. Report PB84-185552, Water Planning Division, Washington DC. 198p

USDA. (1986). Urban hydrology for small watersheds. Technical release, no 55 (TR-55). Soil Conservation Service, Washington, DC.

Van Tonder, G.J. and Xu, Y. (2000). Recharge – Excel-based software to quantify recharge. Department of Water Affairs and Forestry, Pretoria

Van Vururen, C.J. (1981). Depositional model for the Vryheid Formation in the northeastern part of the Karoo Basin – A review. *Geological Survey of South Africa*, 15: 1-11

Van Wyk, W.L. (1963). Groundwater studies in northern natal, Zululand and surrounding areas, Memoir 52, *Geological Survey of South Africa*, 133p

Wang, H.F., Anderson, M.P. (1982). Introduction to Groundwater Modeling: Finite Difference and Finite Element Methods. Academic Press, San Diego, CA, 237p

WHO. (2017). Guidelines for drinking-water quality: fourth edition incorporating the first addendum. Geneva: World Health Organization. Licence: CC BY-NC-SA 3.0 IGO. 631p

Winter, T.C. (2001). The concept of hydrologic landscapes. *Journal of the American Water Resources Association*, 37 (2): 335-349

Winter, T.C., Rosenberry, D.O. and LaBaugh, J.W. (2003). Where does the ground water in small watersheds come from? *Groundwater* 41 (7): 989-1000

Xu, Y. and Beekman, H.E. (Eds). (2003). Groundwater recharge estimation in Southern Africa. UNESCO IHP Series No. 64, UNESCO Paris.

Yang, H and Rose, N. (2005). Trace element pollution records in some UK lake sediments, their history, influence factors and regional differences. *Environment International*, 31(1): 63-75.

Zhang, L., Dawes, W.R., and Walker, G.R. (1999). Predicting the effect of vegetation changes on catchment average water balance. Technical Report 99/12.

APPENDICES

Appendix 1: Hydrometeorological parameters

Appendix 1.1: Monthly rainfall (mm) recorded at different weather station (SAWS, 2018)

Scottburgh

Year	JAN	FEB	MAR	APR	MAY	JUN	JUL	AUG	SEP	OCT	NOV	DEC
1995	118.4	29.5	175.8	225.5	30	60.5	11.3	5.5	22.5	101	83.5	237.5
1996	289	164.5	110	105	58.5	2	337.5	8	15	130	136.5	66
1997	134	62.5	95.5	162.6	23	185	82.2	16.5	88.8	126.5	335.5	74.2
1998	61.4	192	96.7	170.5	36	1	65.1	51	36	68.5	58	88.6
1999	69.2	165.5	154.5	19	14.5	70.5	0	13	31.5	237.5	57.2	244.5
2000	208	275.5	76.5	56	142	1.5	0	0	71.5	105.5	108.2	94.5
2001	61	52	67.5	36	136.5	0	0	1.3	138.3	73	268	261
2002	241.2	140	27.5	90	25	43.5	43.7	80.5	60	24.5	44.5	88.4
2003	31	31	82.5	213	62.5	28.2	16	109	91	24	56.5	185.5
2004	261	105.5	32	50.5	24	0	108.6	15	68	59.5	133	112
2005	72.5	69.5	86.7	47.5	29.5	51.5	1.5	23.5	34.5	50	137.6	119.2
2006	91	349.5	96.5	38.5	63.7	4	0	44	61	157.9	142.5	209.5
2007	103	63	203.7	121.8	5.5	32.5	25.5	15	72.3	63.4	110	41
2008	47	86.5	39.5	105.5	45	49.2	0	2.6	71.5	105.5	108.2	36
2009	246.7	87.1	73.5	16.5	51.5	23.5	0	10.1	88	113.1	153.2	144.4
2010	84.6	40	50.5	13.5	8.5	13.5	0	0	10.5	86.4	81.3	189.2
2011	156	13	29.8	170.8	120.5	77	117	69.5	30	62	308	195
2012	80	24.5	260	87.8	24.5	85.5	6.5	4	145.5	171.9	79	317
2013	93.5	76.1	156	82.3	32.5	0	13	5.7	20	236	46	126.9
2014	82	92.8	82.5	46.5	29	7.5	6.5	36	55	98	95	99.5
2015	26.5	97	71.5	32.5	0	60.5	237.5	0	73.5	48.5	63.5	63
2016	93	107	149.5	15	117.5	0	316	15	55.5	136.5	80.7	80.5
2017	0	206.5	105	48.5	297	0	49	155.5	84	105.5	108.2	94.5

Durban South

Year	JAN	FEB	MAR	APR	MAY	JUN	JUL	AUG	SEP	OCT	NOV	DEC
1995	73.6	32.8	211.2	172.6	44.1	44.4	16.1	11.1	16.2	102.9	82.6	224
1996	448.2	247.5	106.4	36.9	18.7	1.1	261.4	12.7	22.9	120.8	72.7	72.7
1997	187.1	99.5	59.6	167.9	40.5	89.4	159.2	16.6	71.2	151.3	277.2	71.3
1998	93.3	158.3	83.8	237.4	52.2	0	22.9	69.4	25.5	64.5	106.4	132.6
1999	94	239.3	44.2	36.7	36.5	74.4	3.5	12.2	74.1	195.9	59.1	291.8
2000	181.7	157.3	148.8	63.2	167.5	3.8	20.2	17.7	62.8	60.2	142	124.5
2001	65.5	77.4	43.4	89.5	12.5	0	45.3	0.3	145.4	171.3	191.2	142.9
2002	155.8	154.7	21.3	162.6	3.3	23.8	151.5	53.9	43.6	32.4	64.2	113.3
2003	102.1	15.7	96.3	121.8	36.3	61.5	1.9	58.4	121.5	48.5	61.3	93.8
2004	231.7	126	39.5	23.7	2.1	5.3	111.3	12.6	56.4	64.6	51.7	74.2

2005	66.6	128.8	120.7	38.9	3.4	48.3	2.8	20.6	25	44.2	95.1	90
2006	110.8	188.8	77.5	81.6	110.4	5.4	0	71.9	67.4	109.1	178.8	201.9
2007	68.2	80.1	245.4	156	0.8	58.7	21.3	22.7	98.1	139.5	301.2	57.3
2008	133.8	78.7	196.2	122.1	28.4	171.2	3.5	1.8	99.3	81.6	80.5	184.9
2009	159.8	121.7	52	51.5	25	8.9	12.9	54	72.6	94.2	126.8	145
2010	94.3	104.2	28.4	8.5	54	24.6	1.6	0.4	18.2	82.8	100	169.8
2011	124.8	12.2	75	67.8	73.2	47.4	98.4	62.4	47.4	65.4	276.2	55.4
2012	50.6	33.4	282.4	17	18.2	28.4	5.8	80.8	265	209.8	125.6	124.2
2013	165.8	57.2	115.4	87	52.6	28	33.4	13.2	50.6	156.8	83.2	79
2014	69	89.2	65.2	35	17.8	10.4	4.4	5.2	33.6	86.2	119.6	83.8
2015	56	96.8	79.4	25.8	0.8	6.6	199.4	10.8	75.8	39.2	61.4	102
2016	103.2	69.4	129.4	30.8	212.6	6.8	281.2	67.2	85.8	116.6	84.4	55.2
2017	62.4	137	47.8	60.6	217.4	0	34.4	40.8	77.6	166.6	152.3	78.3

Durban Botanicals Gardens

Year	JAN	FEB	MAR	APR	MAY	JUN	JUL	AUG	SEP	OCT	NOV	DEC
1995	40	21.2	252.6	177.1	30	80.1	10.3	9.5	13.2	118.7	79.1	210.4
1996	269	211.8	111.1	41.4	12.8	2	205.3	14.4	9.9	101.3	58.2	71.5
1997	128.7	71.9	61.1	81.3	39.4	76.6	154.7	29.3	64.1	174.4	280.6	58.5
1998	49.8	79.2	78.5	106.3	31.5	0	5.1	67.5	7.7	64.9	64.2	145.9
1999	68.2	315.2	20	25.7	50.6	62	0	18.4	95.5	350	46.1	371.9
2000	171.9	101.5	79.6	89	201.5	0	5	25.7	48.8	64.2	143.4	112.6
2001	142.4	70.3	41.1	108.7	0	0	14.2	1.6	141.8	147.9	171.9	183.9
2002	155.3	94.6	28	169.6	3.5	27.9	140.4	60.1	55.1	38.7	72.7	127.6
2003	82.5	19.9	83.4	40	24.8	73.5	3.7	45.5	143.1	35.5	97.8	71.9
2004	196.8	105.1	61.8	14.6	10.1	2.9	100	25.1	55.8	70.6	125	44.5
2005	83	69.9	85.1	46.3	38	37.8	2.7	20.4	27.8	44.6	110.1	112.4
2006	93.8	142.3	73.5	57.6	108.8	7.1	0	39.2	71.1	94.6	142.7	126.3
2007	37.9	87	175.2	138.9	0.3	34.5	1.3	14.5	83.9	98.5	183.7	43.3
2008	135	76.4	119.5	108.3	22.5	58.3	0	3.1	76.8	29.1	37.8	112.1
2009	109.3	45.2	28.9	29.2	76.4	6.7	4.5	42.2	41.3	112.6	78.4	99.4
2010	93.2	21	21.2	9.8	5.5	11.1	1.3	0.3	10.5	114.5	53.1	123.3
2011	155.5	15	39.1	114.9	55.2	45.6	126.2	53.8	63.5	49.4	311.2	135.1
2012	36.8	31.6	333	11.6	5.2	5.5	6.2	84.4	48.5	174.3	95.7	133.6
2013	126.7	31.2	170.6	12	12	37	25.6	21.7	46.9	177.7	120.1	159.8
2014	78.5	61.1	73	20.5	15.2	17	2.3	5	0	105.7	37.1	59.4
2015	41.2	112.5	89.5	25.5	0	11.2	63.3	7.5	9.9	40.1	35.5	67.8
2016	146.6	130.2	98.5	22.5	203.2	3	343	43.5	6.2	114.3	0	79.6
2017	46.5	137.9	57.6	54	184.4	0	34.4	40.8	77.6	166.6	152.3	78.3

Mount Edgecombe

Year	JAN	FEB	MAR	APR	MAY	JUN	JUL	AUG	SEP	OCT	NOV	DEC
1995	88	22.8	289	173	49	43	9.8	4.4	9.2	106.4	90.8	311.6
1996	314.2	222.6	127.6	34.6	12.4	12.4	216.6	12	6.4	106.2	54.8	62.2
1997	209.2	163.2	52.4	59	35.8	80.4	121	27.8	63.2	163.2	258.4	85.6
1998	76.4	190.8	64.4	65.4	33.4	0.2	14.4	72.4	20.8	64	95	152.8
1999	47.2	263.2	37.8	11.6	46.8	45.6	0.6	20.6	79.8	387.8	61.2	396.2
2000	212.8	245	69	52	117.6	8	4.2	15.4	26.2	49.2	143	174.2
2001	108.6	91.2	28.2	122.2	15.6	0.4	8.4	0.6	46.4	158.2	131.8	257.4
2002	203	98.6	36.8	124	0.8	9	158.4	46.8	37.6	29	49	76.6
2003	100.2	16.2	72	28.2	21.8	23	0.4	10.8	67.8	8.2	64.4	71
2004	171.6	96.4	41.6	25.2	0.8	0.2	57	24.6	39.4	39	79.4	33.4
2005	84.4	50.8	57.2	13	1.4	21.4	0.4	26.6	39.4	52.6	103	78.4
2006	83.4	122.4	55.6	60.2	99.6	1.4	0	65.2	66.4	96.4	87.8	176.6
2007	54.2	53.6	167	26.4	1.2	59.2	7.2	9.6	43.4	110.6	176.4	53.4
2008	111.8	112	36.8	75	6.2	31.4	0.6	1.4	64.6	49.8	64.8	98.6
2009	95.4	84.8	24	29.2	34.4	0.4	0.2	32.8	36.4	72.6	104	155.8
2010	119.2	47.2	17.4	10.6	7.4	12.8	1.8	3.2	16.8	61.4	95	180
2011	193	7	74.6	116.8	63.6	73.2	138.4	71.2	39.6	98.8	280.4	60.2
2012	56.2	22.6	162.6	25.6	11	12.4	4	55	232.8	202.2	154.6	137.2
2013	136	76.4	121.6	80	85.8	60.6	23.4	16.4	41.4	160.8	78.8	90.6
2014	112.8	49.8	99	23	11.6	12	5.2	3.2	33.4	104.4	53.2	82.8
2015	105.2	116.2	100	13.4	0	5	147.2	2.8	45.2	25.8	42	95.8
2016	124.2	47	109.6	21.4	118.8	3.6	263.2	46.4	84	106	82.4	45.2
2017	65.4	167.2	37	51.6	165.8	0.6	20.4	28.8	65.6	112	131	152

Virginia Airport

Year	JAN	FEB	MAR	APR	MAY	JUN	JUL	AUG	SEP	OCT	NOV	DEC
1995	50.4	24.2	158.8	130.2	36	46	15.2	5.6	4.8	63	59.2	168
1996	118.8	113.2	100.6	32	18	5.8	242.8	13.8	7.4	96.6	47.8	73
1997	164.8	114.8	45.2	75.8	30.6	79.6	108.6	25	55	141.4	227.8	66
1998	67.6	159.2	59.4	99.8	49.2	3.4	19.4	80.2	18	66.6	101.6	97.4
1999	54.8	208.8	30.6	15.2	24.6	50	1	27.4	62.6	474.2	32	221.6
2000	184.8	211.6	62.8	57.2	164.6	7	9.2	22.4	36.4	6.2	13	149.2
2001	88.2	90.6	26	121	7	0	22.2	1.6	139.6	153.6	139.2	180
2002	157.4	96.8	39.6	171.8	2.6	23.4	178	59.2	49	35.4	87.8	62.8
2003	100.8	9.8	95	43.8	12.2	41.6	7.6	29.2	90.6	16.8	86.4	5.2
2004	212.6	115.4	52.8	19.6	3.4	1.6	59.8	23.4	43.8	57	39.6	34.2
2005	73	104.2	91.8	16.6	3.6	47	1.8	23.6	27.8	47.4	93.2	65
2006	84.6	86.8	44.4	76.8	57.4	3	0	70.4	66.4	81.6	78	141.2
2007	54.4	56.4	122.2	118.8	0.8	59.8	24.6	12.4	53.4	128.6	136.8	49.8
2008	98.6	103.8	53.6	80.4	8.4	34.4	1.4	5	71	42.4	71.8	127.8

2009	123.2	59.4	27	32.8	36.6	0.2	0.4	46.2	19.4	54.6	87.2	109.4
2010	69.6	67	18.4	23.6	10.8	7.2	1.6	0.4	10	55.8	81.2	160.6
2011	148.6	5	60.2	109.8	49.4	75.8	97	50	37.8	59.4	262.2	54
2012	28	34	263.8	12.6	14	40.6	5.4	82.2	231.8	145.8	100.4	107.6
2013	99.2	50.4	135.2	82	69	52.4	34.8	3	41.6	113.6	85	93
2014	75.4	35.2	69	28.6	20.2	8	4.2	8.8	32.4	105.4	45	80
2015	80.2	58.2	75	28	0.6	0	159.4	0	11.8	17.2	43	64
2016	130	57.4	55.8	26	211.8	2	281.2	46.8	82.4	87	88	44.2
2017	56.8	105	41	71.6	193.6	0	24.6	62.4	67.8	189		

Appendix 1.2**:** Daily monthly mean temperature recorded at different stations (SAWS, 2018)

Mount Edgecombe

Year	JAN	FEB	MAR	APR	MAY	JUN	JUL	AUG	SEP	OCT	NOV	DEC
1995	24.1	25.2	23.5	20.4	19.3	16.9	16.6	18.2	19.7	20.6	21.6	21.9
1996	24.3	24.2	22.4	20.2	19.5	17.5	15.7	16.7	19.2	20.7	22.4	24.4
1997	24.3	24.2	23.4	20.7	18.7	17.7	16.5	18.4	19.2	20.5	21.0	22.8
1998	24.5	24.8	23.8	22.4	19.4	17.3	17.6	17.8	19.3	20.3	22.4	23.3
1999	25.3	24.9	24.8	22.8	20.2	18.2	18.0	18.7	19.1	20.0	23.0	24.3
2000	23.4	25.3	24.8	21.1	18.9	18.3	17.0	18.7	19.4	20.1	21.7	23.4
2001	23.6	23.8	24.1	21.8	19.6	18.7	17.5	18.7	18.9	21.1	23.0	23.4
2002	24.8	23.5	24.0	22.3	19.7	17.3	16.8	18.5	19.3	20.7	20.7	23.8
2003	24.4	25.7	24.5	22.9	19.4	17.3	16.9	17.1	18.8	20.5	21.6	21.5
2004	24.0	23.0	21.9	20.4	17.5	15.0	14.3	17.2	16.7	18.7	21.7	23.1
2005	23.1	23.7	21.8	20.0	18.4	16.3	15.7	17.6	18.3	19.1	20.5	20.5
2006	23.1	23.9	21.1	19.9	16.6	15.1	16.2	16.2	17.8	19.6	20.1	21.9
2007	22.8	23.7	21.7	20.7	20.5	18.1	17.7	18.7	20.8	21.0	22.0	23.3
2008	24.6	25.4	24.1	21.3	20.5	18.6	18.1	19.4	19.3	20.5	22.3	24.2
2009	24.6	24.8	23.9	21.7	20.4	19.1	17.2	18.3	19.4	20.8	21.1	22.8
2010	24.5	25.7	24.8	23.4	21.7	18.2	18.3	18.9	21.0	21.3	22.8	23.4
2011	24.5	24.9	25.5	21.5	19.8	17.2	15.9	17.3	19.8	20.4	21.5	23.6
2012	25.6	25.6	24.5	20.7	20.7	18.7	17.8	19.8	19.6	21.1	22.4	23.9
2013	23.9	23.9	22.6	20.2	18.8	17.3	17.9	17.9	19.8	19.6	21.3	21.8
2014	24.0	24.4	23.5	20.8	19.0	17.2	16.3	18.5	19.6	19.2	21.0	23.1
2015	24.1	23.2	23.2	20.6	20.6	18.3	16.9	18.4	18.9	21.3	21.3	23.9
2016	24.4	24.4	23.9	22.2	19.3	17.8	16.0	17.8	19.0	19.3	21.5	24.0
2017	23.5	24.2	23.9	21.6	19.9	18.2	17.7	17.9	19.8	20.7	21.4	22.8

Virginia Airport

Year	JAN	FEB	MAR	APR	MAY	JUN	JUL	AUG	SEP	OCT	NOV	DEC
1995	24.0	24.7	23.3	20.8	19.3	17.4	16.8	18.1	19.5	20.9	21.6	21.9
1996	24.3	24.4	22.6	20.8	19.9	18.1	16.2	17.1	17.9	22.5	24.0	25.8
1997	25.5	26.1	24.7	21.5	19.6	18.2	17.5	18.9	17.4	19.5	20.7	22.3
1998	23.7	23.7	23.2	22.7	17.4	19.7	19.7	19.8	21.1	22.2	23.9	25.0

1999	27.1	23.7	26.6	24.5	22.2	20.6	19.9	20.5	20.7	21.7	24.7	24.5
2000	23.5	25.3	24.8	21.4	19.4	18.5	17.5	19.0	19.3	20.3	22.0	23.3
2001	23.7	24.1	24.3	22.1	20.1	19.5	18.2	19.0	19.0	20.9	22.8	23.6
2002	24.4	23.7	24.2	22.5	20.1	18.3	17.5	18.8	19.6	20.7	20.9	23.5
2003	24.0	26.3	25.2	23.7	20.0	17.8	17.0	17.0	18.2	20.0	21.1	21.6
2004	24.2	24.8	23.7	22.6	20.0	17.7	16.9	19.1	18.5	20.3	23.0	24.4
2005	24.5	25.3	23.8	21.8	20.3	18.9	18.1	19.3	20.0	20.9	22.2	22.3
2006	24.5	25.5	23.1	21.9	19.2	18.0	18.8	18.8	19.8	21.5	22.1	23.8
2007	24.7	25.6	24.0	22.5	20.4	18.5	17.9	18.3	20.5	20.6	22.0	23.5
2008	24.8	25.7	23.9	21.0	20.4	18.4	17.9	19.1	18.9	20.1	21.8	23.5
2009	24.1	24.3	23.8	21.7	20.4	19.3	17.0	17.8	18.3	19.3	19.1	20.3
2010	24.3	26.0	25.0	23.4	22.0	19.0	18.7	18.9	21.1	21.5	22.6	23.3
2011	24.7	24.9	25.2	21.9	20.3	17.9	16.8	17.5	20.0	20.4	21.3	23.5
2012	25.5	25.4	24.5	21.0	20.8	18.7	17.6	18.6	19.0	20.2	21.3	24.0
2013	24.5	24.7	23.5	21.1	20.1	18.9	18.2	18.3	19.3	19.6	22.1	23.5
2014	25.9	26.2	25.4	22.8	21.2	19.7	18.6	20.3	21.2	20.7	22.5	24.4
2015	25.6	25.1	24.9	22.9	22.3	20.2	19.4	20.4	20.4	22.7	22.4	25.3
2016	25.7	25.6	25.8	22.5	19.5	18.8	17.6	18.7	20.4	24.7	22.8	25.8
2017	28.5	25.9	26.5	23.0	22.7	18.6	18.7	18.7	20.5	18.3	21.0	22.3

Durban South

Year	JAN	FEB	MAR	APR	MAY	JUN	JUL	AUG	SEP	OCT	NOV	DEC
1995	24.5	25.5	23.6	20.6	19.2	16.5	16.1	18.0	19.8	20.6	21.8	21.9
1996	24.2	24.7	22.9	20.8	19.1	16.5	15.4	16.7	19.0	20.5	22.2	24.4
1997	24.5	24.4	23.8	20.8	18.4	16.8	16.3	18.7	19.5	20.5	20.8	22.8
1998	24.3	24.9	23.8	22.6	19.0	16.4	17.3	18.0	19.5	20.6	22.6	23.3
1999	25.6	25.3	25.5	23.2	19.9	17.8	17.6	18.7	19.3	20.4	23.0	24.4
2000	23.7	25.6	24.7	21.0	18.6	17.7	16.6	19.0	19.3	20.1	22.1	23.8
2001	24.4	24.5	24.8	22.0	19.9	18.7	17.5	18.6	19.2	21.3	23.0	23.7
2002	25.0	23.9	24.7	22.7	19.6	17.3	16.7	18.6	19.7	21.3	21.2	24.1
2003	24.7	26.3	24.8	23.0	19.3	17.0	16.2	17.0	18.7	20.4	22.0	23.4
2004	24.4	25.0	23.6	22.3	19.5	16.8	15.8	18.9	18.3	20.4	23.1	24.8
2005	24.7	25.2	23.5	21.7	19.8	17.5	17.0	18.7	19.8	21.2	22.3	22.1
2006	24.5	25.4	22.7	22.0	18.2	16.5	17.6	18.1	20.0	21.8	22.5	23.8
2007	24.6	25.4	23.5	22.3	19.2	17.3	16.7	17.7	20.4	20.4	21.4	22.8
2008	24.3	25.0	23.8	20.7	20.0	17.3	17.0	18.3	18.5	19.8	21.8	23.5
2009	23.8	24.4	23.5	21.4	19.6	18.4	16.3	17.7	18.7	20.5	20.9	22.5
2010	24.6	25.8	24.6	23.1	21.5	17.5	17.8	18.5	21.0	21.3	22.5	23.3
2011	24.8	25.7	25.8	21.3	19.5	16.9	16.0	17.3	19.9	21.1	21.7	23.9
2012	26.5	26.6	25.2	21.2	20.7	17.4	16.7	18.8	18.8	20.2	21.1	24.4
2013	24.7	25.1	24.0	21.2	19.9	17.3	17.4	18.0	19.2	19.7	21.9	22.7
2014	25.1	25.5	24.1	21.6	19.7	17.5	16.6	18.9	20.2	19.6	21.2	23.3
2015	24.7	24.2	24.2	21.5	20.8	18.1	17.5	18.6	19.2	21.5	21.2	24.7
2016	25.6	25.3	25.4	23.7	20.5	17.7	16.4	17.9	19.5	19.8	21.8	23.7
2017	24.0	24.7	24.2	21.9	19.7	17.7	17.4	17.8	19.6	19.9	19.9	21.7

Appendix 1.3: Monthly Average humidity recorded at 8:00 at different weather stations

Durban South

Year	JAN	FEB	MAR	APR	MAY	JUN	JUL	AUG	SEP	OCT	NOV	DEC
1995	73	73	79	78	80	75	75	72	72	73	72	78
1996	83	78	81	76	83	77	77	66	74	76	73	76
1997	77	79	81	78	77	76	81	83	81	75	82	77
1998	79	85	83	84	78	74	79	71	71	69	71	73
1999	74	78	76	73	75	69	75	71	68	73	75	80
2000	77	79	81	79	80	76	73	76	67	75	74	73
2001	66	69	69	73	69	67	59	67	69	76	76	72
2002	76	76	74	76	73	73	68	80	76	69	63	75
2003	75	76	74	79	76	77	74	71	79	73	74	71
2004	78	78	79	74	71	68	68	77	68	72	75	73
2005	80	77	78	78	75	70	75	74	74	71	75	70
2006	84	80	77	74	71	68	71	68	74	77	71	74
2007	75	75	76	76	64	71	69	69	77	76	76	75
2008	79	77	77	75	81	78	73	73	64	77	80	79
2009	81	77	78	80	81	68	69	73	79	82	78	82
2010	80	79	77	74	76	72	72	66	71	78	76	79
2011	80	71	74	75	77	74	77	76	73	69	71	65
2012	67	69	70	67	68	67	64	65	68	77	73	73
2013	74	69	70	69	69	66	77	66	67	68	71	73
2014	71	73	75	69	74	66	65	80	68	69	70	72
2015	72	73	77	74	75	72	80	78	77	73	69	71
2016	72	72	72	69	76	75	75	75	71	71	70	69
2017	68	72	71	68	74	67	71	70	68	61	78	82

Mount Edgecombe

Year	JAN	FEB	MAR	APR	MAY	JUN	JUL	AUG	SEP	OCT	NOV	DEC
1995	82	80	77	79	79	73	73	74	74	73	70	75
1996	81	79	82	84	79	65	70	66	72	72	70	72
1997	75	75	78	75	72	62	74	79	78	71	77	72
1998	74	81	78	80	72	65	66	70	70	69	70	72
1999	72	79	78	72	75	73	74	75	72	71	71	78
2000	77	79	78	75	75	70	67	74	66	74	74	78
2001	72	76	78	83	76	73	68	72	75	79	79	77
2002	76	81	81	82	75	76	69	85	79	73	66	79
2003	78	78	77	83	78	77	69	72	79	74	76	76
2004	82	83	82	81	79	75	73	81	75	76	77	76
2005	84	80	81	84	76	67	70	69	77	72	73	72
2006	80	79	77	78	73	66	69	65	76	77	72	75
2007	74	75	77	74	64	67	66	63	75	76	77	71
2008	78	75	75	75	79	74	69	71	62	77	79	77
2009	78	78	77	79	79	66	67	74	74	78	74	80
2010	78	77	74	73	74	67	67	62	70	75	72	76
2011	79	72	74	79	77	72	78	76	75	76	76	73

2012	72	74	76	76	76	70	66	71	74	80	76	74
2013	77	75	76	72	72	69	81	71	67	66	70	73
2014	70	73	75	65	73	64	63	62	66	67	66	70
2015	70	75	75	73	68	64	73	74	74	70	64	73
2016	73	71	77	74	78	70	73	71	75	76	74	71
2017	72	75	76	73	76	70	74	71	74	69	79	77

Virginia

Year	JAN	FEB	MAR	APR	MAY	JUN	JUL	AUG	SEP	OCT	NOV	DEC
1995	80	81	81	81	80	72	71	75	80	81	81	85
1996	87	86	88	83	83	70	75	74	68	81	82	87
1997	89	86	84	77	73	65	73	80	83	79	85	79
1998	83	89	85	86	75	64	72	74	77	77	82	83
1999	85	88	89	84	81	63	74	77	79	83	85	95
2000	91	92	93	88	85	79	74	84	78	87	86	86
2001	85	85	87	90	82	80	76	82	78	86	86	84
2002	86	85	85	83	73	71	63	86	83	79	73	87
2003	83	84	81	84	76	73	70	72	84	84	83	84
2004	77	79	76	73	67	60	63	77	74	81	87	86
2005	90	79	78	79	72	61	65	72	75	67	47	45
2006	68	73	71	72	65	57	60	58	72	76	70	72
2007	72	71	71	71	53	58	54	59	70	73	73	69
2008	74	71	73	69	71	65	60	64	59	74	77	76
2009	77	74	73	73	72	56	56	67	72	75	73	77
2010	73	72	69	65	65	55	56	53	64	70	68	71
2011	73	69	70	67	66	59	64	63	66	70	70	68
2012	69	68	68	64	64	54	55	61	67	72	71	71
2013	70	68	70	67	62	56	69	61	64	69	70	73
2014	73	72	73	63	66	55	53	61	66	68	68	71
2015	72	74	76	68	63	57	66	68	72	70	67	74
2016	75	73	74	71	71	62	60	63	70	72	72	72
2017	70	73	71	66	68	60	62	63	71	68	52	65

Appendix 1.4: Estimation of monthly runoff using the Curve number method

Land Use	Hydraulic Condition	Hydraulic Soil Group	CN	Weighted CN
Grassland	Fair	B	69	8.25
Agriculture	Good	B/C	82	19.98
Built-Up Area	*	B/C	75	15.97
Forest	Fair	B/C	44	18.06
Bare Soil/Rock	*	B	86	0.0440
Water Bodies	*	B/C	100	1.28
Total				**63.59**
S (mm) =	**145.45**			
R_0=	$\frac{(P-0.2S)^2}{(P+0.8S)}$			

Ro (mm)/month	Jan	Feb	Mar	Apr	May	Jun	Jul	Aug	Sep	Oct	Nov	Dec
R	22.57	10.89	13.65	6.50	0.037	0.019	0.703	0.015	6.05	14.78	28.06	29.51
R_0 (mm/yr)	**132.76**											

Appendix 1.5: Location of weather stations

No	Station Name	Lat	Long
1	Richmond	-29.87	30.27
2	Durban Botanical Gardens	-29.85	31
5	Stanger	-29.33	31.3
7	Pietermaritzburg	-29.633	30.4
8	Scottburgh	-30.2856	30.75469
9	Mount Edgecombe	-29.7	31.05
10	Virginia	-29.33	31.3

Appendix 2: Groundwater level, depth to groundwater and borehole yield data (DWS, 2016)

Site ID	Altitude (m amsl)	Depth to water (m bgl)	Water level (m amsl)	Yield (l/s)	Site ID	Altitude	Depth to water (m bgl)	Water level (m amsl)	Yield (l/s)
2730CCV0003	1198	31.61	1166.39	0.111	2930DD00018	307	12	295	1.4
2930AC00048	1271	8	1263	0.19	2930DD00019	294	15	279	0.15
2930AC00049	1290	15	1275	6.31	2930DD00020	375	25	350	0.7
2930AC00058	1194	10.53	1183.47	0.76	2930DD00021	349	18	331	0.33
2930AC00060	1122	22.37	1099.63	0.5	2930DD00022	346	6	340	1.2
2930AC00064	1058	2	1056	1.51	2930DD00024	122	17	105	10
2930AC00093	1108	43	1065	10	2930DD00026	317	4	313	0.4
2930AC00095	1129	14	1115	0.95	2930DD00028	311	5.4	305.6	0.15
2930AC00096	1114	37.16	1076.84	1.51	2930DD00037	318	5	313	0.17
2930AC00097	1097	1.67	1095.33	0.76	2930DD00042	384	27	357	0.3
2930AD00032	759	24.81	734.19	0.76	2930DD00043	339	8	331	0.01
2930AD00033	782	6.97	775.03	1.01	2930DD00048	150	27	123	0.56
2930AD00037	813	17	796	0.83	2930DD00049	323	17	306	2.22
2930AD00038	786	12.6	773.4	2.16	2930DD00051	307	72.5	234.5	0.66
2930AD00039	794	7.13	786.87	0.34	2930DD00052	249	75	174	2.5
2930AD00040	701	7.05	693.95	0.61	2930DD00053	193	67	126	1.11
2930AD00041	689	9.11	679.89	1.67	2930DD00054	307	7	300	0.07
2930AD00042	699	6.54	692.46	2.02	2930DD00056	295	77	218	0.18
2930AD00043	705	5.77	699.23	0.56	2930DD00057	247	48	199	0.01
2930AD00046	1091	3.66	1087.34	2.5	2930DD00058	214	48	166	0.01
2930AD00047	1092	15	1077	0.25	2930DD00059	332	62.5	269.5	0.83
2930AD00051	1086	0.85	1085.15	2	2930DD00060	176	55	121	0.06
2930AD00052	725	8.28	716.72	0.33	2930DD00061	258	2.9	255.1	0.01

2930AD00053	815	47.68	767.32	3.19	2930DD00062	140	29	111	4
2930AD00054	1062	30	1032	1.94	2930DD00063	207	32	175	1.5
2930AD00056	1156	10.46	1145.54	2.15	2930DD00064	160	33	127	1
2930AD00059	719	17	702	1.51	2930DD00065	132	22	110	14
2930AD00061	750	9.21	740.79	0.56	2930DD00066	241	30	211	4
2930AD00063	715	15.96	699.04	0.08	2930DD00067	175	2.2	172.8	2.5
2930AD00064	786	32.88	753.12	0.39	2930DD00068	175	1.6	173.4	6
2930AD00066	679	18.28	660.72	0.14	2930DD00069	363	16	347	10
2930AD00067	718	70	648	2.5	2930DD00070	349	14	335	5
2930AD00068	713	9.7	703.3	4	2930DD00071	324	8	316	6
2930AD00072	806	17.47	788.53	0.22	2930DD00072	576	76	500	2.5
2930AD00074	674	20.85	653.15	0.22	2930DD00073	244	3.41	240.59	7
2930AD00075	696	6.6	689.4	0.01	2930DD00074	540	15.4	524.6	3.5
2930AD00076	724	9.06	714.94	1	2930DD00075	528	10.6	517.4	0.17
2930AD00077	680	15	665	0.19	2930DD00076	530	1.3	528.7	0.14
2930AD00078	679	6	673	2.86	2930DD00077	547	54	493	0.25
2930AD00080	1039	9.26	1029.74	0.14	2930DD00078	535	12.3	522.7	0.33
2930BC00145	890	26.48	863.52	0.5	2930DD00082	315	3.89	311.11	0.33
2930BC00147	845	14.07	830.93	0.5	2930DD00084	276	3.5	272.5	2.26
2930BC00148	894	27.47	866.53	1.3	2930DD00085	67	52.32	14.68	2
2930BC00149	786	21	765	0.05	2930DD00086	61	32.1	28.9	0.63
2930BC00153	813	27.47	785.53	0.2	2930DD00087	50	19.5	30.5	6.6
2930BC00154	910	30.26	879.74	0.11	2930DD00092	4	1.91	2.09	0.58
2930BC00156	1019	12.81	1006.19	0.5	2930DD00095	10	5.11	4.89	1.1
2930BC00159	948	4.48	943.52	0.13	2930DD00096	10	5.48	4.52	1.11
2930BC00160	1034	21.24	1012.76	1.17	2930DD00098	9	0.93	8.07	9.8
2930BC00162	918	24.26	893.74	0.33	2930DD00099	9	3.8	5.2	19

2930BC00169	950	1.14	948.86	0.33	2930DD00100	9	3.01	5.99	0.83
2930BC00171	897	1.4	895.6	0.3	2930DD00101	7	2.93	4.07	13
2930BC00172	904	1	903	0.2	2930DD00102	7	2.41	4.59	26
2930BC00174	912	20	892	0.22	2930DD00103	6	0.83	5.17	10
2930BCR0005	790	11.55	778.45	0.42	2930DD00104	6	0.9	5.1	6.31
2930BCR0032	983	46.6	936.4	0.42	2930DD00105	7	0.45	6.55	8.33
2930BCR0036	990	66	924	0.42	2930DD00106	7	0.48	6.52	25
2930BCR0037	990	4.7	985.3	0.28	2930DD00107	6	1.05	4.95	25
2930BD00004	514	1	513	2.52	2930DD00108	6	1.08	4.92	5.56
2930BD00067	529	45.3	483.7	0.36	2930DD00109	6	2.06	3.94	4.44
2930BD00068	916	63.1	852.9	0.17	2930DD00110	7	0.84	6.16	1.06
2930BD00069	896	9.4	886.6	0.36	2930DD00111	7	0.88	6.12	0.28
2930BD00073	542	57.39	484.61	0.33	2930DD00112	7	0.64	6.36	1
2930BD00089	862	46.9	815.1	0.17	2930DD00113	7	0.41	6.59	3.79
2930BD00090	963	31.4	931.6	0.22	2930DD00114	7	0.94	6.06	0.13
2930BD00091	681	57.4	623.6	0.39	2930DD00115	7	0.62	6.38	0.81
2930BD00096	1006	23.66	982.34	0.25	2930DD00116	4	1.05	2.95	1.3
2930BD00111	726	31.32	694.68	0.24	2930DD00118	14	1.05	12.95	0.15
2930BD00112	619	25	594	0.06	2930DD00119	14	4.1	9.9	1.82
2930BD00122	660	6.81	653.19	0.08	2930DD00120	12	4.8	7.2	1.25
2930BD00147	611	9.38	601.62	0.22	2930DD00121	12	3.88	8.12	0.1
2930BD00148	541	57.39	483.61	0.36	2930DD00122	10	4.35	5.65	0.25
2930BD00150	660	6.81	653.19	0.01	2930DD00124	13	4.74	8.26	0.23
2930BD00152	783	49.65	733.35	0.14	2930DD00125	16	1.43	14.57	0.57
2930BD00153	614	17.48	596.52	0.45	2930DD00126	16	1.44	14.56	0.39
2930BD00154	562	51.32	510.68	0.67	2930DD00127	8	0.63	7.37	0.47
2930BD00155	608	44.64	563.36	0.7	2930DD00128	11	0.44	10.56	0.5

2930BD00157	858	11.27	846.73	11	2930DD00129	13	4.34	8.66	0.56
2930BD00159	887	3.62	883.38	2.22	2930DD00130	19	3.05	15.95	0.3
2930BD00160	673	34.25	638.75	1.4	2930DD00131	19	2.92	16.08	1.4
2930BD00162	951	43	908	2.5	2930DD00132	53	1.41	51.59	0.34
2930BD00163	588	33.45	554.55	0.77	2930DD00133	53	1.76	51.24	0.09
2930BDM0012	676	57.93	618.07	0.8	2930DD00134	53	1.54	51.46	0.1
2930BDM0013	861	51.03	809.97	0.7	2930DD00135	6	1.44	4.56	0.2
2930BDM0058	557	0.18	556.82	2.5	2930DD00136	7	1.45	5.55	1.66
2930BDM0062	778	49.65	728.35	0.42	2930DD00137	10	1.33	8.67	0.33
2930BDM0063	609	17.48	591.52	1.7	2930DD00138	11	1.56	9.44	0.53
2930BDM0064	557	51.32	505.68	0.44	2930DD00139	8	1.27	6.73	0.15
2930BDM0065	603	44.64	558.36	2	2930DD00140	9	1.99	7.01	0.22
2930BDM0067	853	11.27	841.73	0.17	2930DD00141	9	1.86	7.14	0.08
2930BDM0069	882	3.62	878.38	2	2930DD00142	13	1.87	11.13	0.5
2930BDM0070	668	34.25	633.75	0.67	2930DD00143	14	4.53	9.47	0.07
2930BDM0072	946	43	903	1	2930DDM0095	291	75.9	215.1	1
2930BDM0073	583	33.45	549.55	2	2930DDM0097	212	50.2	161.8	1
2930BDV0002	809	22	787	2.6	2930DDM0124	323	0.61	322.39	6.3
2930BDV0004	918	21.1	896.9	1.89	2930DDM0125	410	27.78	382.22	0.51
2930BDV0006	934	63	871	4.42	2930DDM0160	321	15.26	305.74	0.51
2930BDV0009	1033	44.41	988.59	0.14	2930DDR0001	63	29.04	33.96	1.39
2930BDV0010	514	22.53	491.47	1.67	2930DDR0021	370	9.36	360.64	4.44
2930BDV0012	917	27.8	889.2	2	2930DDR0022	410	29	381	7.58
2930BDV0013	722	15.79	706.21	0.52	2930DDR0024	337	75.04	261.96	0.14
2930BDV0024	693	37.35	655.65	2.5	2930DDR0027	558	4.86	553.14	0.14
2930BDV0025	693	40.98	652.02	2.22	2930DDR0028	325	5.1	319.9	0.67
2930BDV0027	712	49.99	662.01	0.56	2930DDR0030	251	36.88	214.12	5

2930BDV0029	799	5.1	793.9	0.56	2930DDR0031	150	27.36	122.64	1.11
2930BDV0030	863	1.97	861.03	0.42	2930DDR0036	345	42.83	302.17	0.17
2930BDV0031	552	15.34	536.66	0.6	2931AC00031	523	54	469	0.17
2930BDV0032	708	46.18	661.82	1	2931AC00074	234	3.29	230.71	0.5
2930BDV0033	973	13	960	1.1	2931AC00083	417	1.28	415.72	0.09
2930BDV0034	879	0.63	878.37	0.44	2931AC00085	404	17.5	386.5	0.55
2930BDV0035	880	12.82	867.18	6.67	2931AC00086	376	42.1	333.9	0.4
2930BDV0036	753	5.52	747.48	4.17	2931AC00088	366	41.3	324.7	0.1
2930BDV0037	886	3.9	882.1	2.78	2931AC00100	370	16.5	353.5	0.056
2930BDV0038	746	2.35	743.65	0.88	2931AC00101	537	12.15	524.85	0.08
2930BDV0052	666	30	636	2.78	2931ACM0053	329	21.98	307.02	0.08
2930BDV0053	505	45.3	459.7	0.33	2931ACM0060	532	12.15	519.85	0.03
2930BDV0058	489	17	472	0.83	2931ACV0001	621	31.84	589.16	0.03
2930BDV0059	510	37	473	0.83	2931ACV0004	468	32.9	435.1	0.02
2930BDV0060	675	27.56	647.44	0.22	2931ACV0011	635	27.44	607.56	0.08
2930CA00117	1106	6	1100	0.31	2931ACV0032	506	51.34	454.66	0.02
2930CA00118	1110	10	1100	0.61	2931ACV0034	235	3.62	231.38	0.1
2930CA00120	1080	28.35	1051.65	0.67	2931CA00025	103	1.193	101.807	0.08
2930CB00041	754	15	739	1.67	2931CA00026	204	55.4	148.6	0.05
2930CB00046	888	27	861	0.28	2931CA00027	80	52.3	27.7	0.01
2930CB00066	888	10	878	1.39	2931CA00028	95	1.307	93.693	0.1
2930CB00067	883	21.2	861.8	1.11	2931CA00029	188	16.3	171.7	0.34
2930CB00069	696	12.76	683.24	1.14	2931CA00031	123	32.3	90.7	3.79
2930CB00071	701	24.17	676.83	2.78	2931CA00032	114	2.92	111.08	3.33
2930CB00072	679	15.7	663.3	0.5	2931CA00033	101	52.8	48.2	0.4
2930CB00073	881	19.92	861.08	0.76	2931CA00035	133	12	121	0.08
2930CB00075	861	8.42	852.58	0.01	2931CA00036	101	25	76	2

2930CB00076	855	10.47	844.53	2	2931CA00040	195	54.05	140.95	2.48
2930CB00079	1079	43.68	1035.32	0.01	2931CA00041	193	35	158	0.34
2930CB00081	1063	18	1045	3.3	2931CA00042	95	30.24	64.76	0.2
2930CB00082	1059	16.64	1042.36	3.3	2931CA00043	219	47	172	0.88
2930CB00083	1024	62.71	961.29	6.39	2931CA00044	345	12.98	332.02	1.25
2930CB00086	1191	11.36	1179.64	1.94	2931CAM0009	80	58.24	21.76	1.25
2930CB00087	1067	1.4	1065.6	1	2931CAM0050	190	54.05	135.95	0.05
2930CB00088	1143	10.25	1132.75	4	2931CAM0051	188	35	153	5.55
2930CB00096	1120	14.06	1105.94	6.39	2931CAM0052	90	30.24	59.76	2.75
2930CB00097	804	15.23	788.77	20	2931CAM0054	214	47	167	0.66
2930CB00098	787	9.55	777.45	0.67	2931CAM0055	340	12.98	327.02	0.43
2930CB00100	870	36.51	833.49	6.67	2931CAV0002	56	4.8	51.2	10
2930CB00102	932	24.92	907.08	3.05	2931CAV0003	23	52.45	-29.45	0.56
2930CB00106	848	46.75	801.25	1.73	2931CAV0006	65	21.7	43.3	0.03
2930CB00108	790	46	744	1.5	3029CBK0001	76	1.81	74.19	0.01
2930CB00111	660	26.27	633.73	0.45	3030AA00007	900	18	882	0.02
2930CB00112	804	17.61	786.39	0.45	3030AA00008	964	12	952	0.02
2930CB00113	794	13.11	780.89	0.45	3030AA00013	778	10	768	0.03
2930CB00114	648	18.29	629.71	0.45	3030AA00044	493	13	480	0.02
2930CB00116	638	27.43	610.57	0.1	3030AA00046	599	40	559	0.5
2930CB00119	667	19.94	647.06	0.56	3030AA00056	692	20	672	0.02
2930CBR0003	1118	1.5	1116.5	5	3030AA00057	496	20	476	0.01
2930CBR0004	610	12	598	5	3030AA00063	920	10	910	0.02
2930CBR0005	610	5.5	604.5	6.67	3030AA00064	1035	10	1025	0.4
2930CC00012	661	5.5	655.5	11	3030AA00071	1050	20	1030	0.01
2930CC00036	1091	5	1086	4.17	3030AA00076	1044	15	1029	0.4
2930CC00037	1146	18	1128	0.64	3030AA00077	958	30	928	0.08

2930CCE0002	813	4.7	808.3	0.14	3030AA00123	808	21.38	786.62	0.03
2930CCR0010	983	33	950	0.56	3030AAE0003	838	28.9	809.1	0.1
2930CCR0013	874	0.76	873.24	0.56	3030AAG0001	943	12.84	930.16	0.1
2930CCR0015	897	1.2	895.8	1.11	3030AAR0003	1258	28.9	1229.1	0.01
2930CCR0019	920	10.19	909.81	22	3030AAR0022	800	21.38	778.62	0.03
2930CCR0020	980	14.3	965.7	0.56	3030AAV0042	857.4	42.75	814.65	0.1
2930CCR0022	877	5.04	871.96	2.78	3030AB00050	352	7.6	344.4	0.02
2930CD00010	714	9	705	1.11	3030AB00059	537	22	515	0.3
2930CD00011	795	9	786	2.78	3030AB00060	551.07	81	470.07	0.08
2930CD00012	763	9	754	19	3030AB00067	228	17	211	0.2
2930CD00024	859	5.4	853.6	0.61	3030AB00069	405.68	49	356.68	0.38
2930CD00025	859	5	854	2.7	3030AB00077	901	1.1	899.9	0.31
2930CD00043	783	25	758	11	3030AB00080	769	62.7	706.3	0.14
2930CD00049	734	30	704	0.07	3030AB00092	714	10	704	0.14
2930CD00050	748	6	742	1.6	3030AB00093	862	50	812	2.5
2930CD00053	723	40	683	1.4	3030AB00096	785	18	767	0.17
2930CD00055	797	6	791	1.4	3030AB00098	865	11	854	0.2
2930CD00064	672	1.27	670.73	0.08	3030AB00099	852	50	802	1.4
2930CD00065	672	1.2	670.8	0.7	3030AB00100	845	60	785	0.5
2930CD00068	853	5	848	13	3030AB00102	672.08	12	660.08	0.3
2930CD00071	663	1	662	2	3030AB00106	674.82	22	652.82	0.01
2930CD00072	700	25	675	0.01	3030AB00114	445	40	405	0.08
2930CD00077	830	5	825	8.33	3030AB00118	416	61	355	0.39
2930CD00086	838	5.8	832.2	0.01	3030AB00119	421	25	396	0.19
2930CD00128	954	25	929	0.06	3030AB00126	870	6	864	0.14
2930CD00129	936	10	926	5	3030AB00127	847	30	817	1
2930CDR0086	860	0.7	859.3	6.94	3030AB00129	353	88	265	20

2930CDR0092	842	6.37	835.63	0.14	3030AB00133	593.44	1.33	592.11	0.08
2930CDR0093	841	21.43	819.57	0.83	3030AB00138	902	1.096	900.904	0.34
2930CDR0094	845	7.46	837.54	0.12	3030AB00139	895	1.027	893.973	0.71
2930CDR0095	843	6.38	836.62	1.11	3030AB00141	780	2.7	777.3	0.13
2930CDR0098	852	5.55	846.45	1.67	3030AB00149	637.94	0.9	637.04	1
2930CDR0099	840	6.73	833.27	10	3030AB00150	715	0.1	714.9	0.5
2930DA00071	742	7	735	0.69	3030ABK0001	930	76.69	853.31	0.3
2930DA00072	776	12	764	1.11	3030AC00022	851.61	30.5	821.11	0.3
2930DA00077	910	47	863	0.61	3030AC00035	776	38	738	2.5
2930DA00080	908	78	830	0.33	3030AC00038	665	23.5	641.5	2.22
2930DA00081	903	93	810	1.94	3030AC00045	945.18	7	938.18	0.03
2930DA00082	902	78	824	1.82	3030AC00081	892	7.62	884.38	0.01
2930DA00083	838	69	769	8.33	3030ACG0001	946	31.64	914.36	0.04
2930DA00085	852	12	840	0.56	3030ACR0010	976	68.64	907.36	0.01
2930DA00087	811	30	781	5.56	3030ACR0013	940	12.6	927.4	0.1
2930DA00088	693	1.08	691.92	1.11	3030ACR0026	720	0.09	719.91	0.01
2930DA00089	810	6	804	0.74	3030ACR0027	775	0.1	774.9	0.01
2930DA00090	899	1.02	897.98	0.23	3030ACR0028	740	2.4	737.6	0.03
2930DA00091	740	4	736	0.23	3030ACR0039	880	42.8	837.2	0.02
2930DA00092	605	10	595	0.2	3030ACR0049	885	17.86	867.14	0.01
2930DA00093	566	9	557	0.72	3030ACV0029	982.06	60.61	921.45	0.02
2930DA00095	620	1.02	618.98	1.25	3030ACV0032	1082.65	1.013	1081.637	0.03
2930DA00107	804	39.61	764.39	2.78	3030ACV0048	889.4	17.86	871.54	0.02
2930DA00108	805	3.76	801.24	3.06	3030AD00014	929.33	11.4	917.93	0.08
2930DAR0001	700	31.22	668.78	5	3030AD00015	961	28	933	0.5
2930DAR0012	400	11.9	388.1	5.55	3030AD00035	746	3	743	0.03
2930DAR0013	410	26	384	8.33	3030AD00037	911	69	842	0.1

2930DAR0015	415	26.5	388.5	2.5	3030AD00039	906	60	846	0.02
2930DAR0016	320	7.49	312.51	2.78	3030AD00041	754	14	740	0.05
2930DAV0001	223	6.6	216.4	4.17	3030AD00042	965	26	939	0.02
2930DAV0002	215	8.4	206.6	11	3030AD00044	772	54	718	0.02
2930DB00004	484	10	474	3.33	3030AD00046	769	63	706	0.2
2930DB00005	511	28	483	2.22	3030AD00047	757.12	23	734.12	0.5
2930DB00009	607	19	588	8.89	3030AD00051	485	7	478	0.03
2930DB00027	334	30.1	303.9	5	3030AD00055	552	15	537	0.02
2930DB00028	237	49.5	187.5	0.14	3030AD00057	527	8	519	1
2930DB00029	472	53.6	418.4	0.14	3030AD00058	499	6	493	0.6
2930DB00031	498	65.9	432.1	0.02	3030AD00059	501	14	487	0.3
2930DB00032	533	39.4	493.6	0.11	3030AD00060	497	14	483	0.02
2930DB00036	333	13.7	319.3	0.08	3030AD00062	507	40	467	0.03
2930DB00039	377	50.7	326.3	0.14	3030AD00064	461	54	407	0.02
2930DB00040	517	50.6	466.4	0.12	3030AD00069	446	22	424	0.01
2930DB00041	391	46.9	344.1	0.08	3030AD00075	798	80	718	0.02
2930DB00042	777	10	767	0.15	3030AD00091	784	45	739	0.06
2930DB00065	429	49.22	379.78	0.44	3030AD00099	773	63	710	0.2
2930DB00070	488	20.85	467.15	0.02	3030AD00101	485	7	478	0.05
2930DB00085	188	17.26	170.74	0.66	3030AD00105	759	23	736	0.1
2930DB00086	226	59.2	166.8	0.17	3030ADG0002	943	11.6	931.4	0.3
2930DB00087	203	10.14	192.86	0.22	3030ADR0001	924	71.22	852.78	0.08
2930DB00088	270	62.73	207.27	0.68	3030ADR0003	945	14.42	930.58	0.2
2930DB00091	239	34.15	204.85	0.5	3030ADR0004	938	39.2	898.8	4.11
2930DBR0036	194	3.05	190.95	0.4	3030ADR0005	920	1.3	918.7	0.14
2930DBR0037	193	1.59	191.41	0.4	3030ADR0006	575	2.38	572.62	0.72
2930DBR0038	193	10.14	182.86	0.61	3030ADR0007	500	20.75	479.25	0.57

2930DBR0039	227	59.23	167.77	0.08	3030BA00005	266	24.49	241.51	0.34
2930DBR0054	630	40.14	589.86	0.01	3030BA00035	270	18	252	0.56
2930DBR0055	400	54.02	345.98	1.5	3030BA00037	276	2	274	0.22
2930DBR0056	460	38.3	421.7	0.3	3030BA00051	329	8.5	320.5	0.22
2930DBR0057	630	55.38	574.62	0.17	3030BA00053	344	12	332	1
2930DBR0060	500	40.46	459.54	0.29	3030BA00063	276	8	268	0.17
2930DBR0061	180	10.8	169.2	0.67	3030BA00065	142	4.2	137.8	0.2
2930DBR0063	220	19	201	0.33	3030BA00067	506	30	476	10
2930DBR0069	340	9	331	0.14	3030BA00068	655	3.4	651.6	0.2
2930DBR0071	400	51	349	0.17	3030BA00069	654	7	647	2.9
2930DBR0072	405	23.94	381.06	0.17	3030BA00070	115	24	91	0.3
2930DBR0074	430	20.4	409.6	0.25	3030BA00071	383	38	345	1.5
2930DBR0076	440	10.5	429.5	2	3030BA00072	631	4	627	0.1
2930DBR0077	450	22.4	427.6	0.33	3030BA00074	640	30	610	1
2930DBR0078	450	26.63	423.37	0.01	3030BA00083	337	9	328	0.27
2930DBR0079	450	21.3	428.7	1	3030BA00084	177	6.2	170.8	1
2930DBR0080	405	19.7	385.3	1.33	3030BA00085	315	19	296	0.2
2930DBR0081	270	12.61	257.39	1	3030BA00089	492	15	477	0.71
2930DBR0082	320	46.4	273.6	0.33	3030BA00097	350	6	344	0.1
2930DBR0083	250	5.15	244.85	0.33	3030BA00104	484	6	478	0.6
2930DBV0005	273	3.38	269.62	0.17	3030BA00112	360	8	352	0.6
2930DBV0006	367	35.69	331.31	0.33	3030BA00115	482	3	479	0.08
2930DBV0007	392	35.1	356.9	1.66	3030BA00120	222	1.126	220.874	1.5
2930DBV0008	261	6.98	254.02	0.07	3030BA00122	581	96	485	0.1
2930DBV0009	486	5.08	480.92	0.24	3030BA00126	358	41.5	316.5	1.2
2930DBV0011	515	6.55	508.45	1.5	3030BA00135	409	40	369	0.66
2930DBV0012	452	48.5	403.5	3.3	3030BA00141	705	22	683	1

2930DBV0014	314	85.94	228.06	12	3030BA00142	700	19	681	2
2930DBV0019	693	52.75	640.25	0.24	3030BA00144	642	12	630	4
2930DBV0020	371	3.65	367.35	0.07	3030BA00153	207	25.45	181.55	0.76
2930DBV0021	407	4.18	402.82	1.66	3030BA00154	413	8.18	404.82	4
2930DBV0023	466	44.49	421.51	0.66	3030BA00155	253	69.53	183.47	0.42
2930DBV0024	488	27.96	460.04	0.25	3030BA00157	98	45	53	0.7
2930DBV0025	527	5.8	521.2	2	3030BA00158	185	0.79	184.21	0.5
2930DBV0028	299	19.92	279.08	2.3	3030BA00159	136	3.27	132.73	0.5
2930DBV0031	502	2.92	499.08	1.1	3030BA00160	275	25.34	249.66	7
2930DBV0032	293	56.7	236.3	0.8	3030BAK0006	198	40.4	157.6	0.14
2930DBV0034	449	7.12	441.88	0.1	3030BAK0010	450	8.63	441.37	0.27
2930DBV0035	313	49.8	263.2	0.55	3030BAM0075	202	25.45	176.55	0.4
2930DBV0037	247	23.65	223.35	0.5	3030BAM0077	270	25.34	244.66	0.27
2930DBV0039	183	12.5	170.5	0.7	3030BAM0078	408	8.18	399.82	0.02
2930DBV0043	422	34.4	387.6	0.1	3030BAM0079	248	69.53	178.47	0.28
2930DBV0044	243	4.74	238.26	0.6	3030BAM0086	180	0.79	179.21	0.28
2930DBV0045	188	42.25	145.75	0.2	3030BAM0087	249	15.85	233.15	0.28
2930DBV0046	404	47.5	356.5	0.3	3030BAM0088	131	3.27	127.73	1.39
2930DBV0047	366	27.7	338.3	0.2	3030BAM0089	263	13.27	249.73	0.31
2930DBV0048	534	1	533	0.2	3030BAM0090	309	46.76	262.24	0.14
2930DBV0049	609	0.5	608.5	0.11	3030BAM0091	152	14.35	137.65	1
2930DBV0050	495	28	467	0.13	3030BAM0105	265	13.87	251.13	0.54
2930DBV0051	395	49	346	10	3030BAM0107	140	6.38	133.62	3.33
2930DBV0052	497	76	421	0.12	3030BAM0108	377	29.15	347.85	0.61
2930DBV0053	475	9	466	0.01	3030BAM0109	326	38.75	287.25	1.4
2930DBV0054	640	20	620	0.41	3030BAM0110	165	56.73	108.27	0.53
2930DC00049	421	10	411	0.16	3030BAM0111	238	2.97	235.03	0.42

2930DC00050	498	3	495	0.23	3030BAM0112	322	43.08	278.92	0.63
2930DC00054	723	1.4	721.6	0.11	3030BAM0113	164	12.3	151.7	0.19
2930DC00056	679	1.29	677.71	0.08	3030BAM0114	349	1.99	347.01	0.69
2930DC00057	576	15	561	1.94	3030BAM0117	369	60.33	308.67	0.13
2930DC00059	696	1.36	694.64	3.06	3030BAM0118	711	6.13	704.87	0.89
2930DC00060	713	6	707	6.67	3030BAM0119	443	10.8	432.2	0.13
2930DC00062	731	15	716	1.17	3030BAM0122	646	8.24	637.76	0.25
2930DC00063	738	6	732	5.69	3030BAM0123	633	11.95	621.05	0.72
2930DC00065	639	35	604	1.17	3030BAM0136	160	60.33	99.67	0.06
2930DC00068	772	13	759	1.94	3030BAM0137	138	6.38	131.62	0.24
2930DC00070	819	32	787	1.39	3030BAM0138	199	26.7	172.3	0.3
2930DC00075	739	12	727	1.81	3030BAM0139	137	11.7	125.3	2.03
2930DC00076	679	30	649	0.13	3030BAM0140	103	8.18	94.82	0.2
2930DC00084	780	69	711	2.78	3030BAM0141	359	8.71	350.29	0.47
2930DC00085	668	25	643	2.78	3030BAM0142	373	40.55	332.45	0.19
2930DC00099	492	47	445	0.5	3030BAM0144	391	21.23	369.77	0.06
2930DC00102	692	17.9	674.1	0.7	3030BAM0145	178	48.77	129.23	0.69
2930DC00103	672	19.85	652.15	0.37	3030BAM0146	146	4.95	141.05	0.13
2930DC00104	660	8.8	651.2	0.69	3030BAM0148	179	16.1	162.9	0.89
2930DC00105	655	13.5	641.5	3.79	3030BAM0151	753	18.6	734.4	0.25
2930DC00106	695	94.5	600.5	0.7	3030BAM0152	237	1.58	235.42	0.11
2930DC00108	427	5.07	421.93	0.88	3030BAM0153	264	55.75	208.25	0.72
2930DC00129	503	2.77	500.23	0.44	3030BAM0154	158	3.65	154.35	0.26
2930DC00130	453	4.6	448.4	0.01	3030BAM0156	400	26.14	373.86	0.19
2930DC00131	575	16.41	558.59	0.25	3030BAR0001	620	35.09	584.91	0.69
2930DC00132	547	37.43	509.57	0.17	3030BB00025	251	5	246	0.069
2930DC00133	523	49.1	473.9	0.17	3030BB00026	307	54	253	0.31

2930DC00134	547	8.22	538.78	0.07	3030BB00027	382	6	376	0.18
2930DC00136	548	14.93	533.07	0.25	3030BB00028	233	13	220	0.02
2930DC00137	563	46.88	516.12	0.2	3030BB00029	306	6	300	0.69
2930DC00138	491	41.74	449.26	0.4	3030BB00030	325	8	317	0.17
2930DCM0096	520	23	497	0.08	3030BB00031	151	8	143	1.25
2930DCM0098	555	23	532	0.09	3030BB00033	198	36	162	0.16
2930DCM0099	518	0.53	517.47	0.1	3030BB00034	158	40	118	0.17
2930DCM0100	524	13.77	510.23	1.43	3030BB00035	146	64	82	0.28
2930DCM0101	558	11.12	546.88	0.8	3030BB00036	124	11.5	112.5	0.66
2930DCM0102	446	46.7	399.3	2.78	3030BB00038	156	62	94	0.68
2930DCM0127	576	54.61	521.39	0.03	3030BB00039	77	31	46	1.43
2930DCM0128	484	41.36	442.64	0.67	3030BB00040	83	24	59	0.22
2930DCM0130	535	36.45	498.55	1.4	3030BB00042	144	32	112	0.8
2930DCM0131	574	23.78	550.22	3.5	3030BB00043	288	33	255	0.95
2930DCM0132	547	22.76	524.24	0.4	3030BB00044	126	5	121	0.02
2930DCM0133	519	0.27	518.73	42	3030BB00045	325	7	318	0.08
2930DCM0134	519	35.48	483.52	14	3030BB00047	120	12	108	0.44
2930DCM0135	574	30.2	543.8	4.22	3030BB00048	140	30	110	2
2930DCM0159	574	42.53	531.47	6.94	3030BB00049	114	10	104	0.24
2930DCR0007	478	2.95	475.05	2.14	3030BB00050	292	10	282	0.05
2930DCR0011	500	25	475	1.75	3030BB00052	138	5	133	0.04
2930DCR0014	650	34.5	615.5	2.33	3030BB00054	195	6	189	0.28
2930DCR0019	565	57.03	507.97	12	3030BB00058	210	5.27	204.73	0.14
2930DCR0023	580	22.68	557.32	1.51	3030BB00059	158	11	147	1.43
2930DCR0025	561	30.92	530.08	0.75	3030BB00060	187	1.2	185.8	0.08
2930DCR0026	668	9.92	658.08	1.34	3030BB00074	95	22.7	72.3	0.55
2930DCR0028	630	8.8	621.2	0.67	3030BBR0001	155	13	142	0.28

2930DCR0029	570	55.88	514.12	0.1	3030BBR0003	142	0.8	141.2	0.34
2930DCR0031	521	23.71	497.29	0.03	3030BBR0009	323	3.62	319.38	0.3
2930DCR0036	705	1.25	703.75	1	3030BBR0011	299	7.53	291.47	6.6
2930DCR0038	710	4.04	705.96	1.67	3030BBR0014	160	10.35	149.65	0.33
2930DD00001	284	3	281	0.72	3030BBR0016	139	4.02	134.98	0.44
2930DD00006	561	1.8	559.2	0.04	3030BBR0021	357	0.3	356.7	0.15
2930DD00008	188	18	170	0.23	3030BBR0030	140	4.26	135.74	0.2
2930DD00009	168	41	127	0.8	3030BC00020	250	15	235	0.1
2930DD00010	254	45.6	208.4	2	3030BC00039	74	1	73	0.1
2930DD00011	320	40.96	279.04	1.5	3030BC00048	435	78	357	0.3
2930DD00013	251	33	218	2.5	3030BC00050	578	30	548	1.3
2930DD00014	282	37	245	1.3	3030BC00052	436	1	435	10
2930DD00015	331	39.5	291.5	0.2	3030BC00053	418	80	338	0.75
3030BC00091	199	11	188	0.22	3030BC00061	564	30	534	0.42
3030CA00054	242	29.5	212.5	1.94	3030BC00063	330	1.41	328.59	0.38

Appendix 2.2: Transmissivity

Site ID	T (m^2/day)	Site ID	T (m^2/day)	Site ID	T (m^2/day)	Site ID	T (m^2/day)
2930ACR0041	12.21	2931CAV0002	4.00	2930DBR0043	36.21	3030BA00154	0.10
2930BCR0032	49.00	2931CAV0003	0.20	2930DBV0008	23.07	3030BA00159	0.70
2930BDM0013	2.60	2931CAV0004	2.00	2930DCM0100	0.12	3030BAM0075	0.13
2930BDM0058	1.81	2931CAV0005	0.60	2930DCM0101	0.15	3030BAM0078	0.13
2930BDM0069	1.29	2931CAV0006	2.80	2930DCM0133	0.11	3030BAM0080	0.51
2930CC00011	7.00	3030AB00139	10.00	2930DCM0159	0.88	3030BAM0088	0.71
2930CCE0002	8.00	3030ABR0001	75.90	2930DDM0124	2.19	3030BAM0091	0.50
2930CCR0002	5.50	3030ABR0011	0.30	2930DDM0125	3.13	3030BAM0113	0.17
2930DA00107	0.70	3030ACR0029	19.53	2930DDR0001	0.80	3030BAM0140	1.94
2930DA00108	0.30	3030ACR0039	0.45	2931ACM0053	3.50	3030BAM0142	0.65
2930DAR0001	3.00	3030ACR0049	20.92	2931ACV0001	3.40	3030BAM0152	1.31
2930DB00086	0.30	3030AD00105	2.00	2931ACV0004	0.42	3030BAR0003	0.20
2930DB00088	14.20	3030ADR0004	11.71	2931ACV0034	5.10	3030BAR0004	0.10
2930DB00089	5.40	3030ADR0005	7.32	2931ADV0007	8.60	3030BAR0030	0.76
2930DB00091	37.50	3030ADR0006	16.63	2931CAR0001	24.40	3030BAR0031	0.28
2930DBR0039	0.29	3030ADR0007	4.94	3030BB00074	0.30	3030BAR0033	0.27
2930DBR0040	13.76	3030ADR0008	4.44	3030BB00075	3.70	3030BAR0036	2.08
2930DBR0041	7.68	3030ADR0009	11.55	3030BB00077	2.50	3030BAR0038	0.36
2930DBR0042	1.20	3030BA00153	0.10	3030BBR0001	0.62		

Appendix 3: Hydrochemical data across the study area.

Appendix 3.1: Secondary chemistry data

Site ID	Ca	K	Mg	Na	Cl	F	NO3	PO4	SO4	Si	TAL	pH	EC
2730CCV0003	12.3	0.4	8.5	11.2	14.5	0.29	0.02	0.012	14.2	23.29	83.3	7.83	213
2930AC00048	45.7	4.19	41.4	303.8	19	0.58						6.6	600
2930AC00049	12.7	0.69	8.3	12.2	44.7	0.35	2.326	0.012	31.5	13.09	33.8	7.1	309
2930AC00058	2.6	3.96	3.3	16.8	129.6	1.82	0.105	0.008	17.2	11.3	269.9	7.84	820
2930AC00060	3.4	5.99	3.5	24.1	92.6	0.19	0.128	0.009	8.1	18.82	133.1	7.73	555
2930AC00064	1.6	2.15	2.3	17.4	120.5	2	0.02	0.015	30.5	22.01	265.8	7.37	881
2930AC00093	3.6	3.49	2.3	17.6	458.3	1.1	14.755	0.009	171.9	12.19	330.9	7.62	2290
2930AC00095	9.2	0.73	6.4	15.1	96	1.72	2.826	0.01	25.6	7.69	272.3	8.46	770
2930AC00096	4.2	1.22	3	9.2	917.8	2.98	0.02	0.008	354.8	10.74	369.2	7.73	3840
2930AC00097	1	1	1.54	5.11	8.9	0.39	2.417	0.018	22.8	7.24	51.2	7.77	200
2930AD00032	3.7	0.42	1.4	4.4	50.1	0.45	9.471	0.011	4.8	10.2	79.5	7.84	403
2930AD00033	5.5	0.55	2.5	6	7.7	1.63	0.02	0.014	13	1.89	71.7	7.57	220
2930AD00037	22.3	6.9	8.9	40.2	16	0.3						6.6	170
2930AD00038	21.1	3	8.2	38.1	36.466	0.227	9.903	0.016	19.103	35.202	208.686	8.601	629
2930AD00039	1.5	0.38	2	7	15	0.5	0.02	0.034	17	16.33	91	6.83	247
2930AD00040	1.5	0.4	2	7	338.1	0.72	0.02	0.007	7	11.63	219.2	7.02	1540
2930AD00041	10.6	1.91	9.1	31.3	21.5	0.55	3.899	0.065	2	18.14	60.3	7.06	240
2930AD00042	9.6	2.64	5.5	34.3	36.4	0.33	1.811	0.023	4.4	15.79	126.6	7.48	381
2930AD00043	16.7	2.07	17.4	23.6	273.5	0.99	0.802	0.025	31.7	9.68	253.7	7.97	1390
2930AD00046	53.3	0.67	24.3	47.5	9.78	0.1						6.75	104
2930AD00047	21.2	2.78	12.1	82.2	113	0.1						6.87	865
2930AD00051	21.5	1.36	33.2	99.8	57	5.8						7.2	660
2930AD00052	6.3	5.4	6.7	31.3	83.2	0.99	8.637	0.037	4.2	24.53	72.8	6.78	509
2930AD00053	6.3	5.4	6.7	31.3	30.6	1.43	0.79	0.01	6.8	22.77	119.9	7.73	373

2930AD00054	40.6	3.1	50.2	1.776	12.7	0.19	0.02	0.18	2	11.22	24.7	6.75	110
2930AD00056	33.5	2.27	28.7	205.1	6.48	0.1						6.14	42.6
2930AD00059	25.6	1.56	14.1	139.1	210	0.1						7.8	1100
2930AD00061	11	3.99	12.6	36.9	46.83	0.27	0.104	0.157	6.497	14.564	346.722	7.976	781
2930AD00063	11	4	12.6	36.9	183.332	0.716	11.266	0.015	139.013	17.572	178.603	8.378	1213
2930AD00064	15.3	1.31	16.3	103.1	258	0.1						6.6	1310
2930AD00066	1.9	2.03	1.3	3.1	16.8	0.25	0.25	0.021	8.8	25.21	62.1	6.25	187
2930AD00067	35.4	1.39	18.2	78.1	148	0.388						7.44	1120
2930AD00068	17.8	0.53	17.7	70.5	17	0.8						7.59	416
2930AD00072	159.4	2.11	109.3	364.9	93	1.32						6.8	1250
2930AD00074	90.3	4.32	17.6	274.4	16	0.05						6.9	140
2930AD00075	88.3	2.87	42.5	271.1	766	1.6						7.06	3530
2930AD00076	19.2	0.93	10	33.8	13.5	0.42	4.597	0.008	18.5	19.09	249.6	7.78	573
2930AD00077	19.9	1.88	12.9	97.6	20	0.25						7.2	170
2930AD00078	11.6	1.93	4.4	34.8	34.4	0.49	4.095	0.066	2	21.35	77.4	7.17	291
2930AD00080	30.7	1.94	26.8	172.6	11.5	0.13						7.71	117
2930BC00145	32.4	0.7	11.6	52	10.4	0.21						7.23	162
2930BC00147	52.1	0.62	29.3	110.7	135	0.1						7.1	1000
2930BC00148	25	1.71	24.8	132.5	19.2	0.176						7.44	205
2930BC00149	44.5	2.73	26.7	95.4	98	0.94						7.4	800
2930BC00153	19	2.95	11.2	51.1	13.3	0.1						6.45	149
2930BC00154	20	2.7	13	43	22.8	0.1						5.75	242
2930BC00156	2.3	1.9	3.2	18	107.6	13.19	0.02	0.021	25.1	7.44	305.9	7.94	908
2930BC00159	24.1	0.93	8.7	35.9	65.591	0.117	6.638	0.145	46.733	8.699	105.219	7.815	575
2930BC00160	8.3	2.68	6.7	24.6	125.8	0.43	5.013	0.017	49.9	9.48	76.4	7.77	641
2930BC00162	27.6	2.8	12.7	30.6	35.3	1.45	0.02	0.265	6.4	16.61	139.3	8.17	397
2930BC00169	27.6	2.79	12.7	30.6	15	0.58	0.098	0.019	4.3	17.87	33.9	6.48	128
2930BC00171	48.3	1.51	34.6	170	16.1	0.1						8.08	220
2930BC00172	17.8	3.19	5.4	16.5	217.5	1.61	18.222	0.007	13.6	14.13	119.8	7.56	1044

2930BC00174	6.3	0.74	4.6	23.2	192	0.43	0.414	0.038	42.5	8.33	255.9	8.17	1126
2930BCR0005	1.7	1.4	2	18.7	1.5	0.18	0.319	0.011	4.5	12.73	55.8	7.2	103
2930BCR0032	7.5	1.27	13.4	21.8	51.9	1.79	0.084	0.017	13.6	14.25	143.6	8.43	459
2930BCR0036	53	3.8	11	52	9	0.1						6.9	190
2930BCR0037	43.2	1.36	36.9	105	310	0.1						7.2	1430
2930BD00004	128.1	3.15	51.3	299.9	69	0.35						6.7	630
2930BD00067	52.2	1.87	34.5	99.6	50	1.4						7.4	480
2930BD00068	35.7	1.12	35.4	140.5	159	0.49						7.4	876
2930BD00069	18	0.8	13	38	199.011	0.612	13.26	0.018	71.081	19.729	252.65	7.959	1197
2930BD00073	1.61	3.51	1.16	3.98	1967.6	3.09	9.94	0.006	621.9	11.12	231.3	7.7	6800
2930BD00089	41.1	1.4	26.1	45.5	19.2	0.1						6.71	151
2930BD00090	41.1	1.38	26.1	45.5	55	0.33						7.41	988
2930BD00091	45.536	1.19	31.062	33.049	46.6	0.45	8.373	0.008	11.9	19.85	59.8	6.77	372
2930BD00096	12.8	0.83	8.3	14.4	205.8	1.15	0.624	0.006	91.5	9.79	221.7	7.84	1148
2930BD00111	70.2	2.38	25	89	27	1.5						7.1	290
2930BD00112	12.8	0.76	6.4	7.8	342	16.89	0.02	0.017	36.9	8.9	682	8.7	2360
2930BD00122	11.7	0.77	8.2	13.6	192.6	0.73	0.053	0.023	38.6	18.87	134.6	8.17	929
2930BD00147	17.6	0.65	13.3	8.6	88.7	0.45	0.02	0.021	10.1	13.23	211.8	8	655
2930BD00148	7.7	0.71	4.9	7.8	208.1	2.3	0.056	0.006	34.1	7.12	394.1	8.12	1390
2930BD00150	24.8	0.65	5.6	17	33.9	0.41	0.02	0.009	7.2	10.06	163.9	8	430
2930BD00152	8	0.57	3.9	6.3	10	0.48	0.02	0.017	13.9	12.24	69	7.51	183
2930BD00153	18	0.49	6.1	32.3	29.4	0.7	3.038	0.055	2	28.61	112	7.7	340
2930BD00154	5.8	0.7	5.1	9.3	30.9	0.54	0.02	0.012	2	18.32	97.6	7.21	284
2930BD00155	5.8	0.7	5.1	9.3	148	1.4	0.916	0.006	152.7	8	278.1	7.77	1241
2930BD00157	79.386	5.763	40.902	117.211	939	0.662						7.12	3620
2930BD00159	24	1.9	15	1.53	29.3	0.26	4.35	0.029	2	15.63	55	6.7	262
2930BD00160	17	2.85	12.2	36.8	167.685	0.167	11.058	0.222	52.322	16.373	122.66	8.036	942
2930BD00162	26.331	5.372	8.459	74.644	173	3.8						7.2	900
2930BD00163	5	5	3	14	189.2	0.33	2.589	0.012	20.1	22.05	222.9	7.31	1072

2930BDM0012	15.05	3.13	10.716	85.35	15	1.1						7.1	140
2930BDM0013	41	2.5	22	92	30	1.9						7.2	440
2930BDM0058	41	2.7	22	83	24.8	2.02						7.44	319
2930BDM0062	9.283	4.551	4.503	76.573	60	1.2						7.1	470
2930BDM0063	48	4.8	46	1.8	12.7	0.2	0.09	0.18	2	11.31	25.9	6.75	111
2930BDM0064	40.84	2.581	13.724	127.372	282.89	1.01						7.77	1250
2930BDM0065	1.23	4.83	76.4	4.92	18.2	0.41	1.484	0.026	5.9	18.56	32	7.77	147
2930BDM0067	32.2	3.8	11.8	110.2	271	0.1						7.1	1350
2930BDM0069	147.6	29	88.8	375.7	59	0.33						6.9	520
2930BDM0070	9.9	1.47	5	17	236.6	2.9	0.02	0.008	30	15.04	207.5	7.71	1156
2930BDM0072	16	0.4	3	12	104	0.67	0.15	0.006	7.3	9.1	195.4	8.02	686
2930BDM0073	14	0.9	8	14	456.8	0.56	13.006	0.011	39.3	23.5	185.3	7.54	1930
2930BDV0002	5	0.2	3	3	1.5	0.17	0.09	0.076	2	14.22	56.6	6.7	123
2930BDV0004	49	1	14	33	107.3	0.66	25.783	0.007	2	14.87	46.8	6.86	654
2930BDV0006	9	0.4	2	14	264.9	0.37	6.775	0.012	10.1	21.63	117.8	7.3	1128
2930BDV0009	22	2.6	12	95	24	0.21						6.1	220
2930BDV0010	28	1.1	18	46	15.6	0.115						7.56	250
2930BDV0012	34	1.4	29	1.13	38.2	1.9	0.06	0.032	11	15.83	160.6	7.8	454
2930BDV0013	14	1.9	4	8.7	35.1	0.45	0.02	0.008	11.6	16.62	76.1	7.26	305
2930BDV0024	8	0.4	4	3	20.9	0.59	4.76	0.013	11.9	1.71	153.9	7.8	416
2930BDV0025	34	1.8	9	29	17.8	0.46	0.02	0.021	2	11.68	38.4	7.83	147
2930BDV0027	13	1.7	4	17	7.9	0.34	0.02	0.014	2	16.91	50.4	7.8	127
2930BDV0029	30	0.86	15	29	35.9	0.66	0.02	0.028	9.3	23.31	60	7.93	273
2930BDV0030	21	0.86	12	19	6.8	0.15	0.439	0.01	2	3.14	31.8	6.73	102
2930BDV0031	49	1.6	12	1.23	22.1	0.57	0.02	0.032	5.5	12.48	82.6	7.95	269
2930BDV0032	13	0.5	4	10	22	1.45	0.431	0.009	11.7	16.75	137.9	7.53	331
2930BDV0033	28.7	1.72	15.7	36	105.596	0.129	0.452	0.047	40.682	7.665	25.154	6.753	504
2930BDV0034	29	0.6	15	10	38	1.13	0.02	0.017	20	17.07	140.3	7.41	399
2930BDV0035	9	4.7	4	24	232.1	0.24	0.075	0.017	12	27.41	113.2	7.49	955

2930BDV0036	18.1	5.82	17.4	86.3	30	0.59						7.2	240
2930BDV0037	29.6	3.7	14.1	1.44	23.4	0.41	0.02	0.029	6	12.82	128.5	7.72	358
2930BDV0038	31.1	3.16	13.8	48.8	41.7	0.1						6.22	200
2930BDV0052	33.2	2.99	15.2	49.4	12.2	0.1						6.67	106
2930BDV0053	51.8	5.55	24.6	1.46	23.5	0.66	0.02	0.047	5.9	13.09	130.6	7.65	365
2930BDV0058	11.5	2.87	4.6	11.7	390.8	1.13	28.532	0.007	58.9	17.54	274.8	7.88	1930
2930BDV0059	8.9	17.22	5.1	14.9	463.2	1.79	5.375	0.015	68.8	13.39	187.9	7.77	1900
2930BDV0060	8	1.4	3	20	11.9	2.36	0.069	0.012	14.2	6.07	135.5	8.24	339
2930CA00117	20	4.8	7	23	424	1.46	25.233	0.02	45	17.46	234.6	8.2	2090
2930CA00118	13.9	2.44	4.6	16.9	86	0.67	1.999	0.008	10	10.36	99.4	7.28	497
2930CA00120	42.4	3.61	18.4	114	264	0.1						7	1420
2930CB00041	4	6.5	5.8	19.9	25.9	0.31	1.946	0.011	7.1	19.27	105	7.42	340
2930CB00046	4	6.46	5.8	19.9	14.3	0.15	0.055	0.022	8.5	15.68	102.5	8.25	256
2930CB00066	23.8	0.59	14	36.7	245.071	0.2	0.09	0.185	73.142	13.932	70.278	6.927	946
2930CB00067	9	3.9	6	21	383.7	1.15	5.888	0.018	86.4	15.17	252.8	7.85	1810
2930CB00069	13.7	0.52	13.7	16.5	68	4.52	0.065	0.009	10.4	11.41	206.6	7.97	606
2930CB00071	15	1.9	4.2	19	3	0.18	0.076	0.02	2	11.74	41.2	7.18	79
2930CB00072	6.3	2.1	2.8	11.3	14.2	1.47	0.02	0.009	5.8	21.76	71.8	7.22	196
2930CB00073	4	2.8	2.3	18.6	6.3	0.21	1.392	0.013	11.9	15.25	100.3	7.13	224
2930CB00075	4	2.81	2.3	18.6	3.6	0.21	3.39	0.043	2	20.57	84.2	7.14	200
2930CB00076	23.6	2.89	21	131.3	185	1.54						6.89	1050
2930CB00079	13.5	0.75	2.8	7.8	147.3	0.45	16.208	0.005	39.5	14.11	122	6.84	896
2930CB00081	15.7	2.58	10.6	19.6	15.8	0.13	0.681	0.011	7.7	15.87	66.2	7.22	216
2930CB00082	2.6	2.13	2.5	13.2	62.3	0.73	1.732	0.016	13.6	11.73	235.2	7.67	639
2930CB00083	2.5	1.98	2.4	12.7	67.8	0.21	27.151	0.009	22.2	9.52	81.9	7.47	578
2930CB00086	7.4	2.43	1.7	20.1	6.4	0.4	4.284	0.011	2	13.23	62.7	7.59	187
2930CB00087	5.3	2.6	5.5	19	3.1	0.16	0.058	0.013	2	11	33.7	7.06	65
2930CB00088	4.1	6.7	2.2	10.7	16.9	0.36	1.892	0.011	2	17.01	31.6	7.31	140
2930CB00096	29	1.68	11.5	26.7	41.6	0.21	0.816	0.139	6.5	7.95	16.2	7.26	213

2930CB00097	29.1	1.68	11.5	27.2	155.1	0.39	0.02	0.021	16.1	17.85	205	8.14	923
2930CB00098	29.2	1.98	11.5	27.2	280.8	0.43	0.342	0.015	34.4	10.81	235.7	8.01	1410
2930CB00100	11.4	2.43	8.1	25.3	82.6	0.26	0.054	0.009	7.1	18.45	133.5	7.77	482
2930CB00102	37.2	1.38	13.8	35.5	129.19	0.125	0.084	0.245	33.195	13.281	68.599	7.452	606
2930CB00106	10.8	2.6	4.9	16	34.5	0.95	6.303	0.011	2	18.71	53.5	7.45	273
2930CB00108	18.5	1.38	8.7	27.2	16.8	0.47	0.02	0.012	8.7	2.54	46.2	7.74	167
2930CB00111	46.7	4.31	26.9	95	24	5.7						7.4	360
2930CB00112	12.5	2.01	6.39	23	25.8	0.15	0.057	0.013	4.6	5.47	39.9	6.97	188
2930CB00113	12.5	2.15	5.6	15.3	67.3	1.15	7.994	0.012	7.6	17.09	110.6	7.81	481
2930CB00114	32.9	1	23.5	1.39	22.8	0.41	0.02	0.083	7.6	4.28	27.1	9.59	168
2930CB00116	1	2.6	3	23	71.3	0.17	6.267	0.333	29.6	10.34	33.2	7.45	443
2930CB00119	7.9	15.69	6.9	24	1.5	0.32	0.15	0.018	5.6	8.63	13.8	7.28	40
2930CBR0003	59.3	3.4	42.38	1.42	23.5	0.38	0.02	0.036	6.2	13.01	129.5	7.6	365

Appendix 3.2: Primary chemistry data

a. Onsite measured groundwater and surface water hydrochemical parameters in the study area

Sample No.	**source**	**Sample date**	**Elevation m (amsl)**	**Temp (°C)**	**EC (µS/cm)**	**TDS (ppm)**	**pH**	**Eh (mV)**	**DO (mg/l)**	**Sal**	**Alkalinity (mg/l)**
ETM1	Borehole	18/07/2018	11	23	807	403	6.78	13.8	2.53	0.39	147
ETM2	Borehole	18/07/2018	11	23.2	1191	594	7.2	-10.6	2.61	0.59	286
ETM3	Spring	18/07/2018	123	20.49	204	104	6.94	9.5	3.32	0.1	89
ETM4	stream	18/07/2018	10	17.72	381	191	7.5	-17.4	2.13	0.18	116
ETM5	Borehole	19/07/2018	-1	22.5	736	369	7.65	-35.3	3.02	0.36	189
ETM6	Borehole	19/07/2018	17	22.66	501	252	8.07	-55	3.07	0.24	94
ETM7	stream	19/07/2018	16	22.62	566	283	7.93	-50	3.38	0.27	95
ETM8	Borehole	19/07/2018	7	21.01	644	323	8.47	-75.5	3.2	0.31	290
ETM9	stream	20/07/2018	375	18.03	169	85	8.91	-94.3	3.24	0.08	42

ETM10	Spring	20/07/2018	320	18.52	196	99	7.46	-25.1	2.87	0.09	71
ETM11	Borehole	20/07/2018	4	22.13	1530	765	8.55	-79	2.46	0.99	281
ETM12	stream	20/07/2018	12	21.81	605	303	7.89	-7.8	1.88	0.29	120
ETM13	stream	20/07/2018	7	21.28	1500	750	6.92	2.4	2.04	0.76	63
ETM14	stream	20/07/2018	26	21.26	152	76	6.7	10.3	1.65	0.07	71
ETM15	Borehole	23/07/2018	118	22.4	661	331	6.89	-48.9	2.14	0.32	175
ETM16	stream	23/07/2018	235	20.13	381	191	7.7	-41.2	2.41	0.18	121
ETM17	Borehole	23/07/2018	421	22.38	226	114	6.88	13.6	1.82	0.11	109
ETM18	stream	23/07/2018	224	15.45	119	62	8.85	-83	2.75	0.06	45
ETM19	Borehole	23/07/2018	235	21.23	618	312	7.75	-29.7	2.35	0.3	211
ETM20	stream	25/07/2018	15	20.36	322	167	8.29	-56	2.87	0.22	133
ETM21	Borehole	25/07/2018	233	23.88	356	180	6.23	17	1.72	0.17	86
ETM22	Borehole	25/07/2018	795	22.02	107	57	6.95	14.9	2.25	0.05	144
ETM23	stream	25/07/2018	356	18.75	353	177	8.4	-68.7	2.4	0.17	57
ETM24	stream	25/07/2018	13	17.44	434	222	8.11	-54.1	2.89	0.21	119
ETM25	Borehole	26/07/2018	67	22.6	1267	634	7.36	3.4	2.41	0.63	203
ETM26	stream	26/07/2018	277	18.46	478	240	7.55	-24.3	2.52	0.23	109

b. Laboratory measured groundwater and surface water Major ions

Sample ID	EC	Mg	Ca	K	Na	Si	Cl	NO3	SO4	HCO3	Fe
ETM1	807	14.04	36.12	2.72	113.46	18.54	78.32	19.63	25.79	179.23	25.61
ETM2	1191	36.32	27.22	20.74	148.54	24.85	93.25	0.68	0.75	348.37	3629.85
ETM3	204	8.29	8.24	1.71	27.81	6.68	28.52	2.17	8.30	108.49	7069.36
ETM4	381	11.23	13.11	4.63	51.08	8.09	55.28	2.98	17.73	141.07	233.78
ETM5	736	9.45	59.56	7.71	90.01	18.23	44.62	22.86	20.59	229.55	9.98
ETM6	501	5.91	11.32	1.66	92.99	19.30	36.45	24.46	18.54	113.35	25.47
ETM7	566	5.35	6.12	4.07	112.53	16.34	48.14	6.49	34.49	114.92	43.72
ETM8	644	17.63	77.42	7.21	47.87	13.29	33.14	2.39	15.04	0.00	29.94
ETM9	169	7.03	4.01	1.22	28.80	7.45	42.79	0.96	4.54	47.38	499.87
ETM10	196	7.48	7.90	3.85	29.72	4.27	27.92	0.67	3.09	86.37	252.74
ETM11	1530	34.79	49.20	2.04	233.41	4.03	108.98	0.70	1.15	331.05	20.47
ETM12	605	18.67	13.04	1.34	90.33	9.17	72.42	0.79	7.25	145.27	164.69
ETM13	1500	32.95	19.75	9.84	229.08	6.31	72.50	0.65	15.69	76.80	42.27
ETM14	152	5.75	11.19	0.96	15.72	6.01	14.32	0.73		86.58	45.83
ETM15	661	15.60	34.82	3.56	85.30	25.87	69.47	1.05	4.56	213.33	36.12
ETM16	381	13.25	17.28	2.78	51.69	9.16	62.10	1.91	18.40	146.88	70.81
ETM17	226	8.66	15.93	2.44	26.94	22.74	18.47	4.36	10.11	132.88	100.97
ETM18	119	5.07	6.22	1.67	18.59	11.45	17.85	2.73	4.18	51.26	273.27
ETM19	61.8	17.98	42.14	3.02	66.28	21.56	52.95	0.67	1.19	255.98	7250.94
ETM20	322	10.63	17.87	3.92	46.12	7.04	52.33	4.55	17.60	159.15	263.93
ETM21	356	7.25	5.60	1.67	63.93	27.39	54.57	31.83		104.90	361.31
ETM22	107	5.05	3.79	0.71	14.71	5.48	27.91	3.71	3.64	175.52	95.80
ETM23	353	9.36	17.64	4.95	44.03	5.05	49.24	30.08	28.12	67.83	84.68
ETM24	434	12.75	18.71	7.23	61.56	5.05	33.00	3.71	11.92	143.33	175.07
ETM25	1267	31.99	32.64	2.71	199.82	15.59	102.90	1.06	30.26	247.09	16.69
ETM26	478	12.17	16.09	8.99	74.36	1.08	40.68	6.31	14.84	132.51	93.28

c. Trace metals (Concentration is in ppb)

Sample ID	Li	B	Al	V	Cr	Mn	Co	Ni	Cu	Zn	Se	Rb	Sr	Mo	Sb	Hg	Pb
ETM1	5.04	183.74	32.33	1.26	4.27	0.86	0.05	8.19	1.37	37.54	1.19	0.82	143.10	0.56	3.01	0.04	0.18
ETM2	6.16	536.54	25.41	4.09	2.52	278.44	0.36	5.14	2.69	125.55	0.10	15.28	257.97	0.20	1.32	0.11	0.26
ETM3	<3	89.17	391.05	1.17	1.03	80.00	0.87	4.30	1.86	113.83	0.06	2.19	62.29	0.04	1.03	0.05	0.60
ETM4	<3	122.92	40.01	0.56	0.38	83.41	0.37	3.35	1.95	133.94	0.15	3.71	75.14	0.21	1.20	0.05	0.32
ETM5	3.09	271.97	14.47	1.14	12.14	0.59	<0,05	1.57	0.59	13.77	2.05	5.72	369.67	<0,12	0.79	0.02	0.07
ETM6	5.74	153.56	32.85	3.15	10.56	0.85	0.06	3.53	1.11	23.87	1.45	0.22	53.52	<0,12	2.26	0.06	0.14
ETM7	<3	271.59	49.17	2.50	0.50	14.31	0.19	2.08	2.58	56.50	1.91	2.28	60.16	0.14	0.95	0.05	0.66
ETM8	7.56	115.63	30.61	0.33	1.34	6.39	0.09	2.68	2.38	31.97	0.07	6.83	620.50	1.45	1.21	0.04	0.30
ETM9	<3	88.91	77.78	0.32	0.37	26.54	0.20	1.78	2.13	100.70	<0,06	0.95	42.28	0.04	0.79	0.03	0.25
ETM10	<3	87.95	55.82	0.20	0.21	19.94	0.15	2.70	2.02	114.06	0.06	1.41	60.19	<0,12	0.86	0.08	0.26
ETM11	31.90	146.40	37.22	0.06	0.40	341.28	0.07	3.67	1.93	22.75	<0,06	4.36	462.71	0.34	1.86	0.07	0.17
ETM12	<3	61.05	27.32	0.25	2.56	274.93	0.27	2.90	1.71	21.71	0.07	0.53	95.45	0.39	0.95	0.02	0.12
ETM13	<3	121.29	28.73	0.56	0.35	28.75	0.09	3.59	1.63	30.00	<0,06	2.64	221.02	0.32	1.33	0.05	0.17
ETM14	<3	41.37	26.53	0.91	0.26	0.80	0.05	2.05	1.51	20.39	<0,06	0.37	83.37	<0,12	0.88	0.02	0.21
ETM15	25.61	67.27	29.06	0.06	0.27	167.37	0.07	2.76	2.05	20.10	<0,06	1.44	221.00	0.31	1.03	0.03	0.17
ETM16	<3	69.48	75.14	0.27	0.29	157.09	0.28	2.36	2.41	24.16	0.09	1.74	106.47	0.85	1.23	0.05	0.24
ETM17	7.29	47.48	91.44	0.28	1.53	38.75	0.12	4.17	3.67	153.43	0.79	1.03	337.42	0.33	1.18	0.04	0.41
ETM18	<3	49.88	54.33	0.69	0.28	13.34	0.09	3.05	2.10	26.84	<0,06	1.46	47.25	0.11	0.89	0.04	0.28
ETM19	24.24	48.00	30.03	0.04	0.11	476.87	0.05	2.97	1.64	30.15	<0,06	6.21	350.62	0.39	0.84	0.02	0.22
ETM20	<3	121.63	34.13	0.67	0.46	273.02	0.43	6.12	2.41	106.58	0.10	3.04	93.49	0.46	1.46	0.03	0.21
ETM21	<3	105.22	25.84	1.08	0.55	29.44	0.19	3.28	1.38	117.74	0.94	0.57	44.32	0.23	1.11	0.04	0.19
ETM22	<3	83.85	40.41	0.08	0.29	136.64	0.49	3.98	1.84	123.05	0.19	0.46	30.86	0.31	1.07	0.05	0.17
ETM23	<3	66.43	53.14	1.90	1.06	27.50	0.33	2.97	3.92	31.62	0.10	4.33	82.95	0.32	0.90	0.04	0.80
ETM24	<3	108.11	41.20	1.24	0.34	130.91	0.47	2.86	2.95	28.19	0.15	4.61	94.49	0.30	0.96	0.06	0.31
ETM25	33.25	155.58	40.71	0.07	<0,2	275.14	0.27	3.46	5.30	57.78	0.39	1.72	316.26	1.89	1.22	0.09	0.39
ETM26	<3	73.76	57.67	0.87	0.47	27.03	0.27	2.61	2.96	22.56	0.11	7.07	85.45	0.44	1.23	0.07	0.22

Appendix 4: Hydrochemical Data from landfill sites.

Appendix 4.1. Primary data from all landfill sites

a. Major ions and physio-chemical data

Sample No.	source	Sample date	EC (µS/cm)	pH	Eh (mV)	Mg mg/L	Ca mg/L	K mg/L	Na mg/L	Si mg/L	Cl mg/L	NO3 mg/L	SO4 mg/L	HCO3 mg/L
Bul Bul Drive														
BB1	Borehole	7/8/2017	1273	6.08		38.673	43.307	15.208	179.195	15.289	156.209	2.206		78.071
BB2	Borehole	7/8/2017	522	7.45		36.264	18.269	2.830	118.212	2.980	137.343	0.276		198.300
BB3	Borehole	7/8/2017	671	7.6	27.9	39.239	33.594	5.039	163.493	6.762	180.232	1.263		351.179
BB5	stream	7/8/2017	1273	6.22	48.6	50.159	6.433	3.244	196.532	31.824	85.358			89.045
BB6	Borehole	7/8/2017	755	6.86	16.9	34.594	54.446	2.463	156.237	12.182	80.814	1.705	18.651	122.399
BB7	Borehole	7/8/2017	2032	7.23	-3.9	62.237	73.506	3.143	274.153	15.416	109.369	5.409		382.429
BB8	Borehole	7/8/2017	1234	7.31	-9.1	23.101	16.300	2.465	387.487	13.275	161.398	5.664	10.180	432.215
BB9	Borehole	7/8/2017	637	6.2	51.5	9.778	2.710	4.515	124.684	30.333	176.842	4.486		84.167
BB10	stream	7/8/2017	507	7.03	7.7	12.120	17.551	7.177	63.599	4.727	31.470	2.631	16.020	134.056
Lovu Landfill Site														
LBH1	Borehole	8/8/2017	1531	7.65	-29.1	34.338	47.437	2.084	238.578	3.690	73.102	0.777	0.867	326.717
LBH2	Borehole	8/8/2017	1214	7.29	-7.1	42.394	52.259	2.374	313.360	13.793	252.800	0.924	7.263	326.322
LBH4	Borehole	8/8/2017	587	7.1	3.5	24.931	17.863	1.882	154.319	26.861	160.559	29.967	27.559	286.339
LBH6	Borehole	8/8/2017	835	7.52	22.6	41.140	84.192	2.575	150.620	7.520	150.658	1.570	11.969	340.470
L2	stream	8/8/2017	1032	7.48	-19	35.339	38.590	39.865	251.460	10.468	180.116	17.185	6.281	357.598
L3	stream	8/8/2017	597	7.38	-12.8	14.436	10.024	1.448	84.843	11.280	64.406		9.159	94.932
Bisasar Road Landfill site														
BS1	Borehole	8/8/2017	2144	6.97	11	137.893	182.016	5.655	482.503	7.145	230.758	1.186	18.150	497.295
BS2	Borehole	8/8/2017	1905	7.25	-5.2	129.251	124.623	17.680	429.633	16.680	143.674		4.330	546.805
BS3	Borehole	9/8/2017	425	7.5	-20.5	171.111	22.333	8.957	665.383	2.017	189.099	2.069	6.204	182.422
BS4	Borehole	9/8/2017	394	7.2	-2.1	19.937	27.162	0.956	41.963	19.745	41.286	2.892	1.504	215.597

BS5	Borehole	9/8/2017	555	7.38	-12.9	19.571	20.148	1.100	121.808	34.012	52.528	9.819	20.766	245.849
BS6	stream	9/8/2017	492	7	9.5	11.915	61.442	10.527	65.614	15.641	78.908		1.110	219.380
BS7	stream	9/8/2017	3339	7.97	-48	51.495	50.059	162.213	474.875	16.787	52.060	17.222	1.668	852.129
Marianhill Landfill Site														
MH1	Borehole	11/8/2017	674	8.16	-59.6	4.558	40.805	3.720	140.261	7.842	43.467	1.418	32.628	324.696
MH2	Borehole	11/8/2017	428	6.14	54.7	13.471	15.493	3.473	52.573	11.370	74.649	7.965	35.000	62.211
MH3	Borehole	11/8/2017	610	7.16	0.2	17.309	53.541	3.185	44.935	11.957	49.293	3.055	8.098	277.758
MH4	stream	11/8/2017	1043	7.16	-7.8	30.887	32.588	27.559	123.717	11.890	140.854	48.018	15.382	293.595
MH5	Borehole	11/8/2017	467	7.18	-1.5	15.784	19.978	2.136	49.513	11.006	77.016	6.727	21.368	104.761
MH6	Borehole	11/8/2017	3317	6.97	10.5	14.449	9.121	1.760	36.334	11.193	37.881	14.048	26.812	75.569
Buffelsdraai Landfill site														
BF1	Borehole	11/8/2017	688	6.38	18.7	48.834	40.645	2.604	132.858	12.209	294.749	10.113	12.118	207.263
BF2	Borehole	14/8/2017	601	7.49	16.5	25.343	26.385	2.745	78.928	16.160	88.373	1.056	8.739	256.014
BF3	Borehole	14/8/2017	546	6.82	-54.3	22.804	9.713	5.139	76.375	2.672	95.950	1.574	1.579	174.841
BF4	Borehole	14/8/2017	660	6.86	-1.4	22.420	27.398	1.046	84.146	19.350	37.980	22.537	10.900	311.847
BF5	stream	14/8/2017	562	8.07	-11.5	17.539	12.092	0.720	77.219	16.666	89.960		9.328	166.766
BF6	stream	14/8/2017	1113	7.18	4.9	4.380	2.745	2.120	26.336	8.150	36.464		2.889	34.119
BF7	stream	14/8/2017	2317	7.35	-27.1	127.386	77.937	9.621	273.809	8.153	455.100	15.167	7.529	719.303
La Mercy Landfill site														
LM1	Borehole	10/8/2017	466	7.08	42.4	3.364	23.780	3.591	10.947	5.692	11.004	2.466	134.809	71.963
LM2	Borehole	10/8/2017	686	7.61	-19.5	3.264	4.547	8.183	130.465	5.997	47.172	3.387	1.926	250.544

b. Trace elements (concentration in ppb)

Sample Id	Fe	B	Al	V	Cr	Mn	Co	Ni	Cu	Zn	As	Rb	Sr	Mo	Sb	Ba	Hg	Pb
Bul Bul Drive																		
BB1	21.00	64.83	26.94	0.06	0.27	1843.30	0.20	7.93	5.13	30.65	0.04	16.00	205.55	0.16	0.666	112.269	0.101	0.369
BB2	8.43	267.53	14.65	0.09	<0,2	0.65	0.06	3.87	1.19	77.21	0.11	1.02	141.10	0.38	0.556	75.833	0.075	0.078
BB3	8.75	134.76	17.88	0.43	<0,2	4.05	0.27	2.80	2.13	10.17	0.26	4.24	277.55	0.62	0.473	51.484	0.090	0.179
BB5	14.26	218.25	18.99	1.55	<0,2	438.04	2.35	16.19	2.45	43.31	0.26	0.56	145.66	0.87	0.791	33.927	0.109	0.274
BB6	342.77	93.75	341.69	1.03	1.07	498.76	0.92	4.91	4.70	56.30	0.19	2.33	113.01	1.10	0.357	147.926	0.051	1.956
BB7	12.57	81.09	18.69	0.25	<0,2	1.37	0.11	2.71	1.99	43.50	0.22	1.95	316.76	0.33	0.664	264.176	0.223	0.265
BB8	9.74	159.28	18.24	4.07	0.29	2.05	0.14	1.92	1.07	20.83	0.17	0.41	89.39	0.25	0.664	20.322	0.239	0.124
BB9	26.51	120.43	22.24	0.43	0.27	199.53	0.17	5.93	1.97	66.27	0.09	4.65	28.86	1.13	0.564	74.239	0.099	0.193
BB10	20.66	38.22	26.76	1.15	0.35	1.35	0.28	4.07	2.87	20.06	0.71	5.32	85.37	0.45	0.972	42.917	0.105	0.275
Lovu Landfill Site																		
LBH1	13.32	110.90	21.53	<0,04	<0,2	307.42	0.14	2.39	0.89	10.27	0.02	4.32	469.40	0.30	0.623	99.192	0.112	0.223
LBH2	160.19	106.10	28.70	0.29	<0,2	233.53	0.12	2.50	4.28	39.93	0.15	5.05	321.95	0.27	0.677	221.728	0.144	0.205
LBH4	31.73	64.06	26.76	14.63	0.40	1.80	0.15	2.71	2.68	30.73	0.90	0.83	25.02	0.40	0.617	13.706	0.046	0.265
LBH6	95.36	95.25	35.43	0.38	0.24	1.08	0.11	2.50	1.50	20.00	0.50	3.04	311.98	0.48	0.746	62.308	0.074	0.480
L2	65.47	188.71	25.97	0.63	7.48	1.10	1.83	11.33	3.05	11.92	1.46	20.38	199.13	2.15	1.029	85.410	0.211	0.152
L3	228.46	41.63	48.15	0.23	0.24	1.21	0.19	2.53	1.38	11.60	0.29	0.99	75.12	0.27	0.682	33.242	0.070	0.173
Bisasar Road Landfill site																		
BS1	19.91	247.42	19.72	0.17	<0,2	1910.05	0.39	2.33	1.32	40.50	0.19	7.63	982.94	0.35	0.750	80.808	0.158	0.875
BS2	15.44	274.43	17.87	0.16	0.31	800.61	2.01	9.12	2.92	42.02	0.80	3.46	663.49	2.68	0.677	235.556	0.094	0.229
BS3	15.96	236.72	17.33	0.05	<0,2	128.20	0.11	1.90	1.19	14.60	0.01	13.26	82.87	0.26	0.678	10.494	0.137	0.179
BS4	12.94	63.31	14.65	0.08	1.30	95.90	0.22	10.81	1.49	38.68	0.43	1.00	119.03	4.93	0.558	42.618	0.059	0.088
BS5	16.53	87.67	23.43	13.67	<0,2	1.79	0.17	2.10	1.69	23.94	0.67	0.74	48.50	0.45	0.688	13.514	0.089	0.454
BS6	11415.3	46.34	56.66	3.67	1.44	1295.64	2.64	6.15	1.83	69.91	3.16	4.40	121.18	0.07	0.562	90.014	0.090	0.688
BS7	659.01	629.95	40.79	10.96	39.42	336.67	15.01	34.22	40.70	44.19	12.33	110.34	321.63	4.53	1.671	185.498	0.114	1.044

Marianhill Landfill Site																		
MH1	148.35	189.04	43.39	0.55	<0,2	6.63	0.12	2.07	6.82	21.61	0.83	3.33	290.82	0.68	0.502	56.912	0.067	0.514
MH2	64.91	37.94	168.92	0.37	0.34	48.45	0.33	2.71	1.94	21.52	0.40	2.87	45.16	<0,12	0.518	88.062	0.044	0.347
MH3	13.04	28.42	18.56	0.48	0.35	1.72	0.20	2.32	1.40	32.13	0.64	3.53	420.88	0.22	0.651	259.050	0.047	0.202
MH4	1203.29	138.95	44.59	0.53	3.88	1824.99	4.10	11.54	11.33	18.62	1.12	9.89	170.46	0.73	1.082	274.386	0.113	0.347
MH5	79.81	41.01	21.84	0.23	<0,2	5.84	0.31	2.47	3.54	13.27	0.17	1.89	99.07	<0,12	0.629	106.741	0.059	0.173
MH6	20.58	42.46	22.15	0.36	<0,2	0.64	0.30	2.40	1.57	12.02	0.19	1.62	73.03	<0,12	0.619	104.499	0.063	0.188
Buffelsdraai Landfill site																		
BF1	39.98	95.13	25.61	0.08	0.25	4.46	0.15	2.56	1.30	18.60	0.10	2.63	110.05	0.48	0.801	311.947	0.062	0.309
BF2	16.96	67.17	26.16	1.09	0.10	834.87	0.60	6.68	3.43	80.45	1.88	2.39	93.13	1.56	1.130	91.705	0.055	7.023
BF3	18.19	78.88	19.67	0.15	0.14	19.37	0.15	2.29	4.97	15.51	0.35	4.26	229.74	0.64	0.558	60.160	0.088	0.290
BF4	10.34	52.20	17.33	7.49	0.22	1.08	0.15	1.77	1.51	17.15	0.70	1.32	82.60	0.19	0.558	38.996	0.047	0.120
BF5	20.31	45.39	18.80	0.61	<0,2	0.81	0.17	2.16	2.28	19.05	0.62	0.61	60.43	0.12	0.597	42.726	0.074	0.109
BF6	189.22	19.90	32.77	0.25	0.27	0.98	0.16	2.09	1.57	12.98	0.16	2.89	23.50	<0,12	0.594	31.511	0.038	0.196
La Mercy Landfill site																		
BF7	17.08	70.63	22.17	2.28	0.97	19.29	1.90	7.99	3.68	19.30	0.71	3.33	572.82	0.27	0.810	219.396	0.191	0.125
LM1	116.24	24.34	20.20	0.08	0.29	105.29	0.34	2.43	1.96	60.30	7.44	4.29	57.21	<0,12	1.157	16.756	0.042	0.282
LM2	86.51	205.40	36.39	0.72	0.19	52.54	0.28	3.03	1.37	17.76	2.70	3.31	15.62	0.91	0.816	10.054	0.175	0.488